

STUDY OF **KNO** SCALING
IN *PP*-COLLISIONS AT \sqrt{s} FROM
0.9 TO 13 TEV USING RESULTS OF
THE **ATLAS** AT THE LHC

Yuri Kulchitsky
JINR, Dubna

09/03/2023 Seminar of the

High Energy Physics and Theoretical Physics Divisions,
Petersburg Nuclear Physics Institute named by B. P. Konstantinov

KNO SCALING: MOTIVATION

In the 2022 Year we celebrated the **50th anniversary** of the famous Equation, the basic result of **Polyakov & Koba, Nielsen, Olesen (KNO)** concerning the asymptotic behavior of the multiplicity distributions. These authors put forward the **hypothesis** that at **very high energies** the probability distributions $P_n(s)$ of producing n particles in a certain collision process should exhibit the scaling (homogeneity) relation

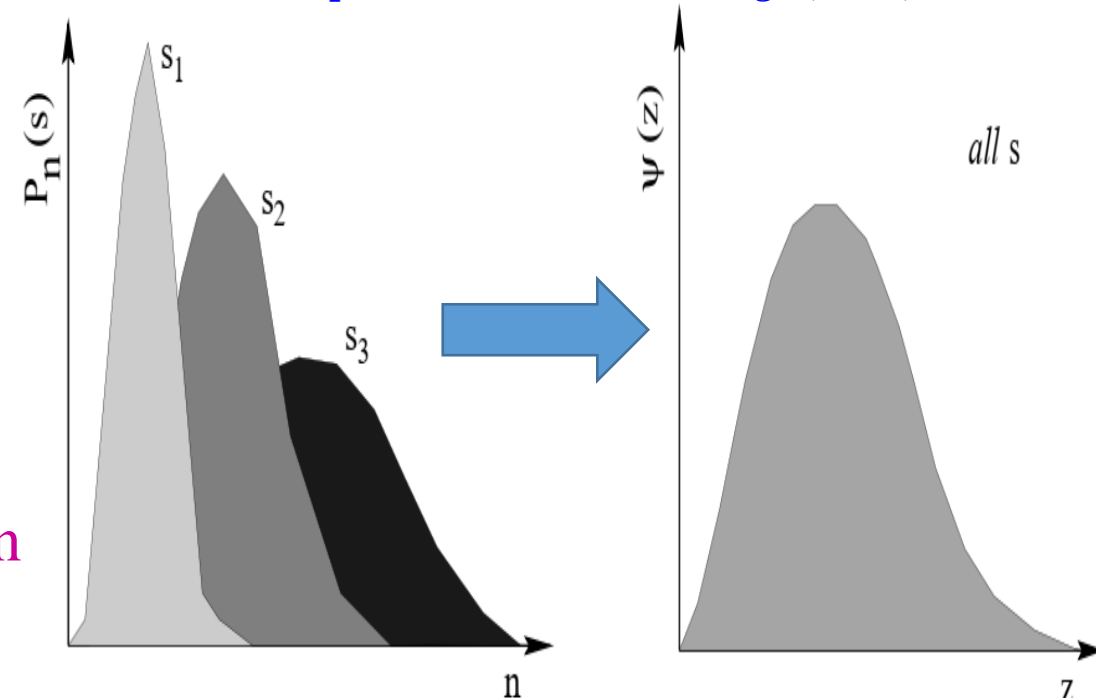
$$P_n(s) = \frac{1}{\langle n(s) \rangle} \psi\left(\frac{n}{\langle n(s) \rangle}\right)$$

as $S \rightarrow \infty$ with $\langle n(s) \rangle$ being the average multiplicity of secondaries at collision energy, S

This so-called **KNO scaling hypothesis** asserts that if we **rescale** $P_n(s)$ measured at different energies via **stretching (shrinking) the vertical (horizontal) axes** by $\langle n(s) \rangle$, these rescaled curves will coincide with each other.

The multiplicity distributions become simple **rescaled copies** of the universal function $\psi(z)$ depending only on the **scaled multiplicity** $z = n(s)/\langle n(s) \rangle$.

1. **A. M. Polyakov**, A Similarity hypothesis in the strong interactions. 1. Multiple hadron production in $e+e$ -annihilation, *Zh. Eksp. Teor. Fiz.* **59** (1970) 542
2. **Z. Koba, H. B. Nielsen and P. Olesen**, Scaling of multiplicity distributions in high-energy hadron collisions, *Nucl. Phys. B* **40** (1972) 317
3. **Z. Koba**, Multi-body phenomena in strong interactions – description of hadronic multi-body final states, p. 171 in *Proceedings CERN-JINR School of Physics, Ebeltoft, Denmark, 17-13 Jun 1973, CERN Yellow Reports: School Proceedings (1973)*



KNO SCALING: MAIN ASSUMPTION

J. F. Grosse-Oetringhaus¹, K. Reygers,
J. Phys. G 37 (2010) 083001

Z. Koba, H. B. Nielsen and
P. Olesen, *Scaling of
multiplicity distributions in
high-energy hadron
collisions*, Nucl. Phys. B 40
(1972) 317

□ KNO scaling main assumption is *Feynman scaling*.

□ KNO scaling is derived by calculating

$$\langle n(n-1)\dots(n-q+1) \rangle = \int f^{(q)}(x_1, p_{T,1}; \dots; x_q, p_{T,q}) \frac{dp_{z,1}}{E_1} dp_{T,1}^2 \dots \frac{dp_{z,q}}{E_q} dp_{T,q}^2$$

which is an extension of the expression used in the derivation of *Feynman scaling*

$$\langle N \rangle = \int_{-1}^1 f_i(x_F) \frac{dx_F}{\sqrt{x_F^2 + \frac{m_T^2}{W^2}}}$$

$$\langle N \rangle \propto \ln W \propto \ln \sqrt{s} \quad \text{with} \quad W = \sqrt{s}/2.$$

that uses a function $f(q)$ that describes q -particle correlations (q particles with energy E_q , longitudinal momentum $p_{z,q}$, transverse momentum $p_{T,q}$, and Feynman-x, x_q). Integration by parts is performed for all x_i and it is proven that the resulting function is uniquely defined by moments. This yields a polynomial in $\ln s$.

□ With a substitution of the form $\langle N \rangle \propto \ln s$ the multiplicity distribution $P(n)$ is found to scale as

$$P(n) = \frac{1}{\langle n \rangle} \Psi\left(\frac{n}{\langle n \rangle}\right) + \mathcal{O}\left(\frac{1}{\langle n \rangle^2}\right),$$

where the first term results from the leading term in $\ln s$, that is $(\ln s)^q$

The second term contains all other terms in $\ln s$, i.e., $(\ln s)^{q'}$ for $q' < q$. $\Psi(z)$ is a universal (energy-independent function). This means that multiplicity distributions at all energies fall on one curve when plotted as a function of z . However, $\Psi(z)$ can be different depending on the type of reaction and the type of measured particles.

STUDY OF MINIMUM-BIAS (MB) EVENTS

Understanding of soft-QCD interactions has direct impact on:

- precision measurements;
- searches for new physics

In this Report

For pp interactions at 0.9 – 13 TeV:

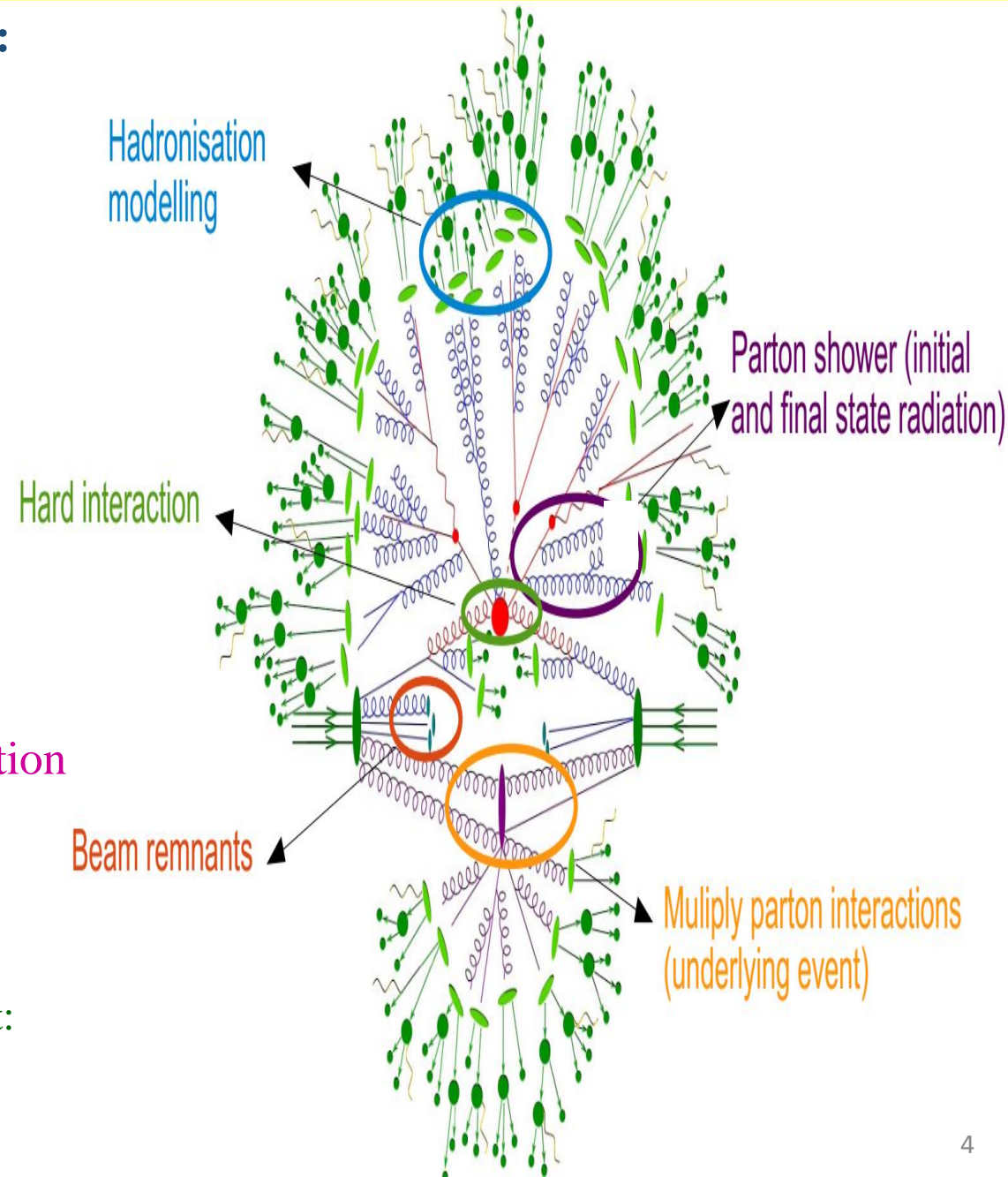
➤ Study Charged-particle distributions

➤ **Study of KNO scaling**

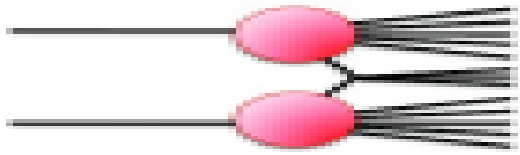
- Study Underlying event distributions
- Study Bose–Einstein correlations (BEC)
- Monte-Carlo generators tuning
- Study an inelastic cross section
- Study particle correlations, hadronization and colour reconnection

Provides insight into strong interactions in non-perturbative QCD regime:

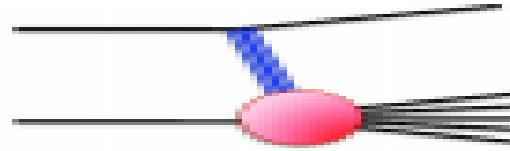
- Soft QCD results used in Monte-Carlo generators tuning,
- Soft QCD description essential for simulating Underlying Event:
 - Multiple Parton Interactions (MPI),
 - Initial & Final State gluon Radiation (ISR, FSR)



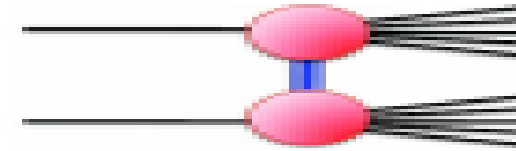
The composition of inelastic p-p collisions:



Non-diffractive



Single-diffractive



Double-diffractive

➤ **Perturbative QCD** describes only the hard-scattered partons, all the rest is predicted with **phenomenological models**

The MC generators used to compare to the corrected data

- **ND:** QCD motivated models with many parameters;
- Pile-up is Background;
- **SD+DD** modelled with large uncertainties
- **Strange baryons** with $30 < \tau < 300$ ps are excluded.

Measure spectra of primary charged particles corrected to particle level

Generator	Version	Tune	PDF	Focus of Tune
PYTHIA 8	8.185	A2	MSTW2008LO	MB
PYTHIA 8	8.186	MONASH	NNPDF2.3LO	MB/UE
EPOS	3.4	LHCv3400		MB
QGSJET-II	II-04	Default		

Multiplicity vs. η

Multiplicity vs. p_T

Multiplicity distributions

$$\frac{1}{N_{ch}} \cdot \frac{dN_{ch}}{d\eta}$$

$$\frac{1}{N_{ev}} \cdot \frac{1}{2\pi p_T} \cdot \frac{d^2 N_{ch}}{d\eta dp_T}$$

$$\frac{1}{N_{ev}} \cdot \frac{dN_{ev}}{dn_{ch}}$$

$$\langle p_T \rangle \text{ vs. } n_{ch}$$

Measurements do not apply model dependent corrections & allow to tune models to data measured in well defined kinematic range

All the events are processed through the ATLAS detector simulation program (based on GEANT4)

A TOROIDAL LHC APPARATUS (ATLAS)

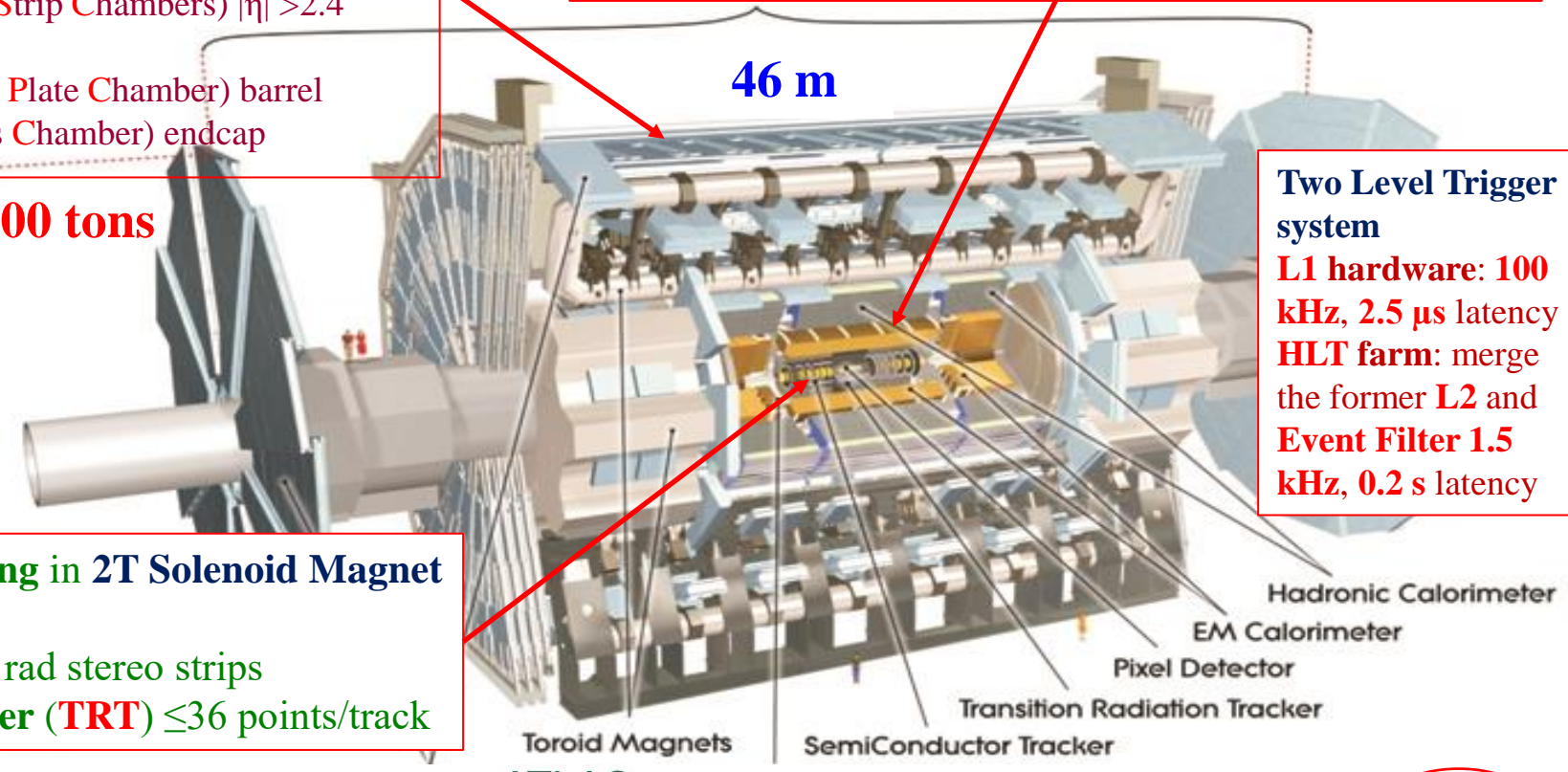


Subdetector	Operational Fraction
AFP	93.8%
ALFA	99.9%
CSC Cathode Strip Chambers	95.3%
Forward LAr Calorimeter	99.7%
Hadronic End-Cap Lar Cal	99.5%
LAr EM Calorimeter	100 %
LVL1 Calo Trigger	99.9%
LVL1 Muon RPC Trigger	99.8%
LVL1 Muon TGC Trigger	99.9%
MDT Muon Drift Tubes	99.7%
Pixels	97.8%
RPC Barrel Muon Chambers	94.4%
SCT Silicon Strips	98.7%
TGC End-Cap Muon Cha	99.5%
Tile Calorimeter	99.2%
TRT Transit Rad Tracker	97.2%

Air-core Muon spectrometer
 (μ Trigger/tracking and Toroid Magnets)
Precision Tracking:
 MDT (Monitored Drift Tubes)
 CSC (Cathode Strip Chambers) $|\eta| > 2.4$
Trigger:
 RPC (Resistive Plate Chamber) barrel
 TGC (Thin Gas Chamber) endcap

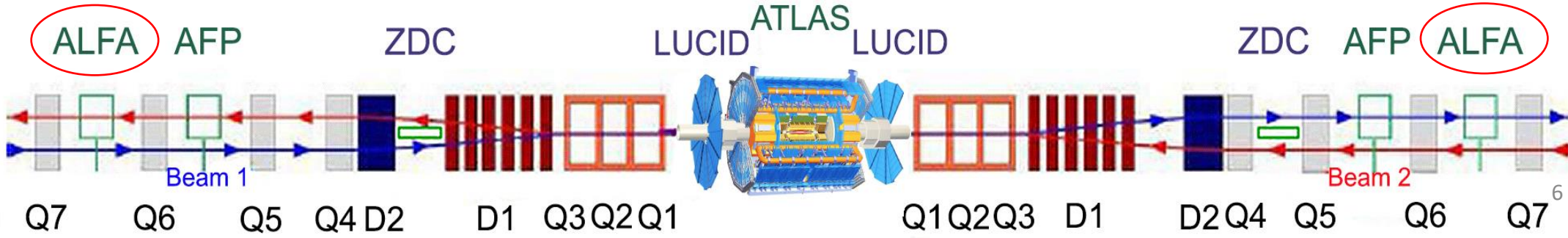
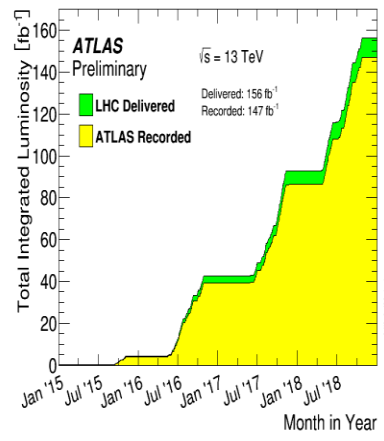
Longitudinally segmented Calorimeter:
 EM and Hadronic energy
 LiquidAr EM barrel and End-cap & Hadronic End-cap
 Tile calorimeter (Fe-scintillator) Hadronic barrel

25 m
 7 000 tons



Two Level Trigger system
 L1 hardware: 100 kHz, 2.5 μ s latency
 HLT farm: merge the former L2 and Event Filter 1.5 kHz, 0.2 s latency

Inner Detector (ID) Tracking in 2T Solenoid Magnet
 Silicon Pixels 50x400 μ m²
 Silicon Strips (SCT) 40 μ m rad stereo strips
 Transition Radiation Tracker (TRT) ≤ 36 points/track

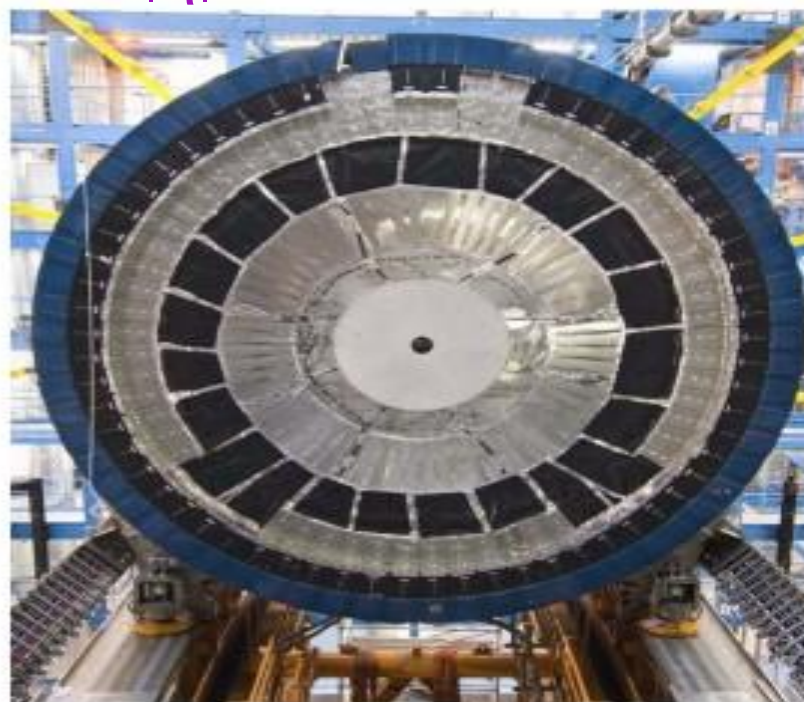
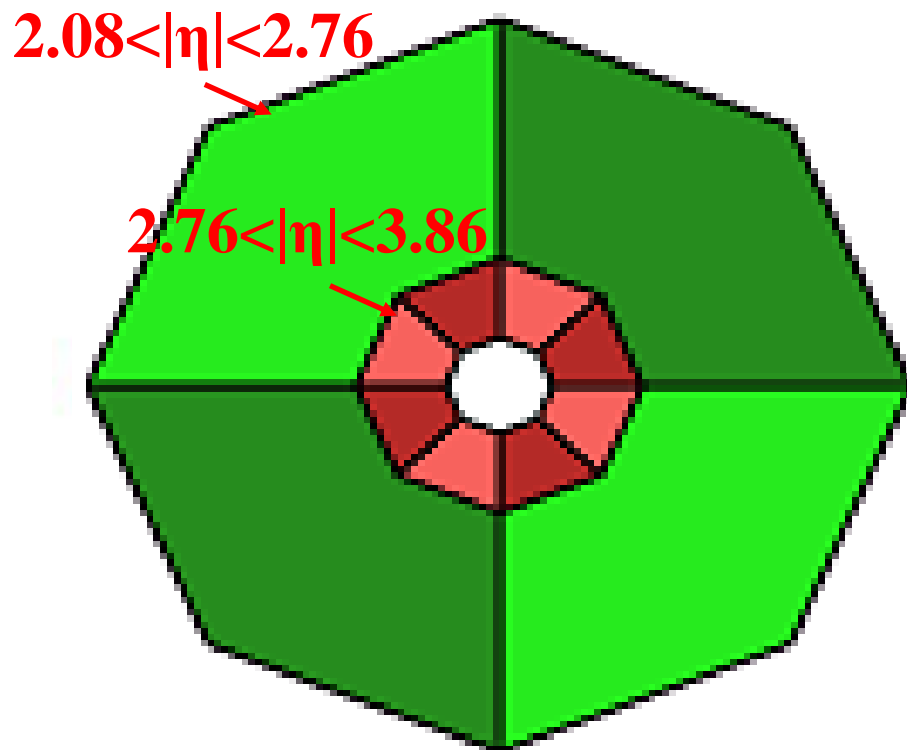


09/03/2023

MINIMUM BIAS TRIGGER SCINTILLATOR

24 independent wedge-shaped plastic scintillators (12 per side) read out by PMTs,

$$2.08 < |\eta| < 3.86$$



Pseudorapidity is defined as

$$\eta = -\frac{1}{2} \ln(\tan(\theta/2))$$

θ is the polar angle with respect to the beam.

- Designed for triggering on min bias events, >99% efficiency
- **MBTS** timing used to veto halo and beam gas events
- Also being used as gap trigger for various diffractive subjects

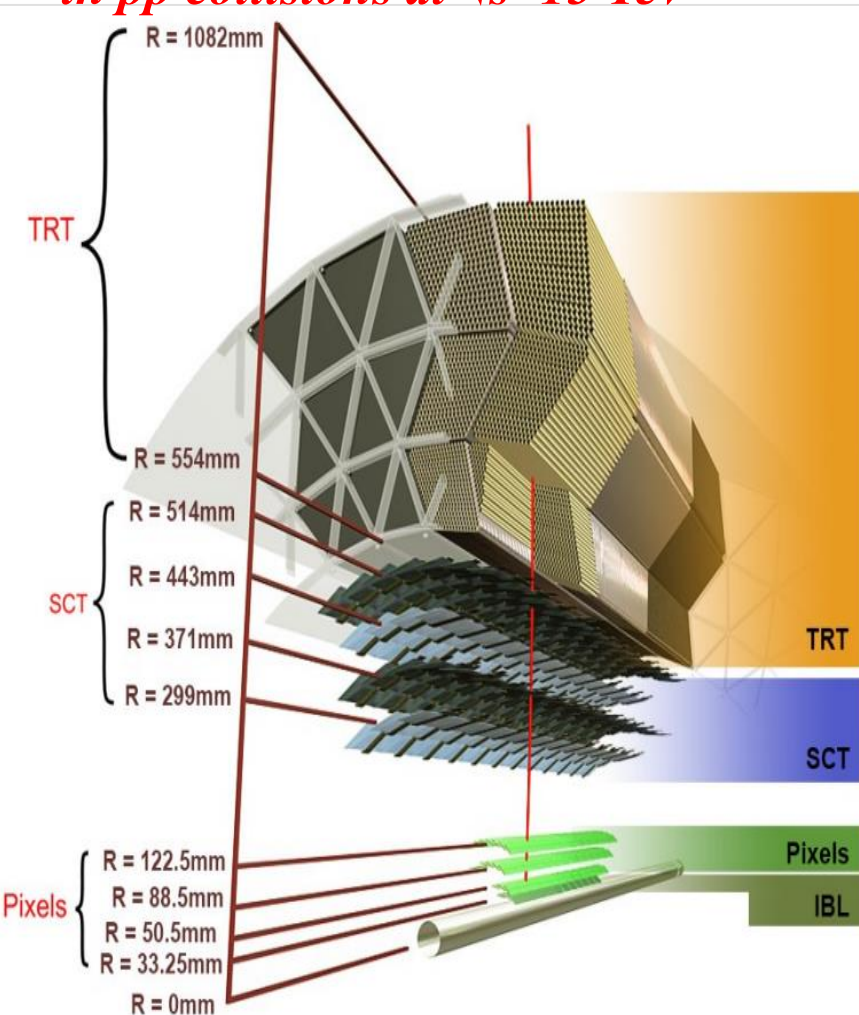
INNER DETECTORS (ID)

The focus of ATLAS is high- p_T physics and provides a window onto important *softer QCD processes*. These have intrinsic interest but also the searches for new physics.

- ▶ *Charged-particle distributions at $\sqrt{s}=13$ TeV in pp interactions*
- ▶ *Charged-particle distributions sensitive to the underlying event in pp collisions at $\sqrt{s}=13$ TeV*

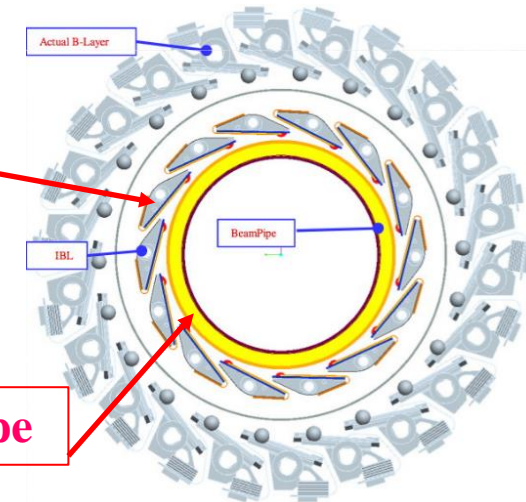


ATLAS tracking detectors:
Pixels, SCT & TRT

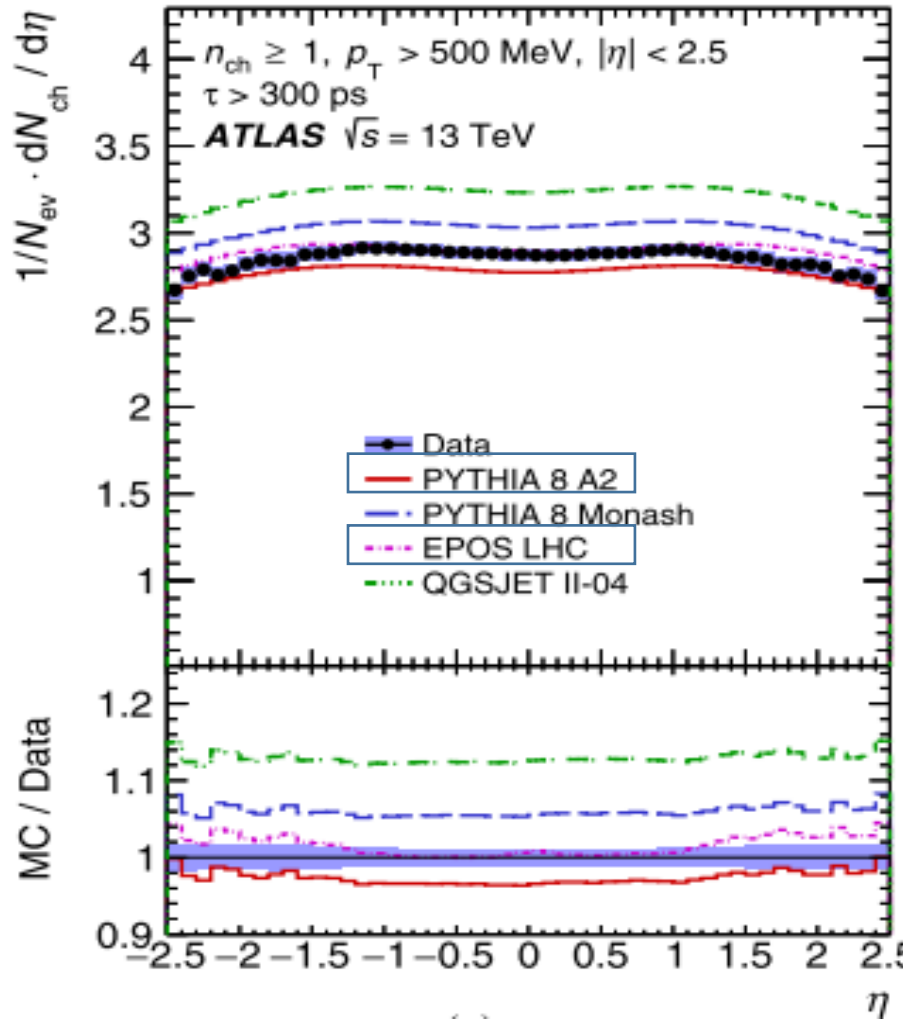


- ❑ **New innermost 4-th layer** for the Pixel detector
[IBL = Insertable B-Layer]
- ❑ Required complete removal of the ATLAS Pixel volume
- ❑ IBL fully operational

New Be beam pipe



Two times better tracks impact parameters resolution at 13 TeV!

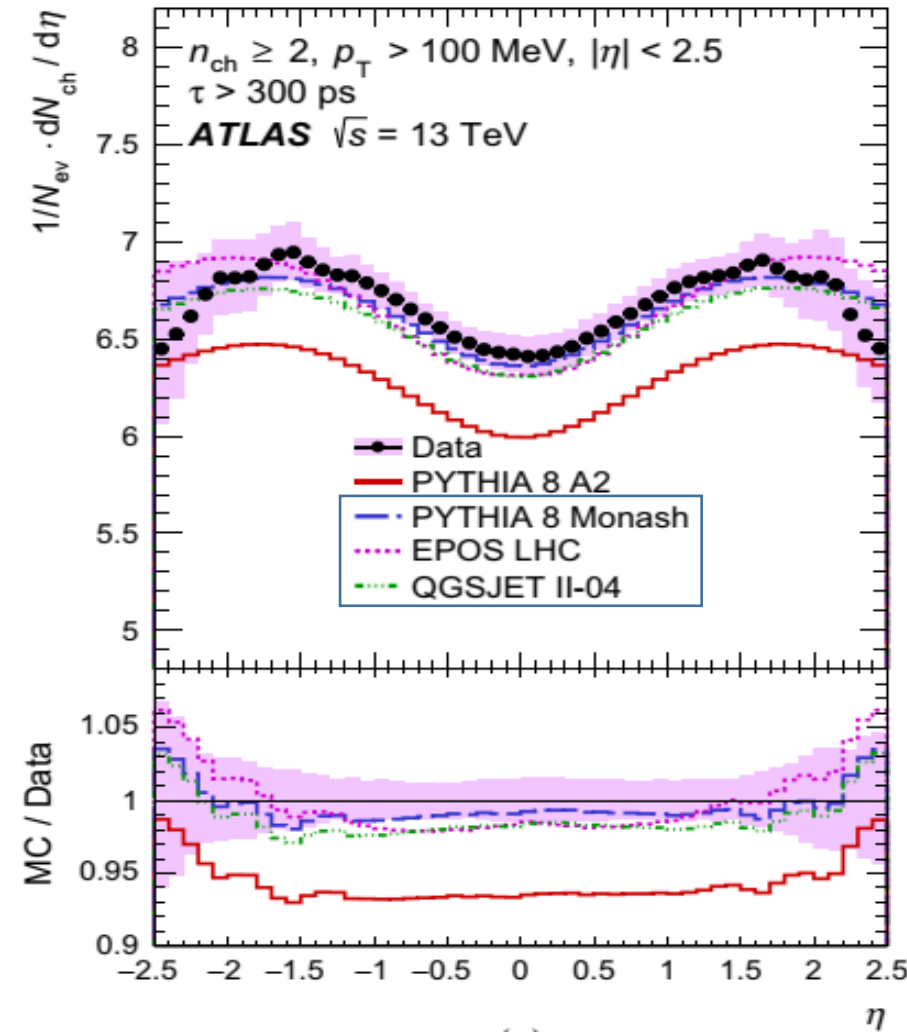


For $p_T > 500 \text{ MeV}$:

- Has the *same shape* in Models but different normalisation
- **EPOS** and **Pythia 8 A2** give remarkably good predictions

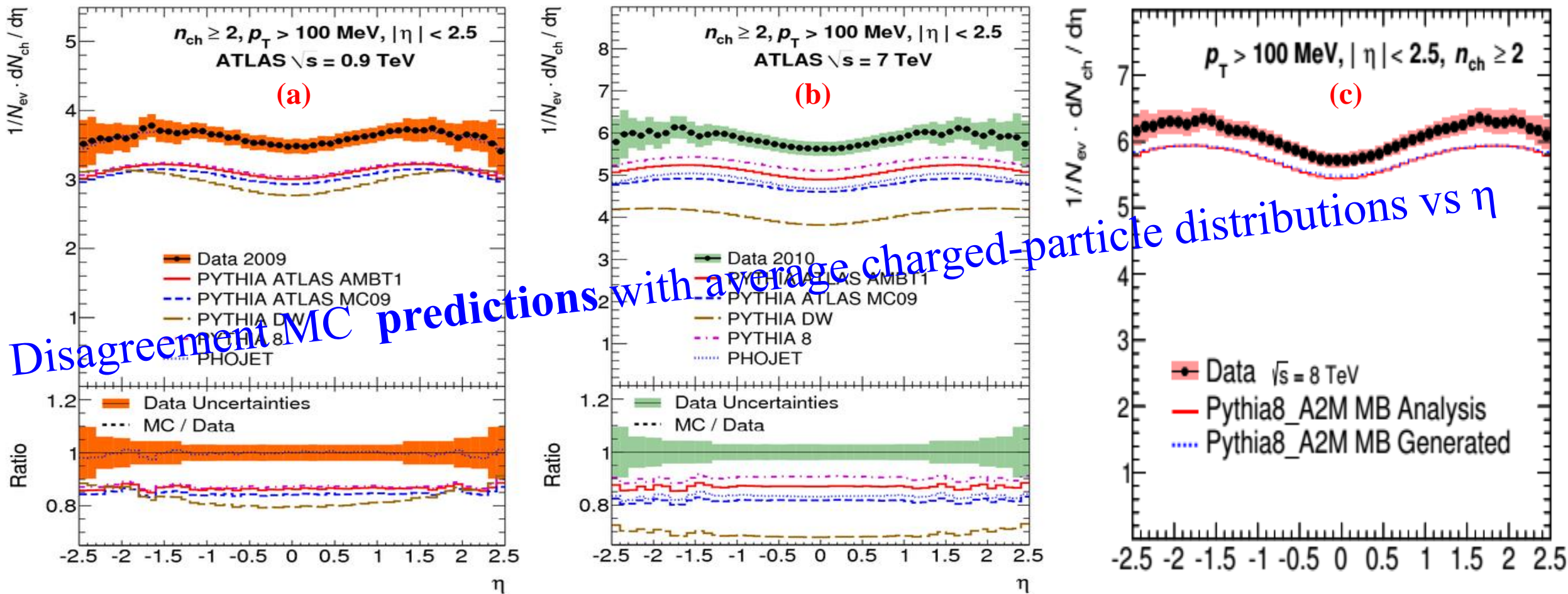
For $p_T > 100 \text{ MeV}$:

- **PYTHIA 8 MONASH, EPOS** and **QGSJET- II** give a good description for $|\eta| < 1.5$
- The prediction from **PYTHIA 8 A2** has the same but lies below the data



Primary charged-particle multiplicities as a function of η for events with $n_{ch} \geq 1, p_T > 500 \text{ MeV}$ and $n_{ch} \geq 2, p_T > 100 \text{ MeV}$

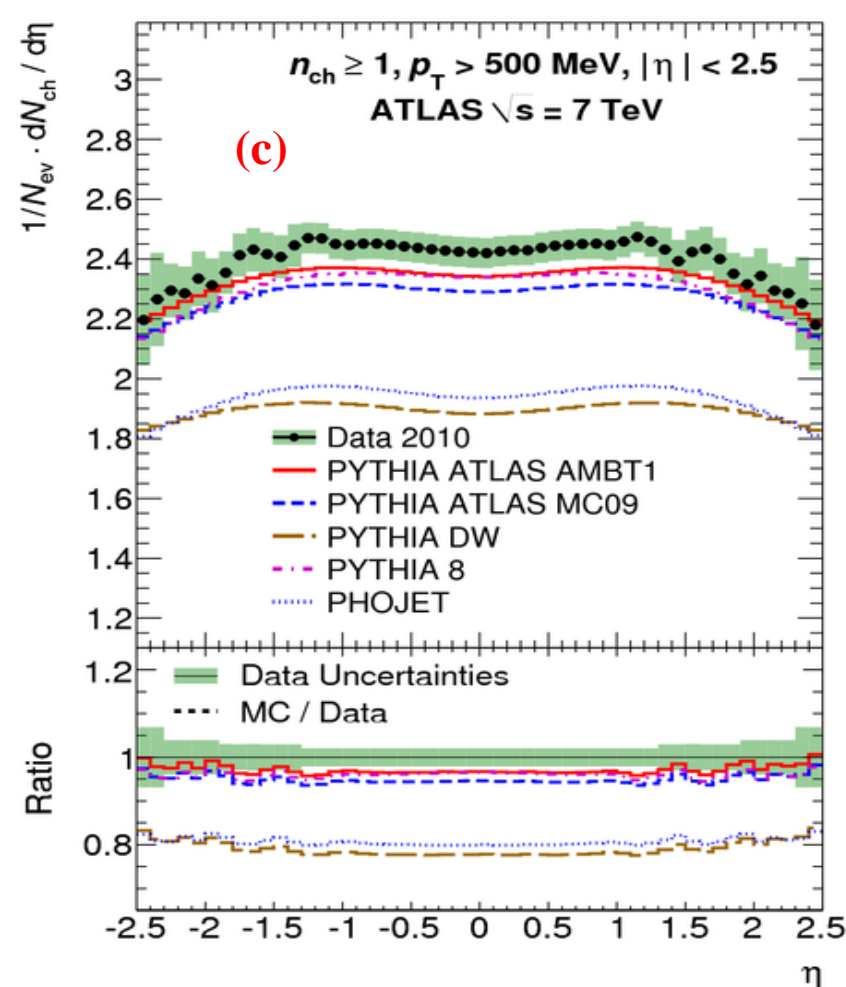
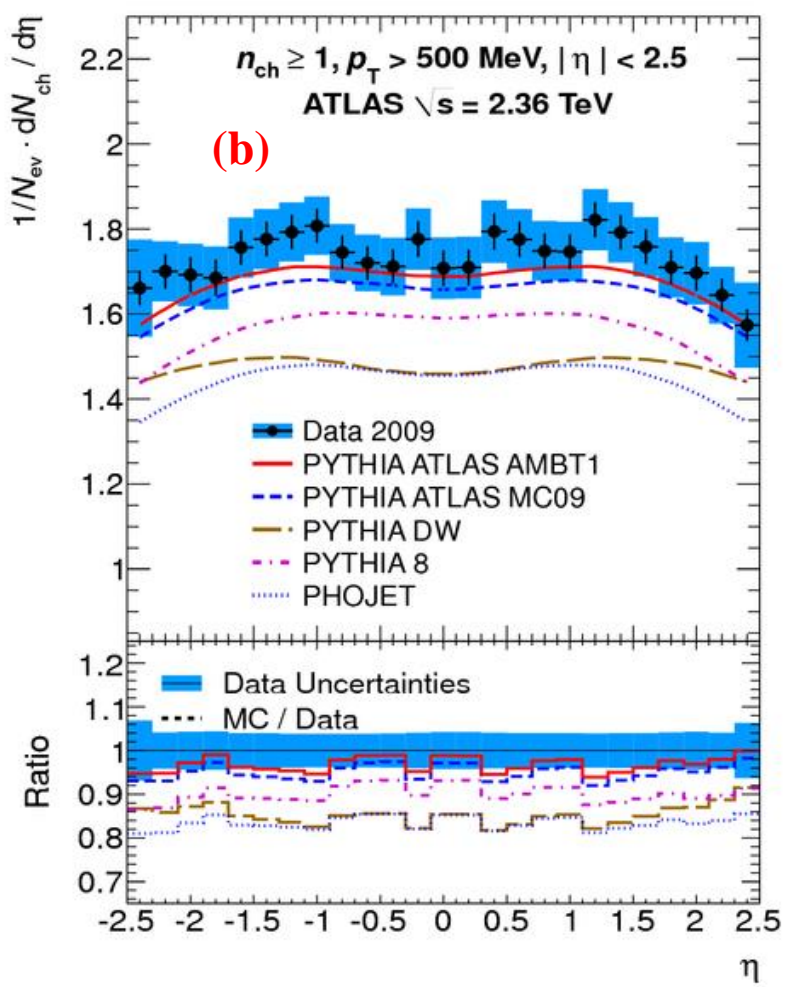
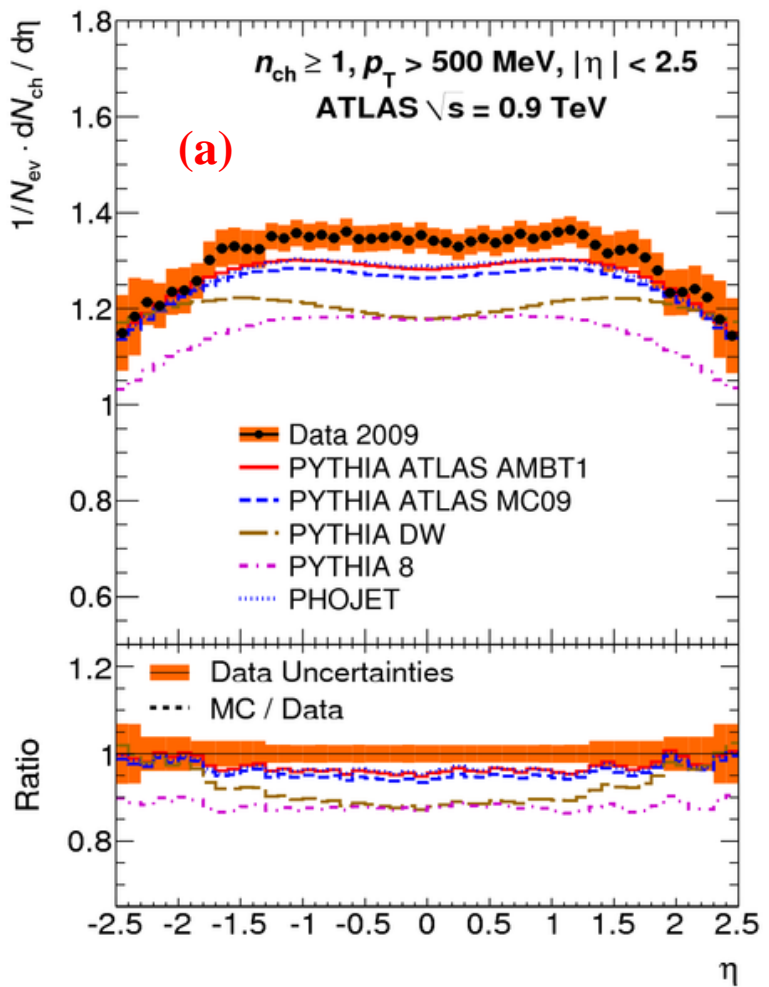
CHARGED-PARTICLE MULTIPLICITIES AS A FUNCTION OF THE η : $p_T > 100$ MeV



Charged-particle multiplicities as a function of the η for events with $n_{ch} \geq 2, p_T > 100$ MeV at $\sqrt{s} = 0.9$ (a), 7 (b) and 8 TeV (c)

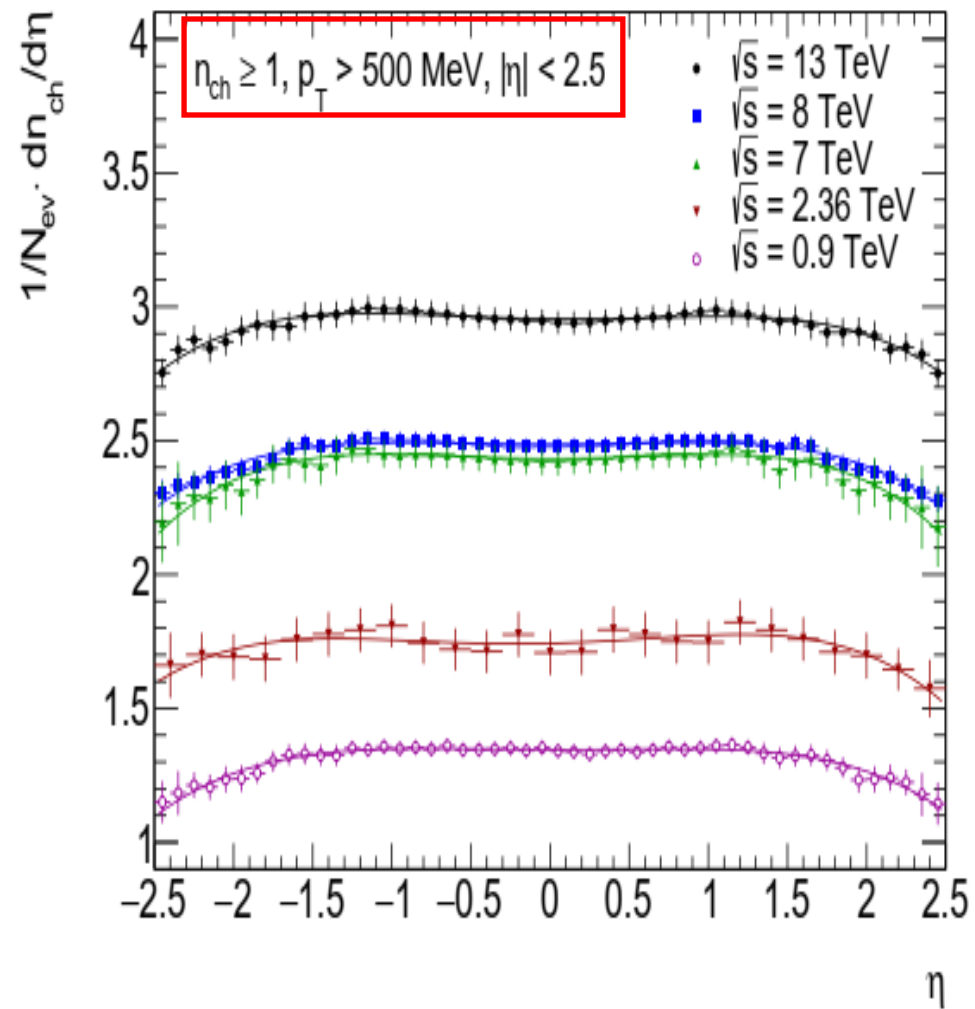
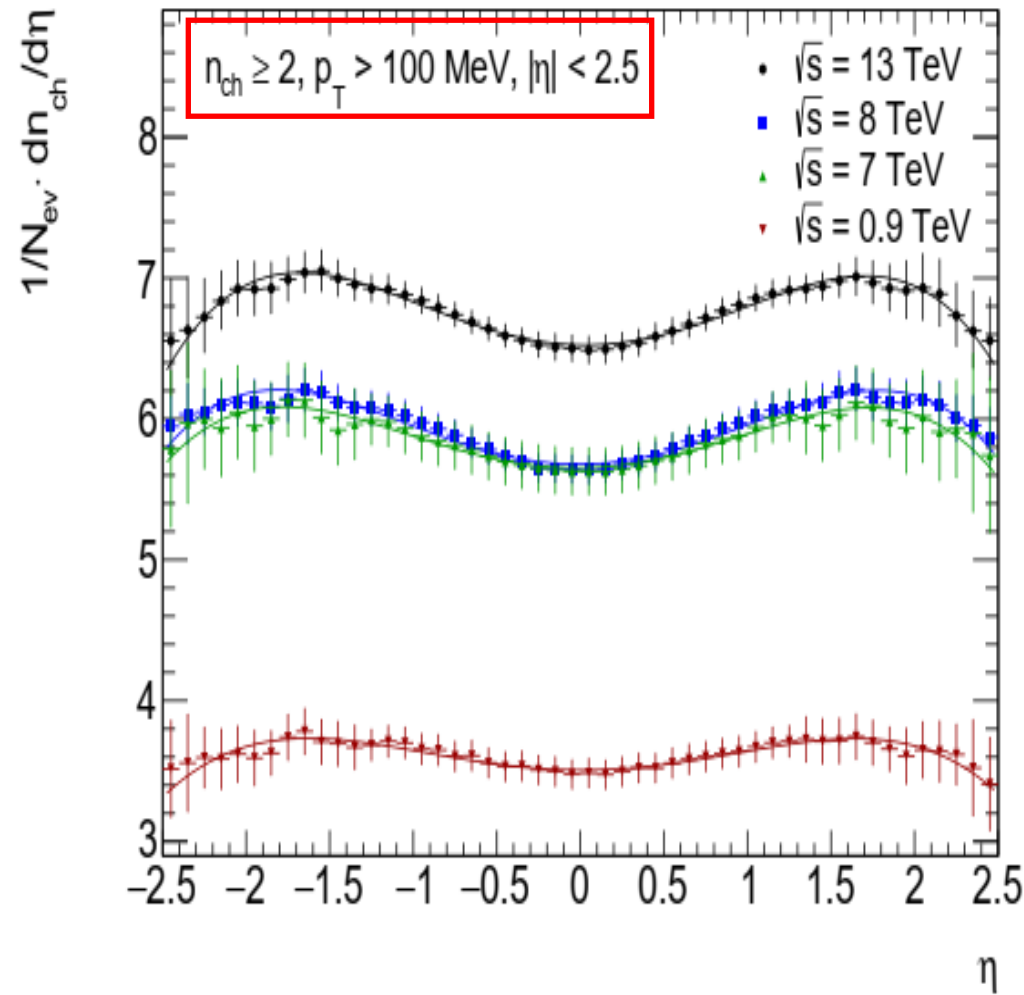
Strong dependence on the **ID** material in the **forward region**. From 7 to 8 TeV, up to **50%** improvement in the central η region & **65%** improvement in the high η region: better knowledge of the ID material achieved at the end of Run 1

CHARGED-PARTICLE MULTIPLICITIES AS A FUNCTION OF η : $p_T > 500$ MeV



Charged-particle multiplicities as a function of the pseudorapidity for events with $n_{ch} \geq 1, p_T > 500$ MeV at $\sqrt{s} = 0.9$ (a), 2.36 (b) and 7 TeV (c)

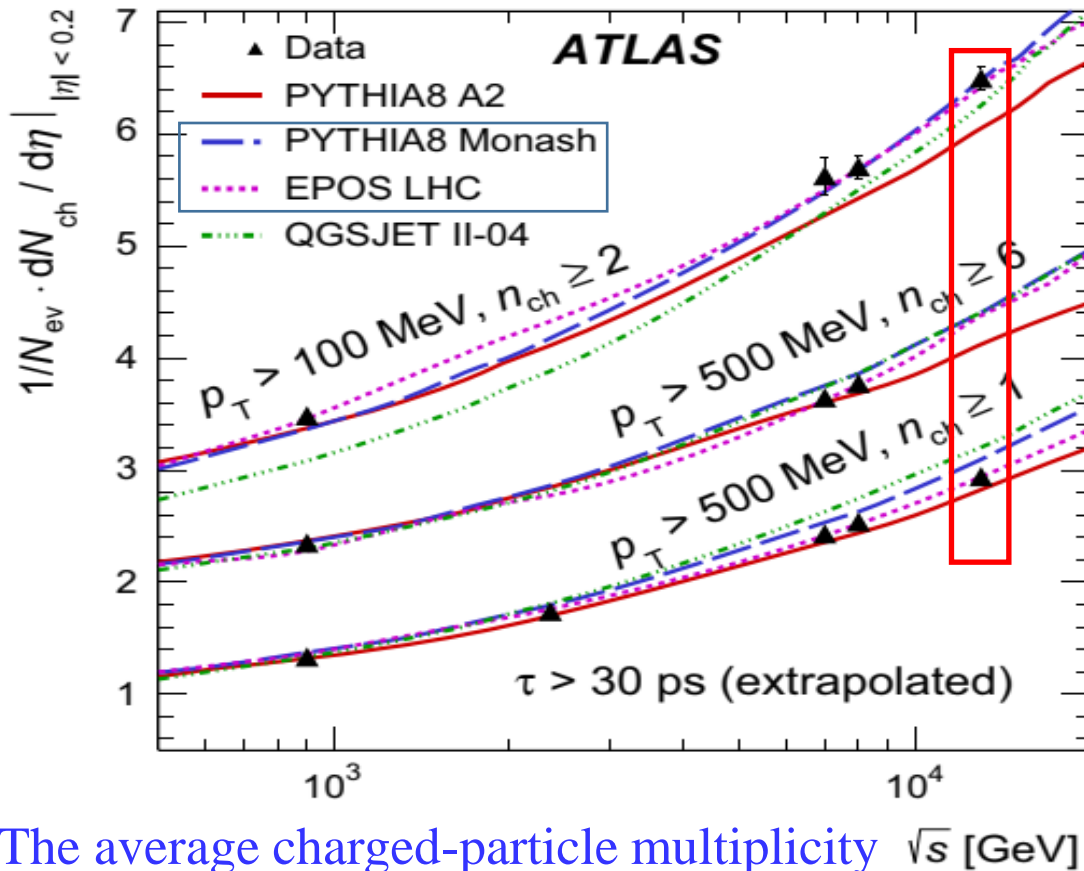
AVERAGE PRIMARY CHARGED-PARTICLE MULTIPLICITY



\sqrt{s} [TeV]	p_T^{\min} [MeV]	Average Multiplicity
13	100	33.88±0.11
	500	14.66±0.04
8	100	29.81±0.10
	500	12.25±0.03
7	100	29.40±0.19
	500	11.98±0.05
2.36	500	8.66±0.51
0.9	100	18.06±0.12
	500	6.53±0.03

$$z = \frac{n_{\text{ch}}(s, p_T^{\min})}{\langle n_{\text{ch}}(s, p_T^{\min}) \rangle}$$

The average multiplicity, $\langle n_{\text{ch}}(s, p_T^{\min}) \rangle$, as the results of the fits with a polynomial function of the average multiplicity distributions on pseudorapidity region $-2.5 < \eta < 2.5$ and the events samples with $p_T > 100 \text{ MeV}$ & $p_T > 500 \text{ MeV}$ at centre-of-mass energies **0.9, 2.36, 7, 8, 13 TeV** using the **ATLAS** Collaboration results.



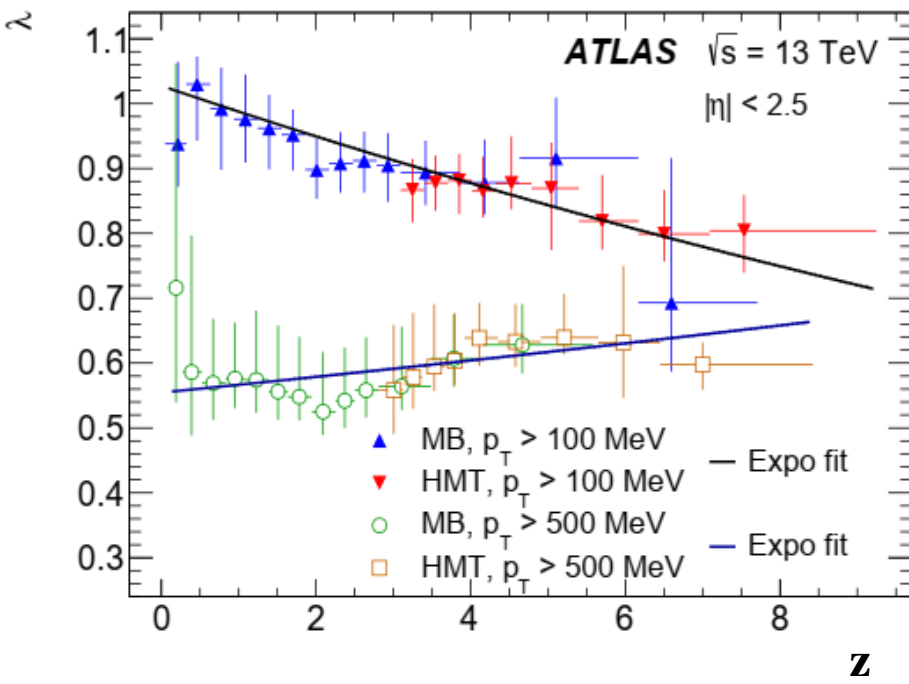
- The values for the other pp energies are taken from previous ATLAS analyses.
- The results have been extrapolated to include charged strange baryons (charged particles with a mean lifetime of $30 < \tau < 300$ ps).
- The data are shown as *black triangles with vertical error bars* representing the total uncertainty.
- They are compared to various MC predictions which are shown as *coloured lines*.
- It is related to the average energy density in pp interactions and it gives reference for heavy-ion collisions
- ❖ For comparison of multiplicity distributions for different energies or different p_T -thresholds a scaled charged-particle multiplicity is introduced as follows:

$$z = \frac{n_{ch}(s, p_T^{\min})}{\langle n_{ch}(s, p_T^{\min}) \rangle} = \frac{n_{ch}(s, p_T^{\min})}{\langle dn_{ch}/d\eta|_{|\eta|<0.2}(s, p_T^{\min}) \rangle \cdot \Delta\eta}$$

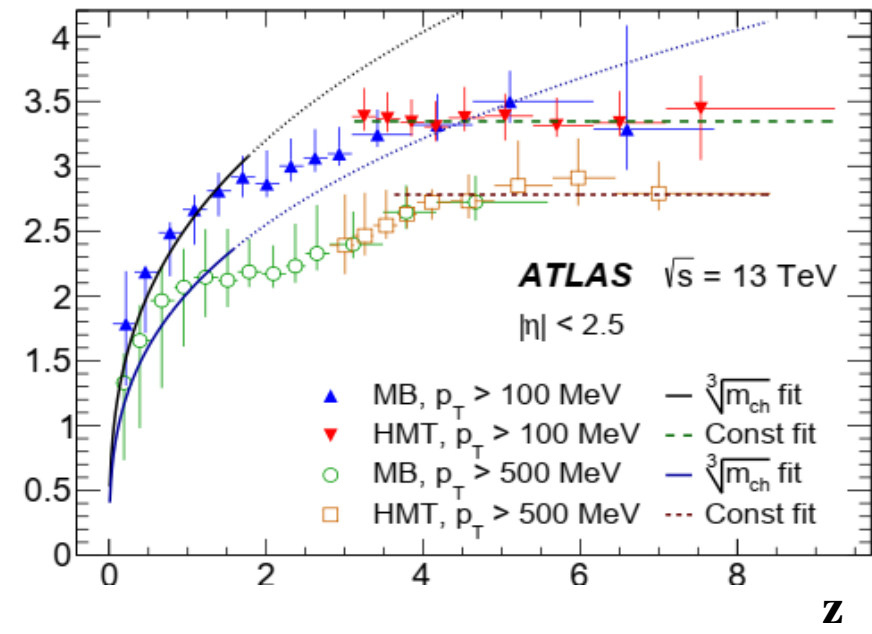
CERN-EP-2021-172
arXiv:2202.02218 [hep-ex]

- For $p_T > 100$ MeV the predictions from **EPOS** and **PYTHIA8 MONASH** match the data well; the predictions from **PYTHIA8 A2** the match is not as good as was observed when measuring particles with $p_T > 500$ MeV
- For $p_T > 500$ MeV the predictions from **EPOS** and **PYTHIA8 A2** match the data well

BEC PARAMETERS VS NORMALIZED MULTIPLICITY

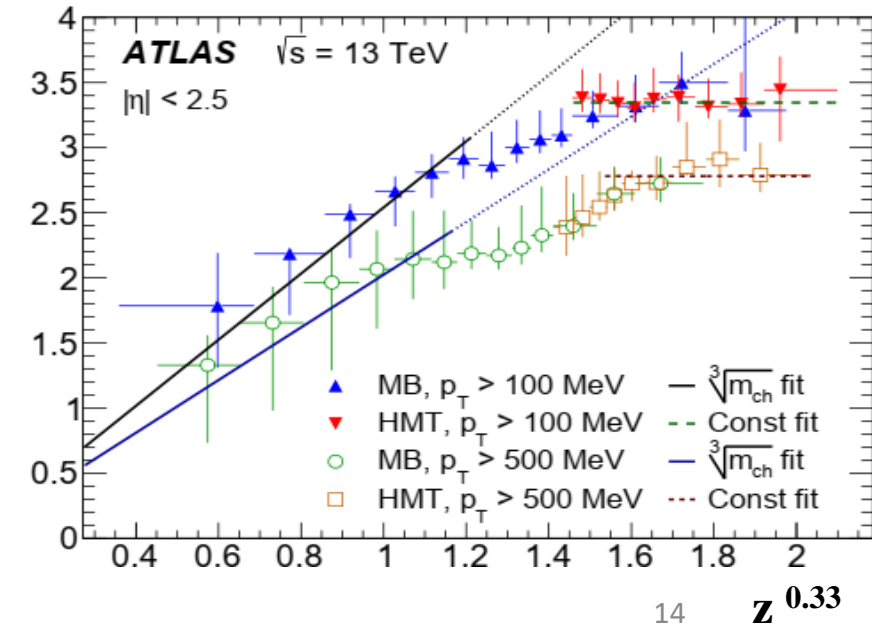


□ The dependence of the $\lambda(z)$ on rescaled multiplicity obtained from the exponential fit of the $R_2(Q)$ correlation functions for tracks with $p_T > 100$ MeV and $p_T > 500$ MeV at $\sqrt{s} = 13$ TeV for the MB and HMT data.



□ The dependence of the $R(z)$ on z and on $z^{0.33}$.

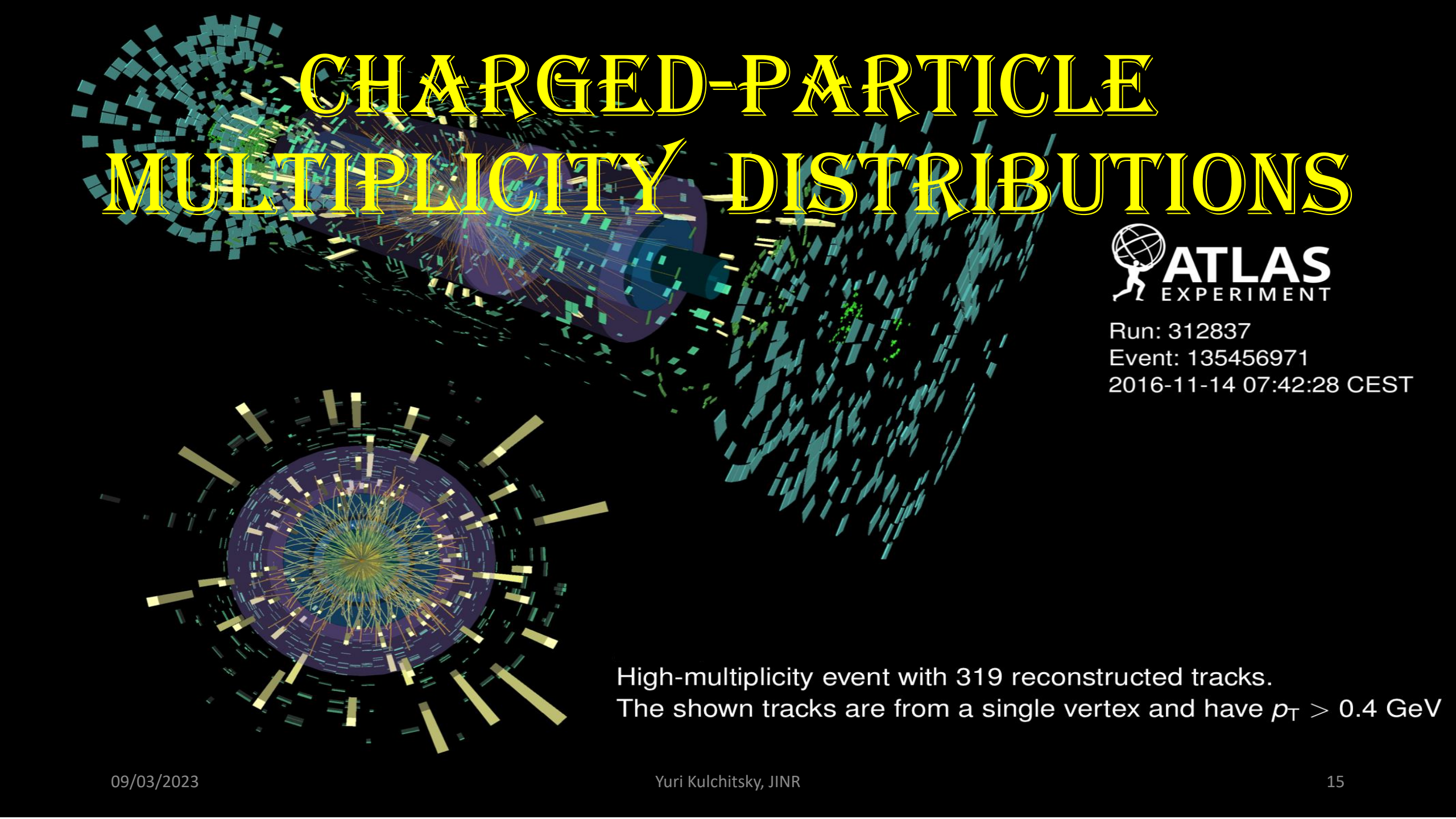
□ The uncertainties represent the sum in quadrature of the statistical and asymmetric systematic contributions.



$$z = \frac{n_{ch}(s, p_T^{\min})}{\langle n_{ch}(s, p_T^{\min}) \rangle} = \frac{n_{ch}(s, p_T^{\min})}{\langle dn_{ch}/d\eta|_{|\eta| < 0.2}(s, p_T^{\min}) \rangle \cdot \Delta\eta}$$

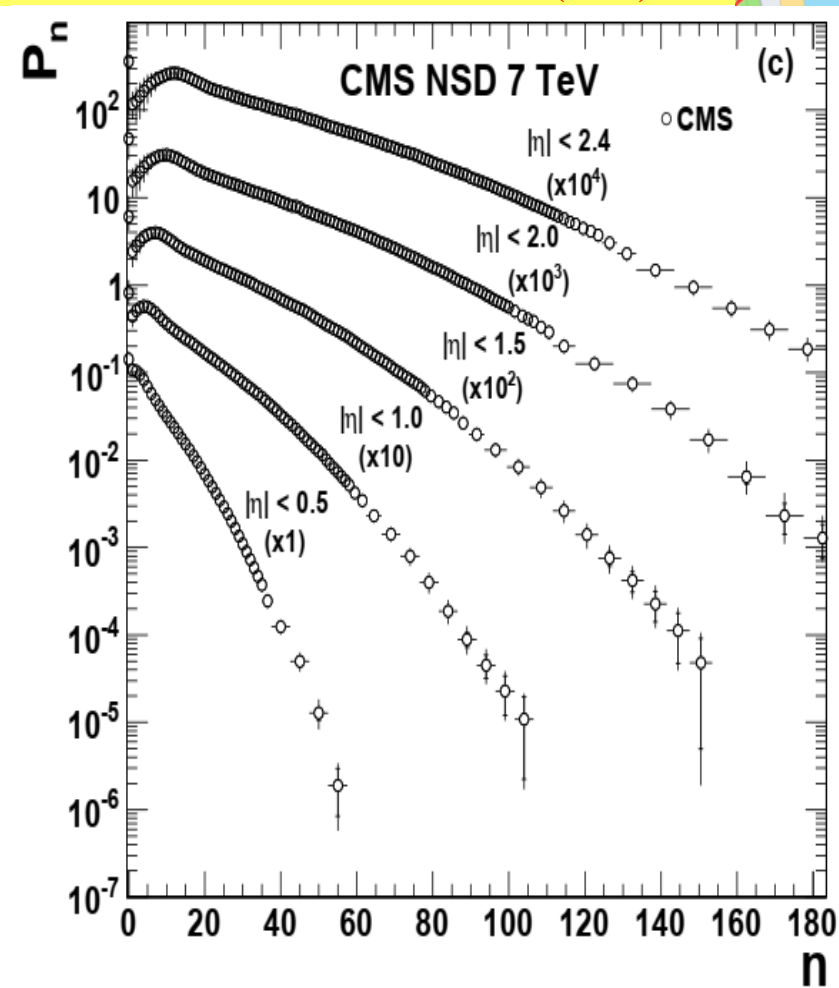
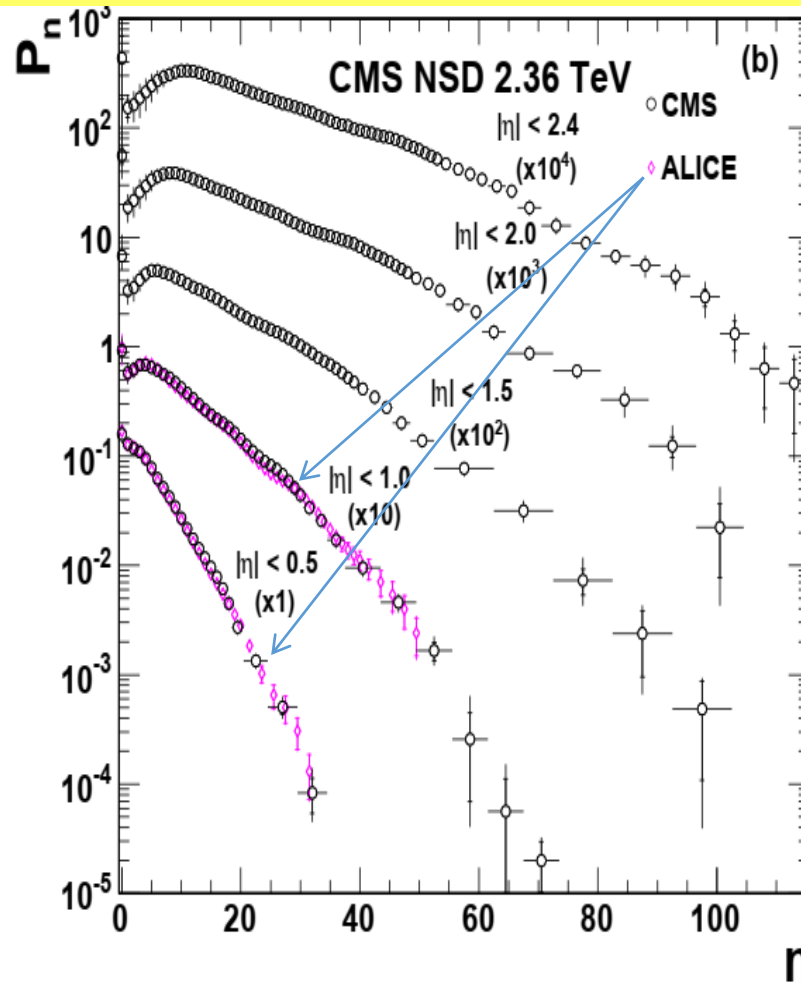
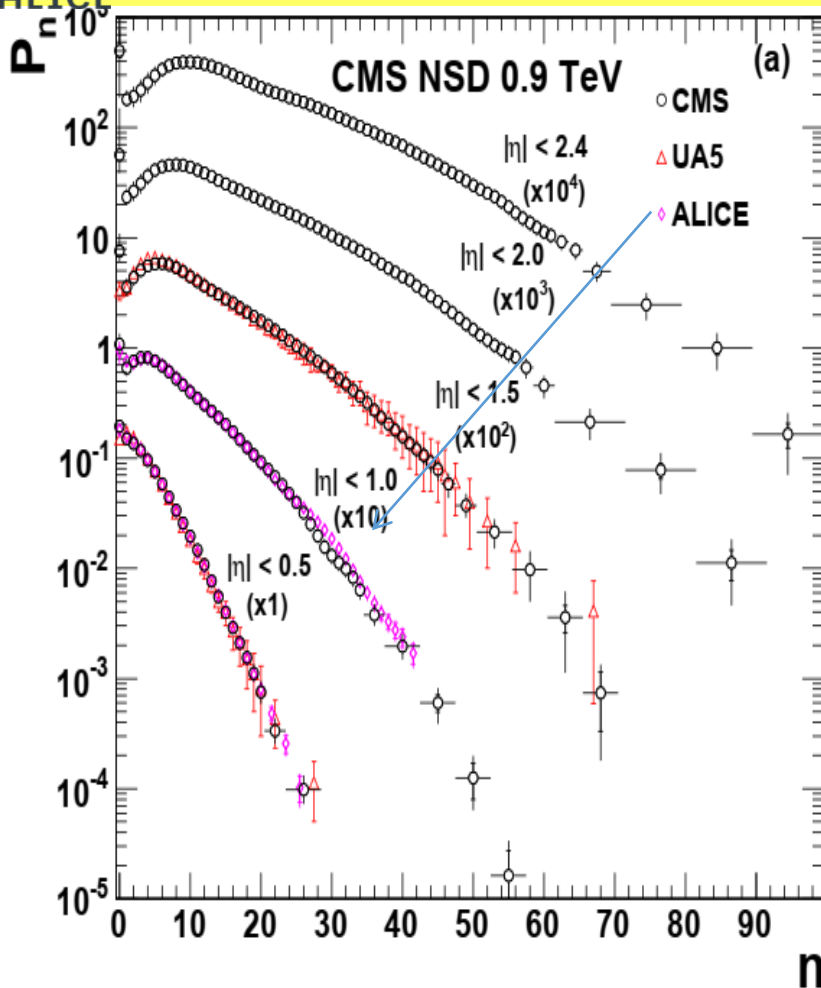
where $\langle dn_{ch}/d\eta|_{|\eta| < 0.2}(s, p_T^{\min}) \rangle$ is the average charged-particle multiplicity per unit pseudorapidity in the region $|\eta| < 0.2$ for different centre-of-mass energies and p_T^{\min} thresholds; $\Delta\eta$ is total pseudorapidity region, equal to 5 in case of ATLAS Inner detector.

CHARGED-PARTICLE MULTIPLICITY DISTRIBUTIONS



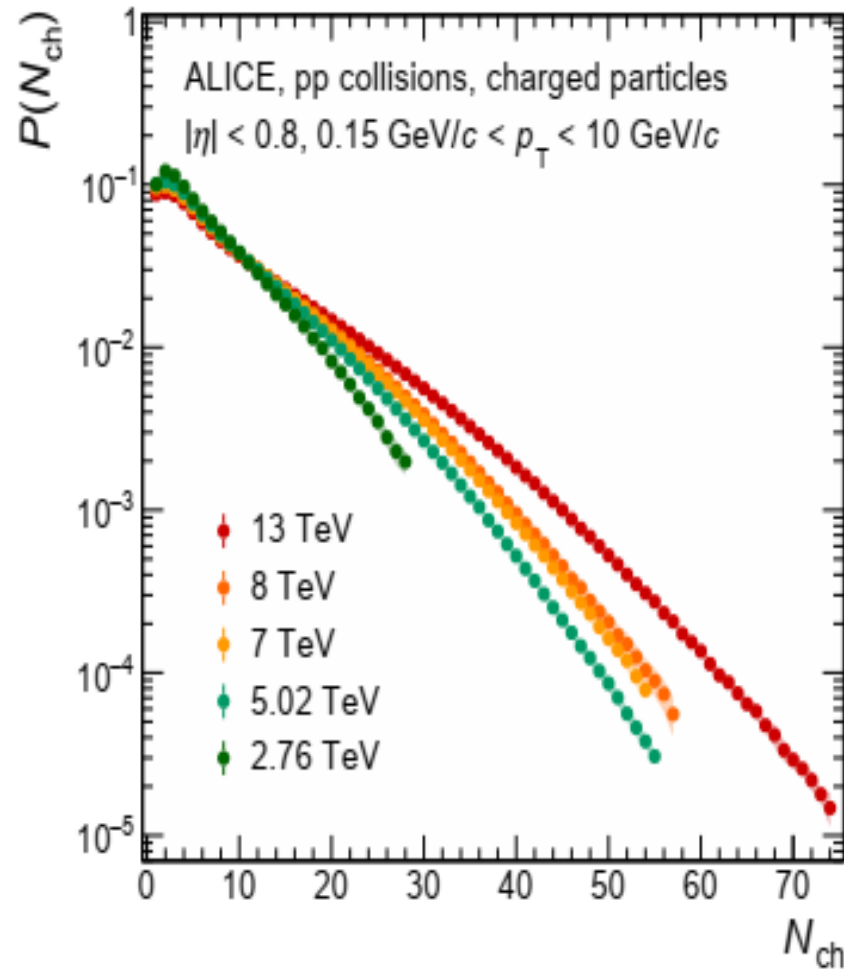
Run: 312837
Event: 135456971
2016-11-14 07:42:28 CEST

High-multiplicity event with 319 reconstructed tracks.
The shown tracks are from a single vertex and have $p_T > 0.4$ GeV

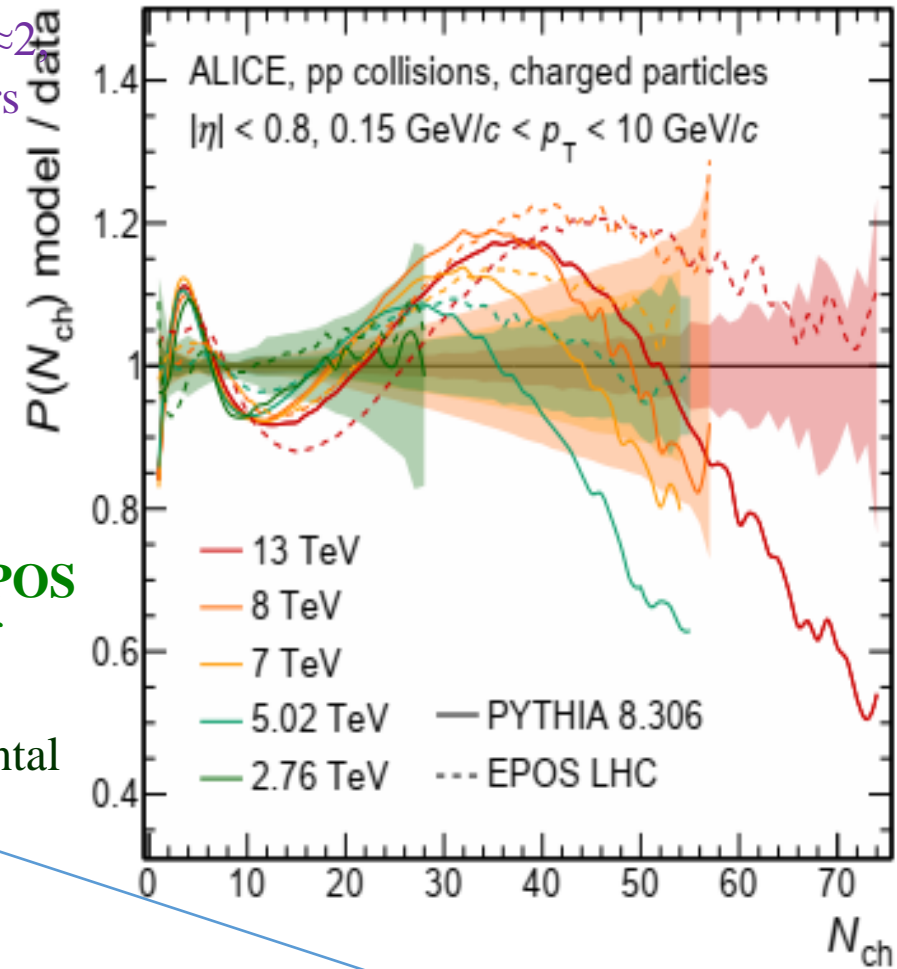


The multiplicity scale is dependent from the energy!

- The CMS fully corrected charged hadron multiplicity spectrum for $|\eta| < 0.5, 1.0, 1.5, 2.0, 2.4$ at **0.9, 2.36, 7 TeV**, compared with other measurements (ALICE & UA5) in the same η interval and at the same \sqrt{s} energy.
- ❖ For clarity, results in different pseudorapidity intervals are scaled by powers of 10 as given in the plots.
- ❖ The error bars are the statistical and systematic uncertainties added in quadrature.



- Distributions reach a max around $N_{ch} \approx 2$ then fall steeply off over several orders of magnitude.
- The slope of the decay with N_{ch} decreases with increasing collision energy. This can be attributed to the larger p_T in the initial hard scattering which results in larger multiplicities.
- ❖ The overall shapes of the multiplicity distribution are better described by **EPOS LHC**, while **Pythia 8** falls sharply off above $N_{ch}/\langle N_{ch} \rangle \approx 4$.
- ❖ Both models agree with the experimental distributions within **25%** with larger deviations at highest multiplicities.



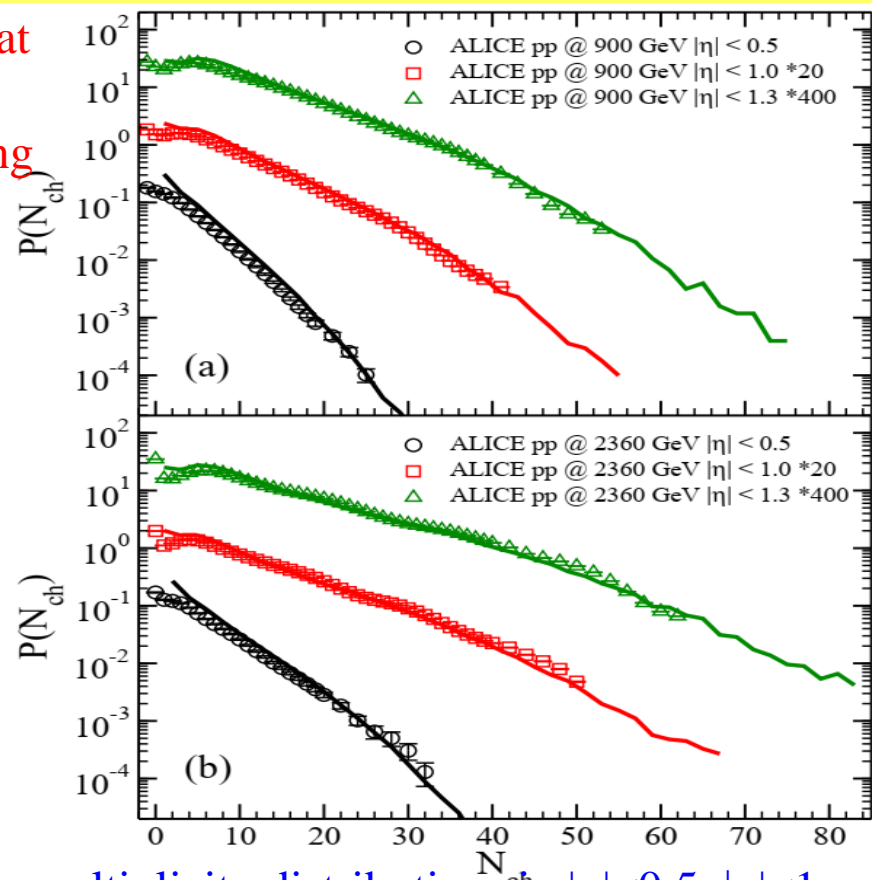
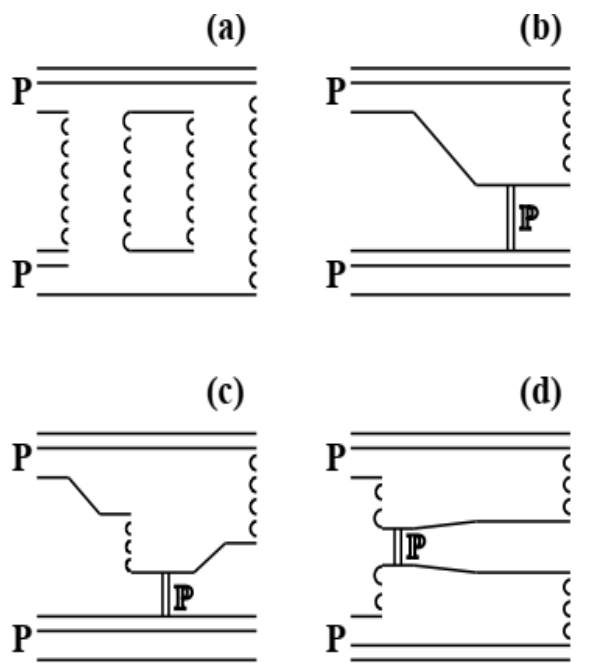
- The ALICE primary charged-particle multiplicity distributions as a function of the multiplicity for pp collisions at the different \sqrt{s} energies for events with $N_{ch} > 0, |\eta| < 0.8, 0.15 < p_T < 10 \text{ GeV}$.
- The ratio of Pythia 8 and EPOS LHC model predictions to data at various energies. The semi-transparent bands indicate the relative systematic uncertainties of the data.

	$\sqrt{s_{NN}}$ (TeV)	$\langle N_{ch} \rangle$
	2.76	7.18 ± 0.24
	5.02	8.21 ± 0.10
pp	7	8.86 ± 0.12
	8	9.05 ± 0.22
	13	10.31 ± 0.09

CHARGED-PARTICLE MULTIPLICITIES DISTRIBUTION: QUARK-GLUON STRING MODEL

Charged-particle multiplicity and transverse momentum distributions in pp collisions at **0.2–14 TeV** within the MC QGSM based on Gribov's Reggeon field theory were studied and the special attention was given to the origin of violation of the KNO scaling

Diagrams of particle production processes included in the modeling of pp interactions at ultra-relativistic energies $\sigma_{pp}^{inel} = \sigma_P + \sigma_{SD} + \sigma_{DD}$, where σ_P is the cross section for the multi-chain processes described by the **cylinder diagram & diagrams with multi-Pomeron scattering (a)**, σ_{SD} is the cross section of **single-diffractive** processes represented by the diagrams with small (b) and large (c) mass excitation, corresponding to the triple-Reggeon and triple-Pomeron limit, respectively, and σ_{DD} is the cross section of **double-diffractive** process shown by the diagram in (d)



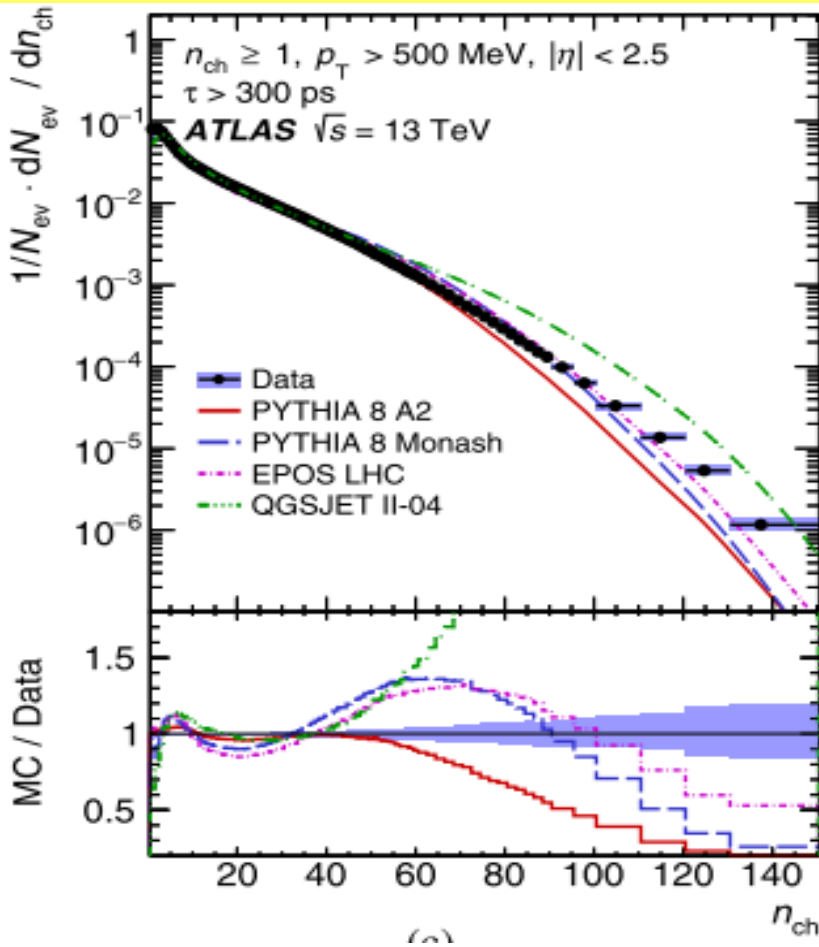
Charged-particle multiplicity distributions in $|\eta| < 0.5$, $|\eta| < 1$, $|\eta| < 1.3$, obtained in QGSM for pp collisions at 0.9, 2.36 TeV

- ❑ The comparison of the QGSM calculations with the **ALICE data**.
- ❑ In this figure the multiplicity distributions of charged particles calculated in NSD pp events **at 0.9 and 2.36 TeV** in three central pseudorapidity intervals are plotted onto the experimental data.
- ❑ **The agreement** between the model results and the data **is good**.
- ❑ The QGSM demonstrates a kind of a **wavy structure mentioned**. Such a wavy behavior in the model can be linked to processes going via **the many-Pomeron exchanges**

1. A.B. Kaidalov, K.A.Ter-Martirosyan, PLB 117 (1982)
2. N.S.Amelin, L.V.Bravina., Sov. J. Nucl. Phys. 51 (1990) 133
3. N.S.Amelin, E.F.Staubo, L.P.Csernai, PRD 46 (1992) 4873
4. J.Bleibel, L.V.Bravina, A.B.Kaidalov, E.E.Zabrodin, *How many of the scaling trends in pp collisions will be violated at 14 TeV? – Predictions from Monte Carlo quark-gluon string model*, Phys. Rev. D 93 (2016) 114012;
5. L.V.Bravina and E.E.Zabrodin, *Scaling trends in proton-proton collisions from SPS to LHC in quark-gluon string model*, J. Phys. Conf. Ser. 668 (2016) 012045

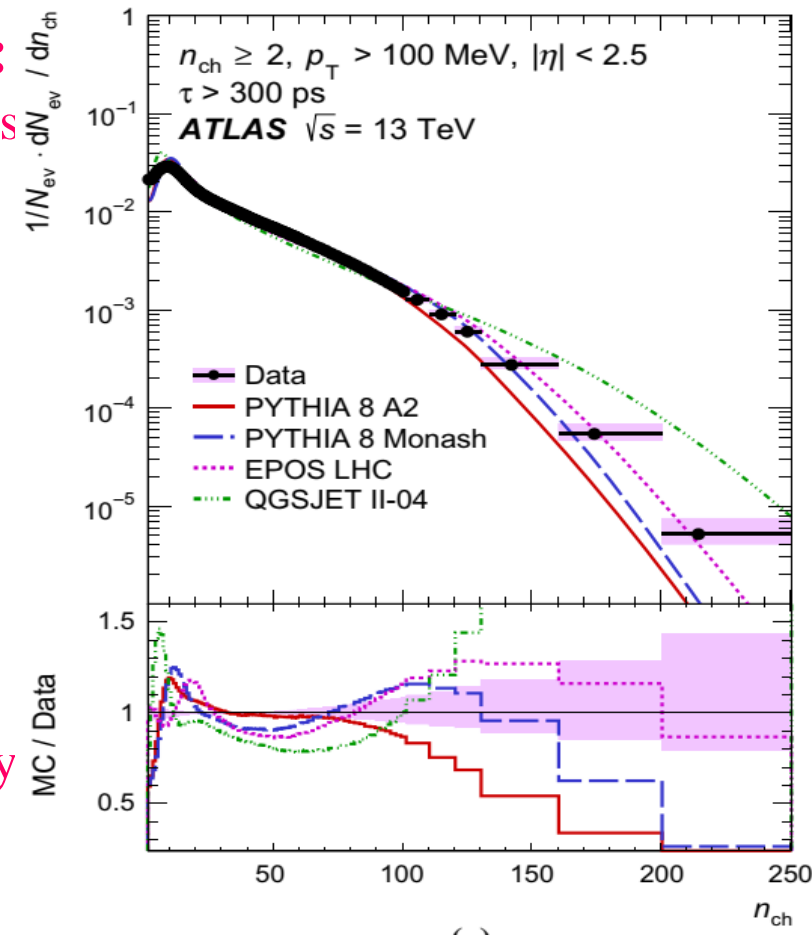
09/03/2023

Yuri Kulchitsky, JINR



For $p_{\text{T}} > 500 \text{ MeV}$ & $p_{\text{T}} > 100 \text{ MeV}$:

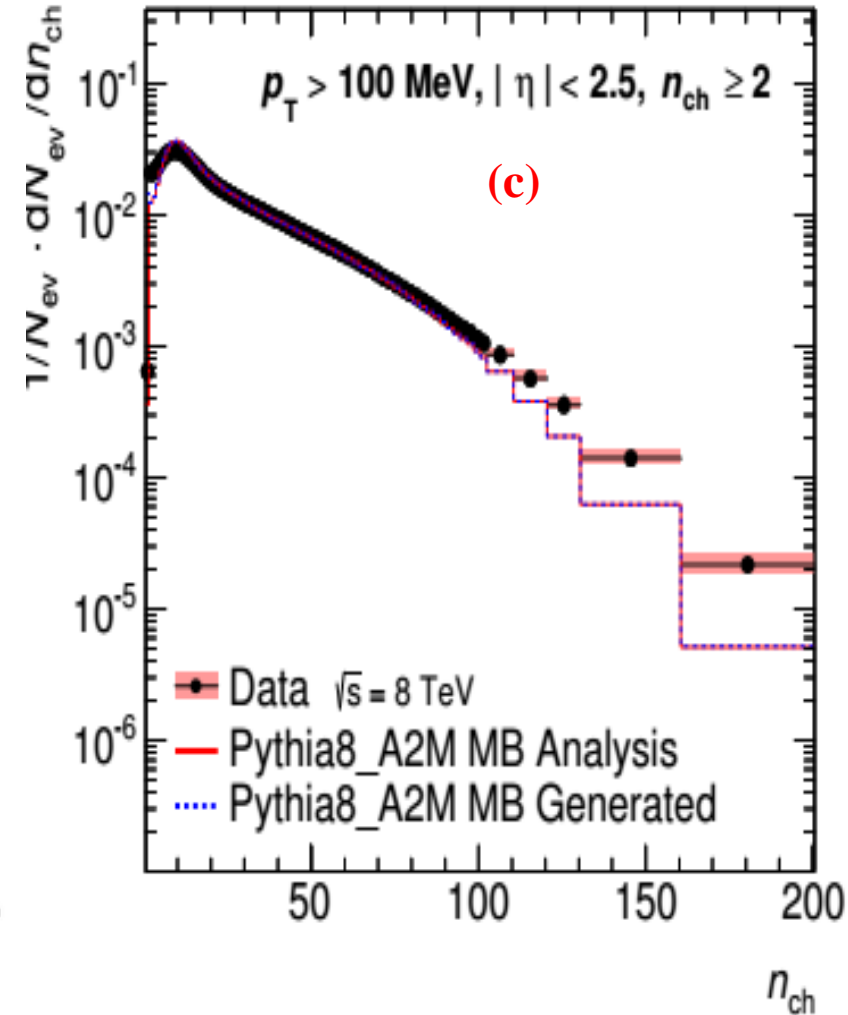
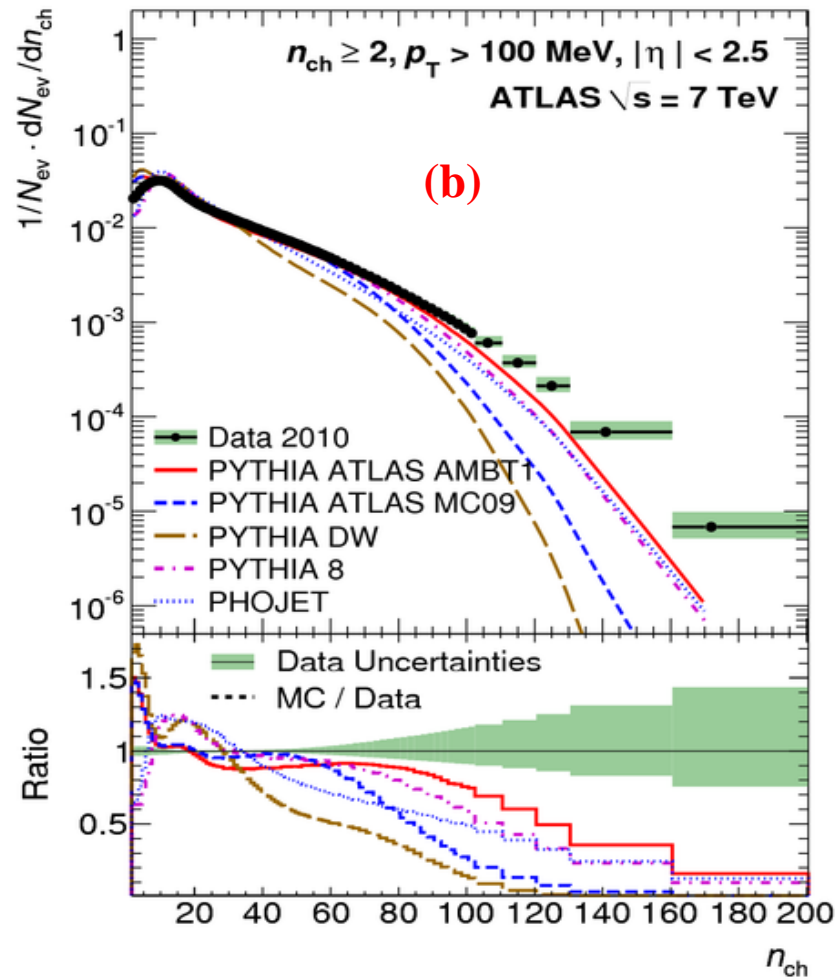
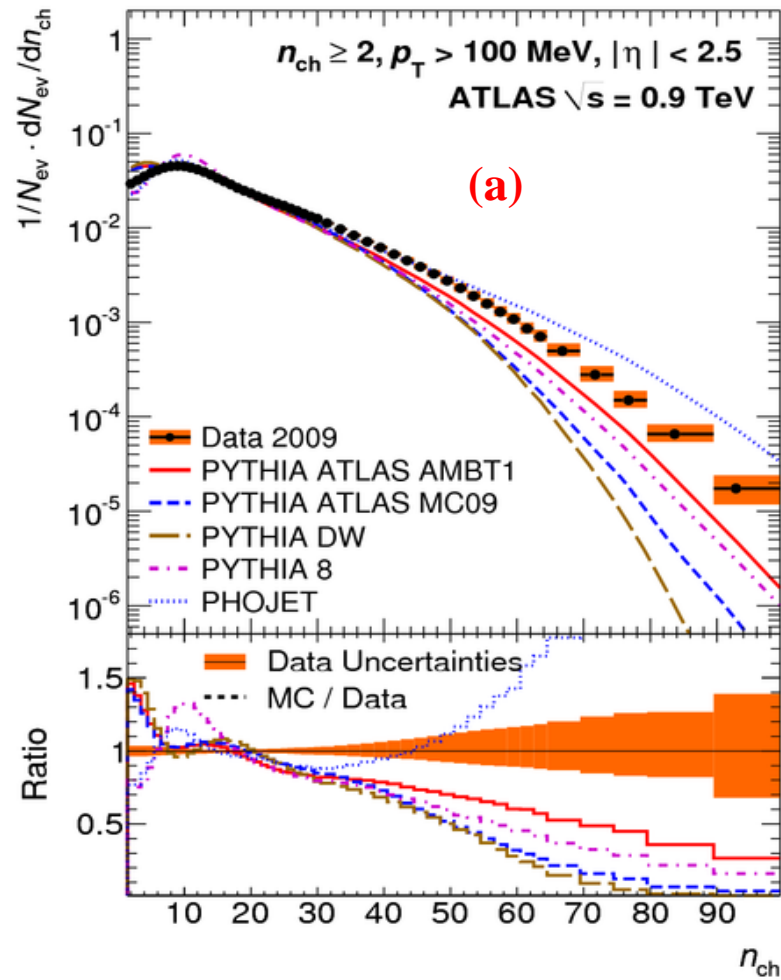
- The form of the measured distribution is reproduced reasonably by all models.
- **PYTHIA 8 A2** describes the data well for middle n_{ch} but underestimates it for higher
- For middle n_{ch} **PYTHIA 8 MONASH, EPOS, QGSJET-II** underestimate the data by up to 10-20%.
- **PYTHIA 8 MONASH, EPOS** overestimate the data for higher n_{ch} and drop below the measurement in the very high- n_{ch} region
- **QGSJET-II** overestimates the data



Primary charged-particle multiplicities versus n_{ch} for events with $n_{\text{ch}} \geq 1, p_{\text{T}} > 500 \text{ MeV}$ & $n_{\text{ch}} \geq 2, p_{\text{T}} > 100 \text{ MeV}$ in $|\eta| < 2.5$. The high- n_{ch} region has significant contributions from events with numerous MPI.

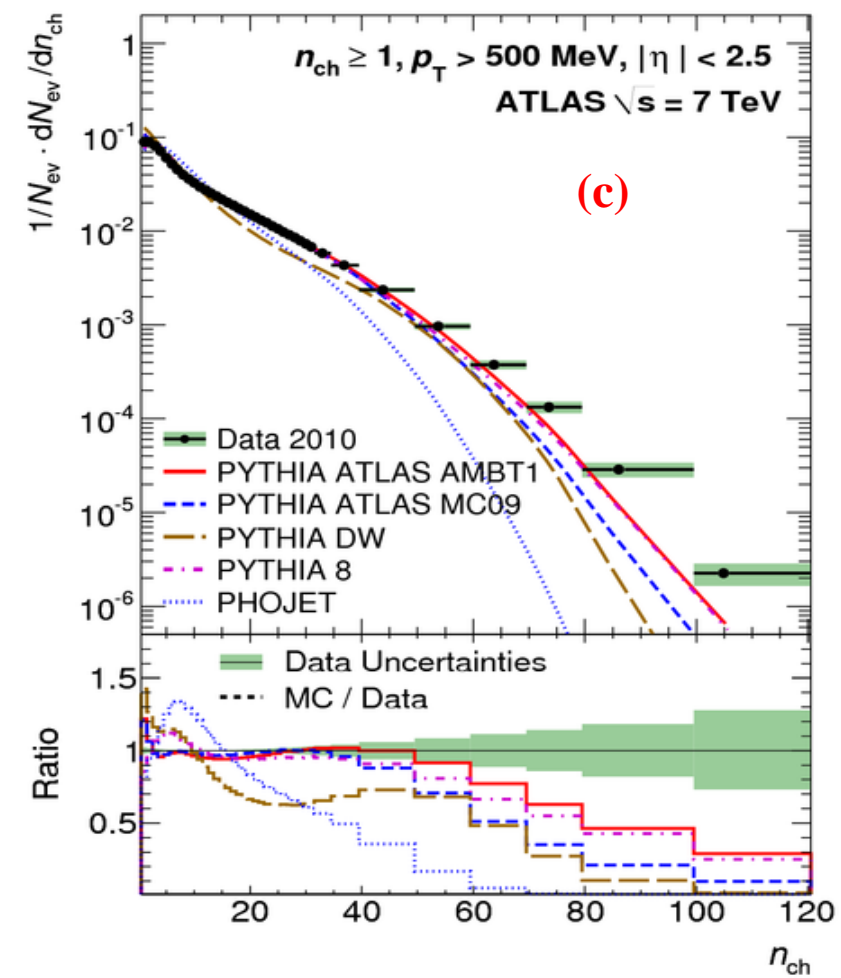
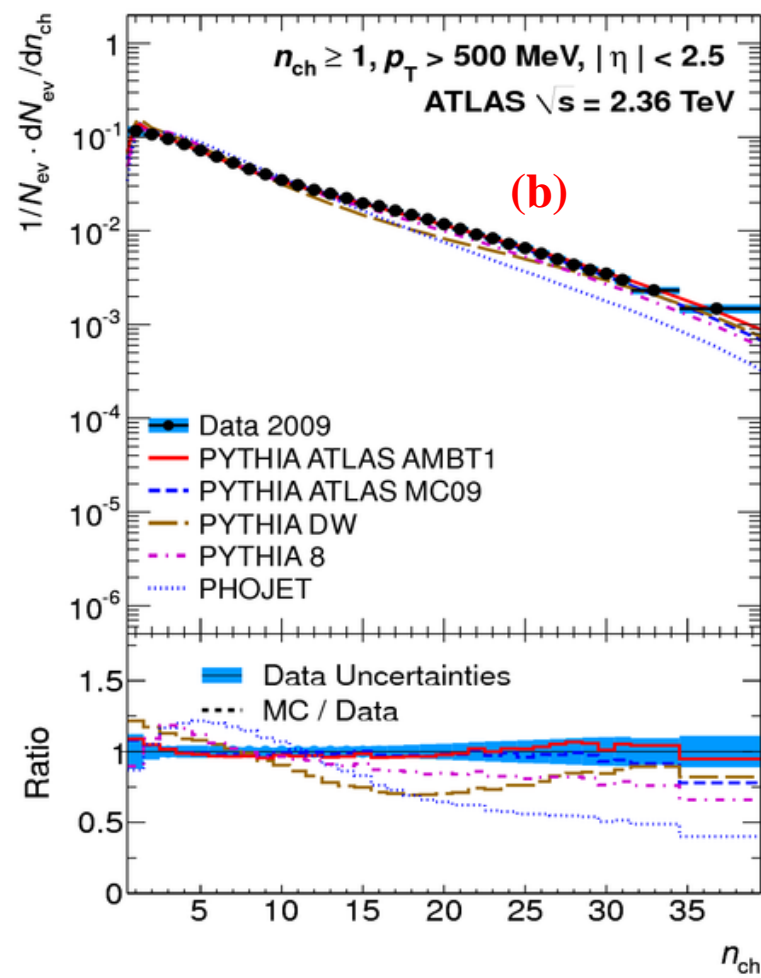
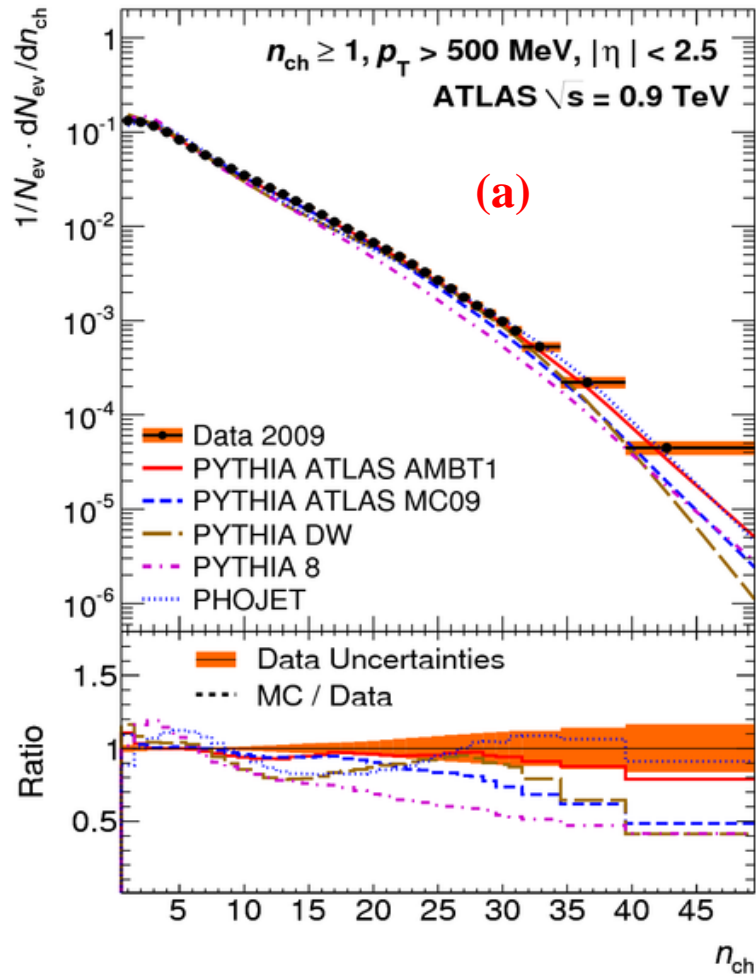
Colour reconnection: strings from independent parton interactions do not independently produce hadrons, but fuse before hadronization

CHARGED-PARTICLE MULTIPLICITIES DISTRIBUTION: $p_T > 100$ MEV



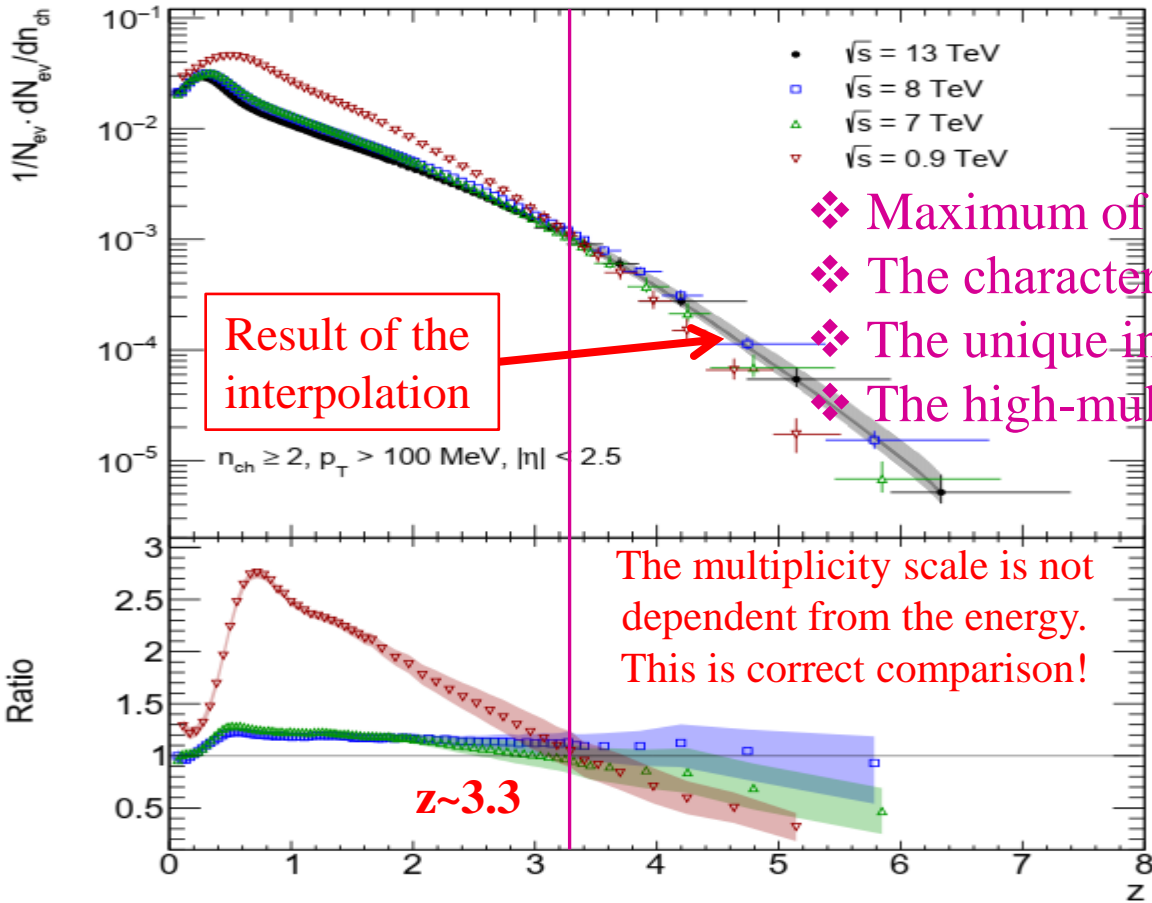
Charged-particle multiplicities distribution for events with $n_{ch} \geq 2, p_T > 100$ MeV and $|\eta| < 2.5$ at $\sqrt{s} = 0.9$ (a), 7 (b) and 8 TeV (c)

CHARGED-PARTICLE MULTIPLICITIES DISTRIBUTION: $p_T > 500$ MEV

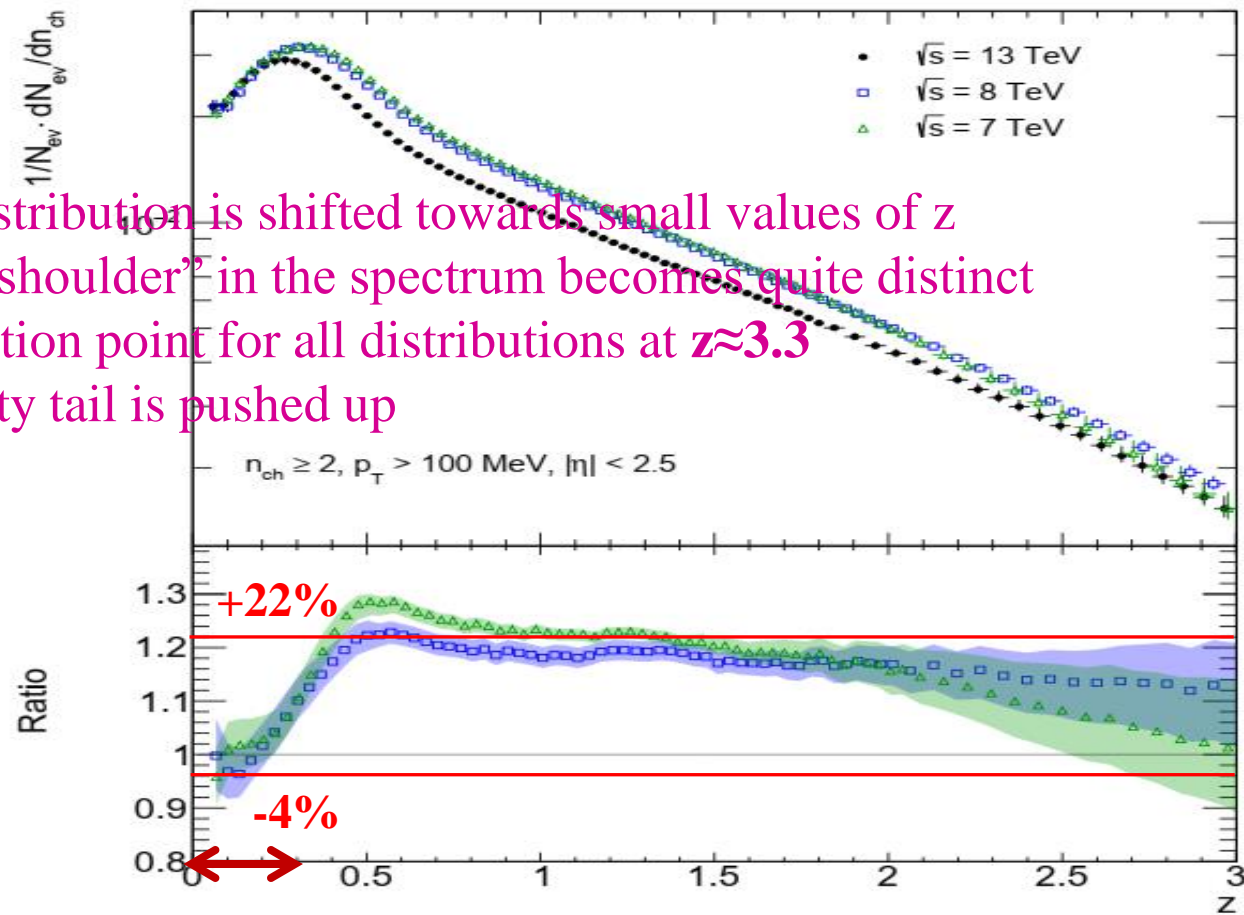


Charged-particle multiplicities distribution for events with $n_{ch} \geq 1$, $p_T > 500$ MeV and $|\eta| < 2.5$ at $\sqrt{s} = 0.9$ (a), 2.36 (b) and 7 TeV (c)

CHARGED-PARTICLE MULTIPLICITIES DISTRIBUTION: ATLAS, $P_T > 100$ MEV



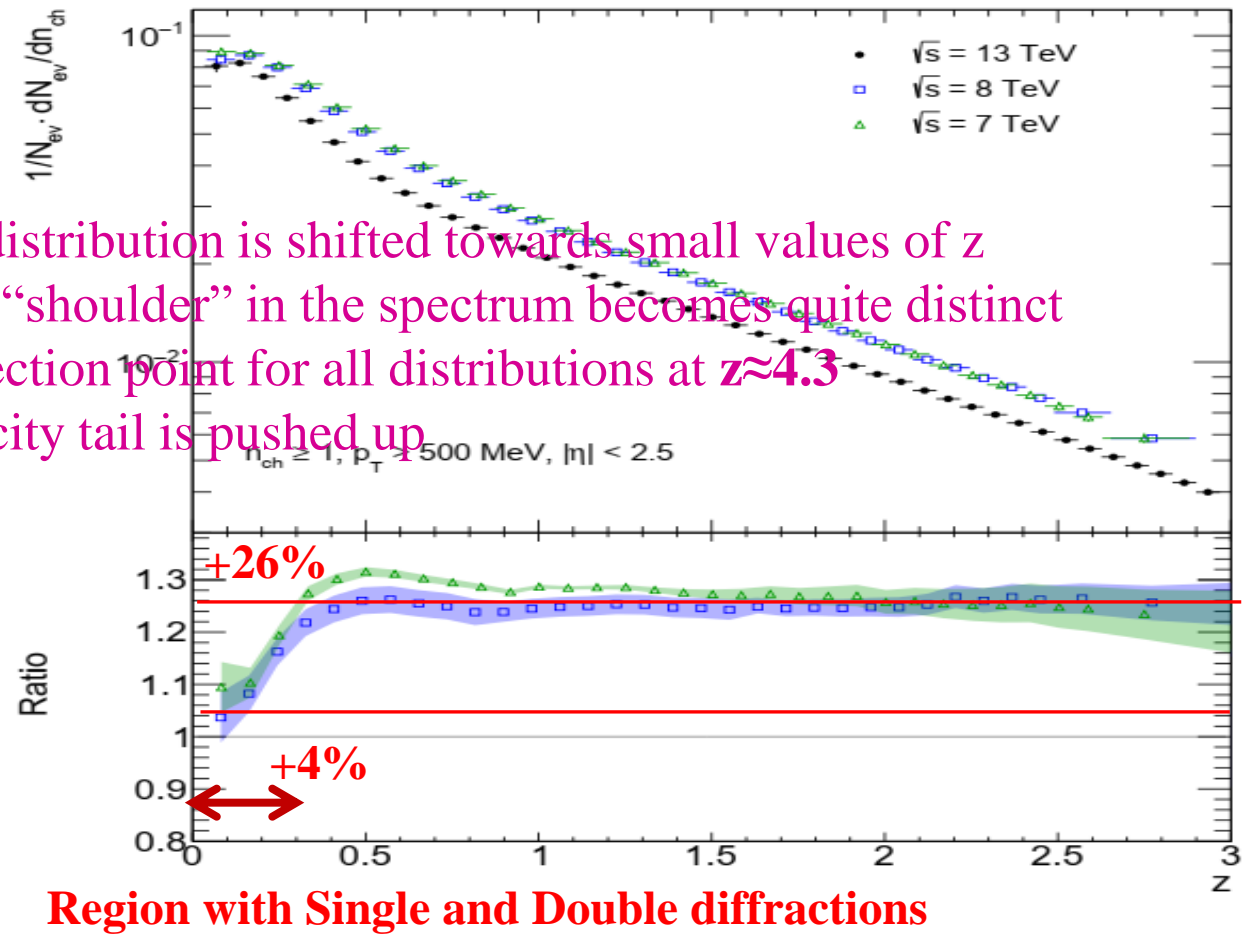
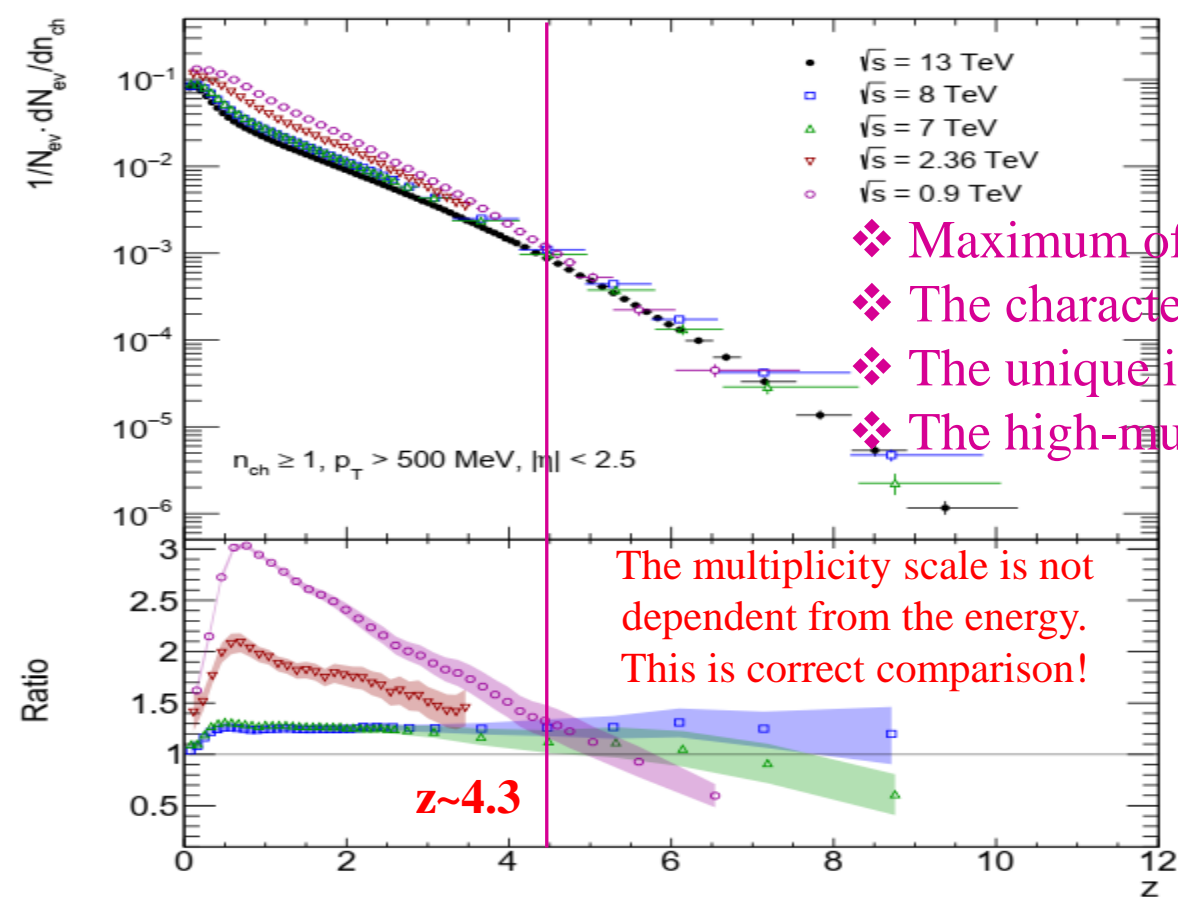
- ❖ Maximum of the distribution is shifted towards small values of z
- ❖ The characteristic “shoulder” in the spectrum becomes quite distinct
- ❖ The unique intersection point for all distributions at $z \sim 3.3$
- ❖ The high-multiplicity tail is pushed up



Region with Single and Double diffractions

- Primary charged-particle multiplicity distributions as a function of a normalized multiplicity for events with $n_{ch} \geq 2$, $p_T > 100 \text{ MeV}$, $|\eta| < 2.5$ measurement by ATLAS at the $\sqrt{s} = 0.9, 7, 8, 13 \text{ TeV}$ for the complete and zoom regions.
- The ratios to the distribution at 13 TeV are shown. Ratios and their uncertainties were obtained by interpolating the distribution at 13 TeV to z step at different \sqrt{s} . Bands represent the total uncertainties of ratios.

CHARGED-PARTICLE MULTIPLICITIES DISTRIBUTION: ATLAS, $P_T > 500$ MEV

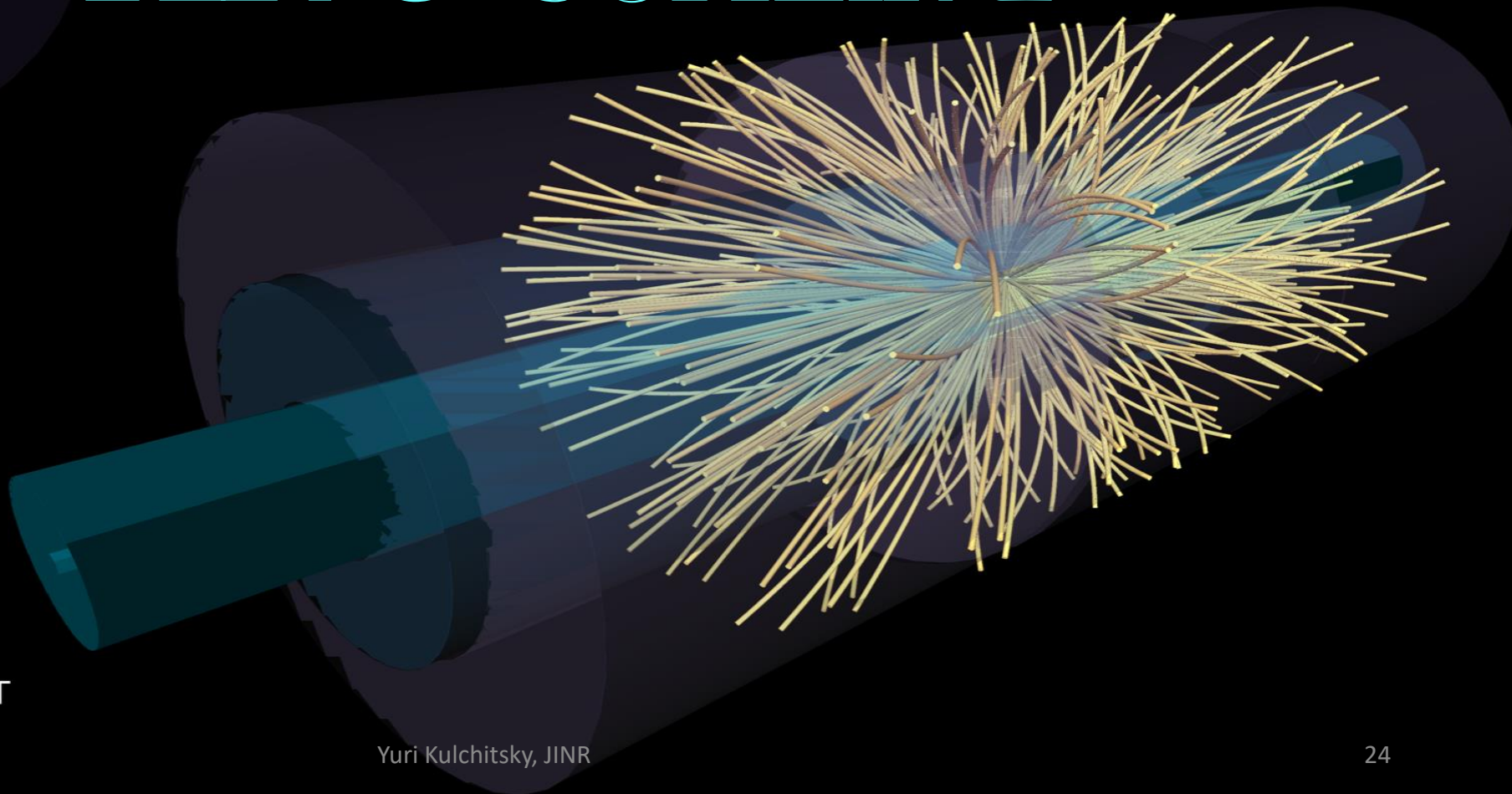
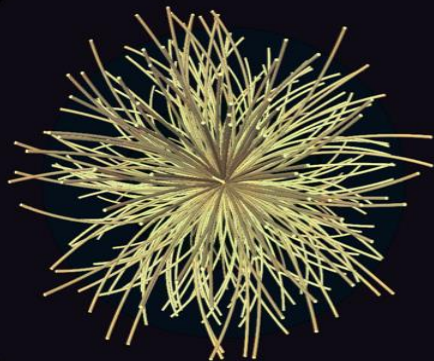


- Primary charged-particle multiplicity distributions as a function of a normalized multiplicity for events with $n_{ch} \geq 2$, $p_T > 500$ MeV, $|\eta| < 2.5$ measurement by ATLAS at the $\sqrt{s} = 0.9, 7, 8, 13$ TeV for the complete and zoom regions.
- The ratios to the distribution at 13 TeV are shown. Ratios and their uncertainties were obtained by interpolating the distribution at 13 TeV to z step at different \sqrt{s} . Bands represent the total uncertainties of ratios.

319 reconstructed charged-particles

The shown tracks are from a single vertex and have $p_T > 0.4$ GeV

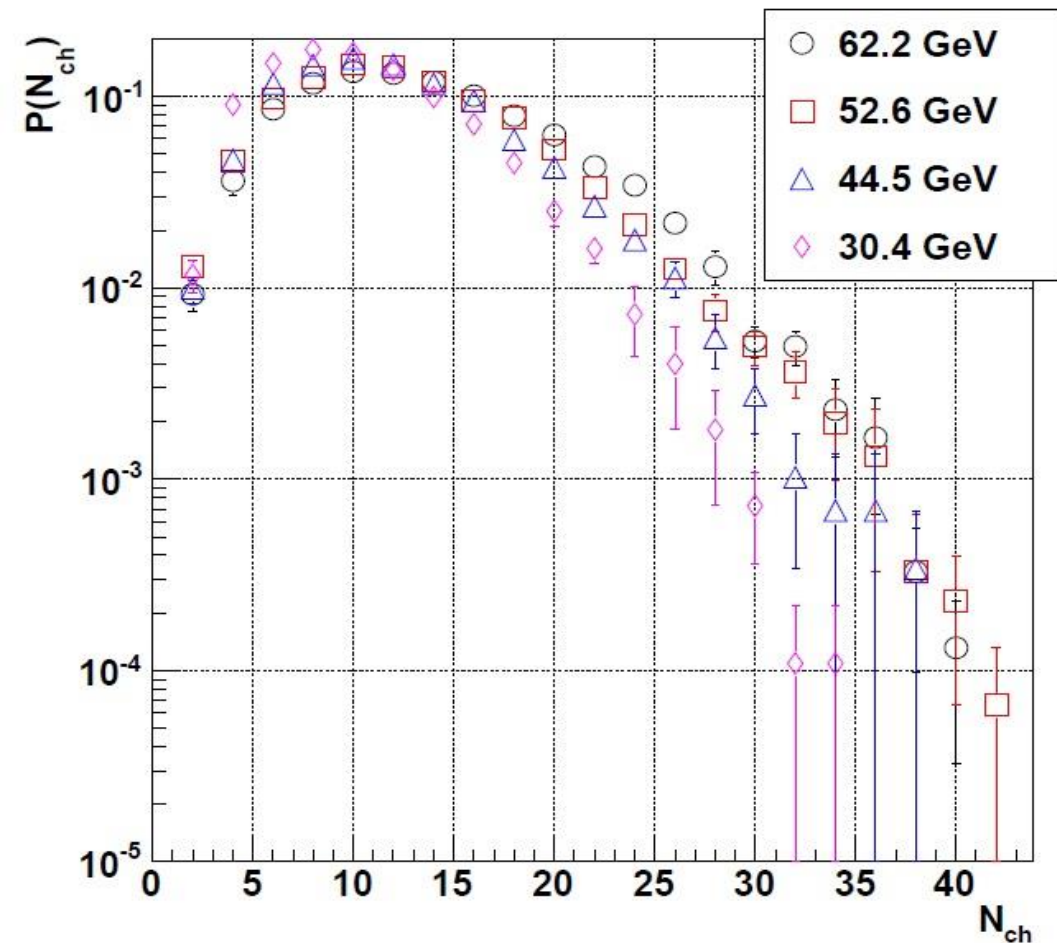
KN0 SCALING



Run: 312837
Event: 135456971
2016-11-14 07:42:28 CEST

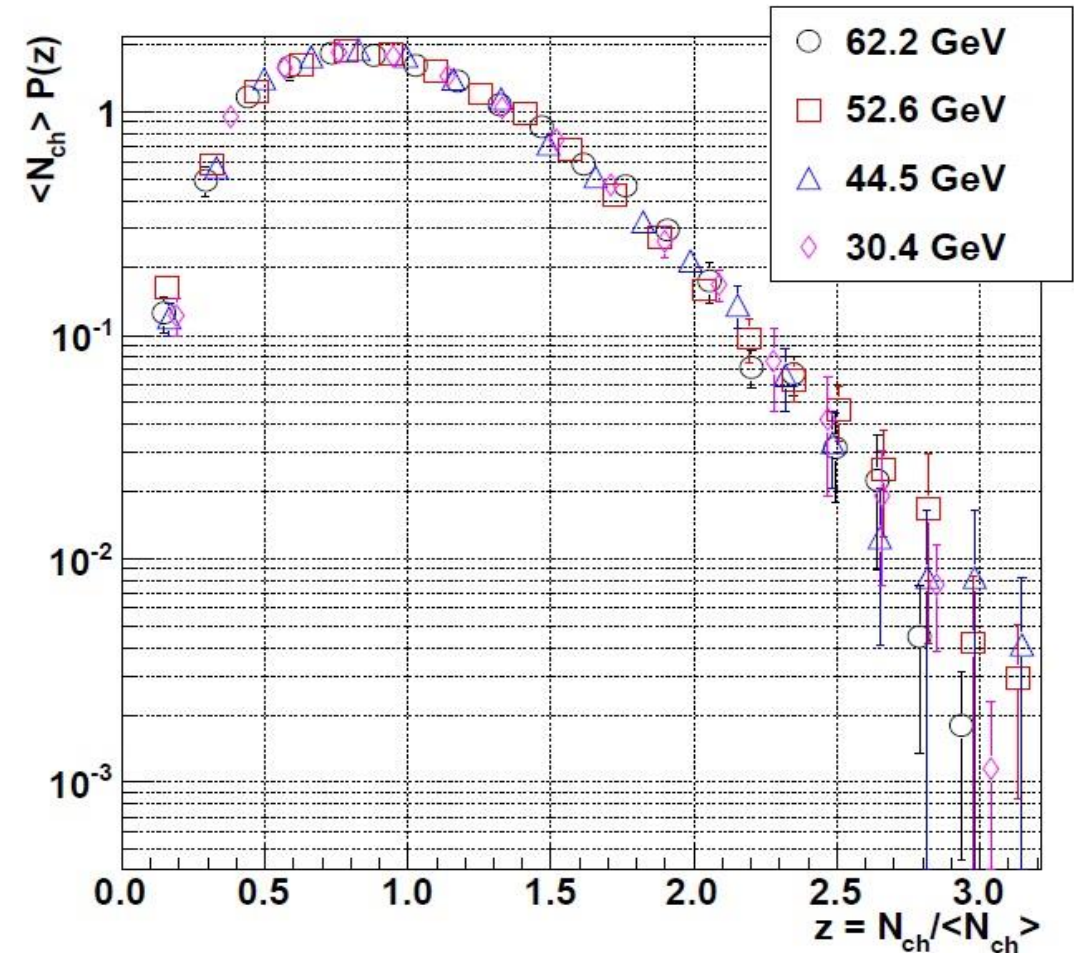
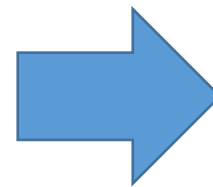
Evolution of the charged particle multiplicity distribution in proton-proton collisions $P(N_{ch})$ with \sqrt{s} follows KNO-scaling with

Scaling variable $z = \frac{N_{ch}}{\langle N_{ch} \rangle}$ and $P(N_{ch}) \langle N_{ch} \rangle = \Psi(z)$ Energy independent function

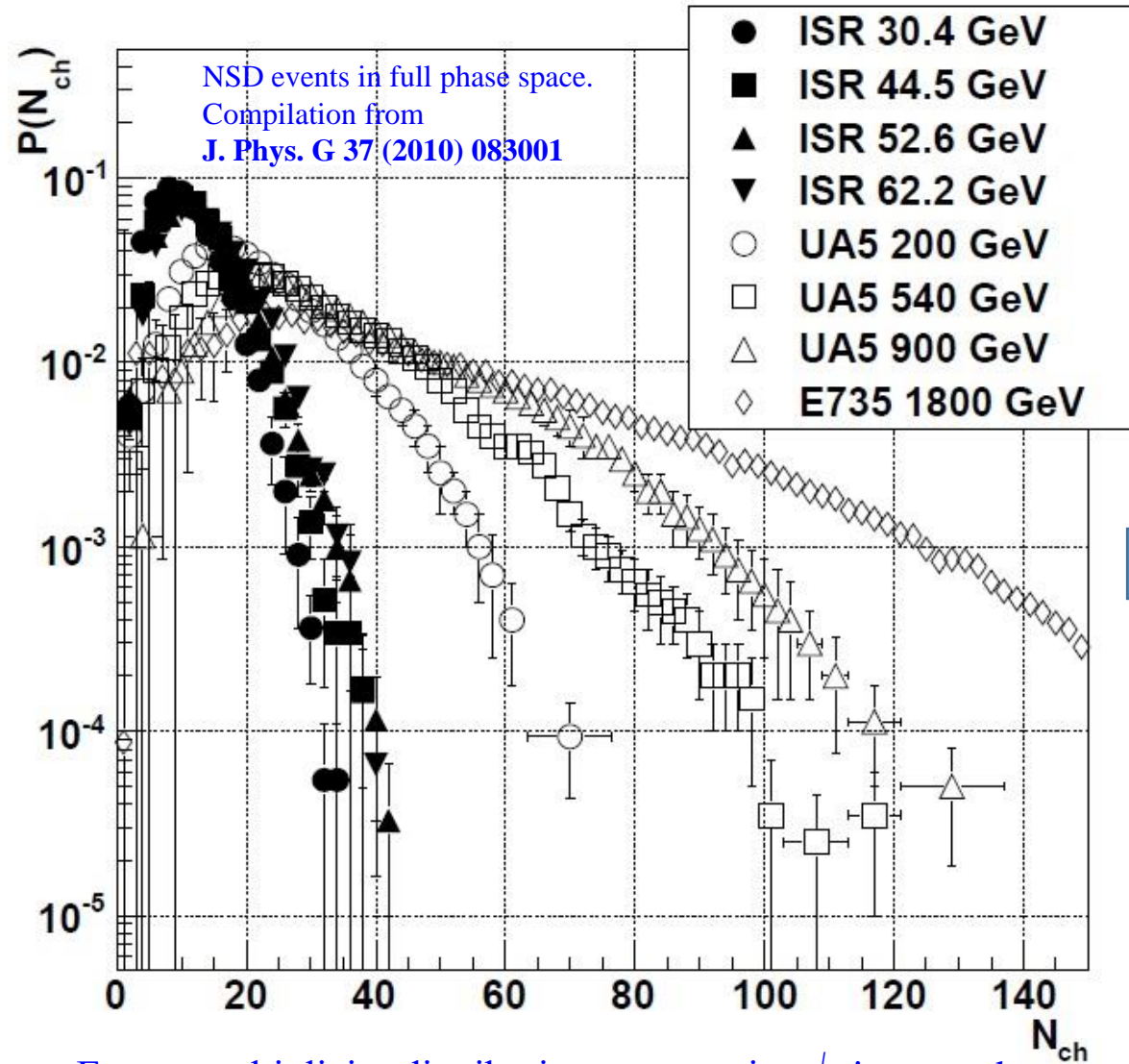


Multiplicity distributions

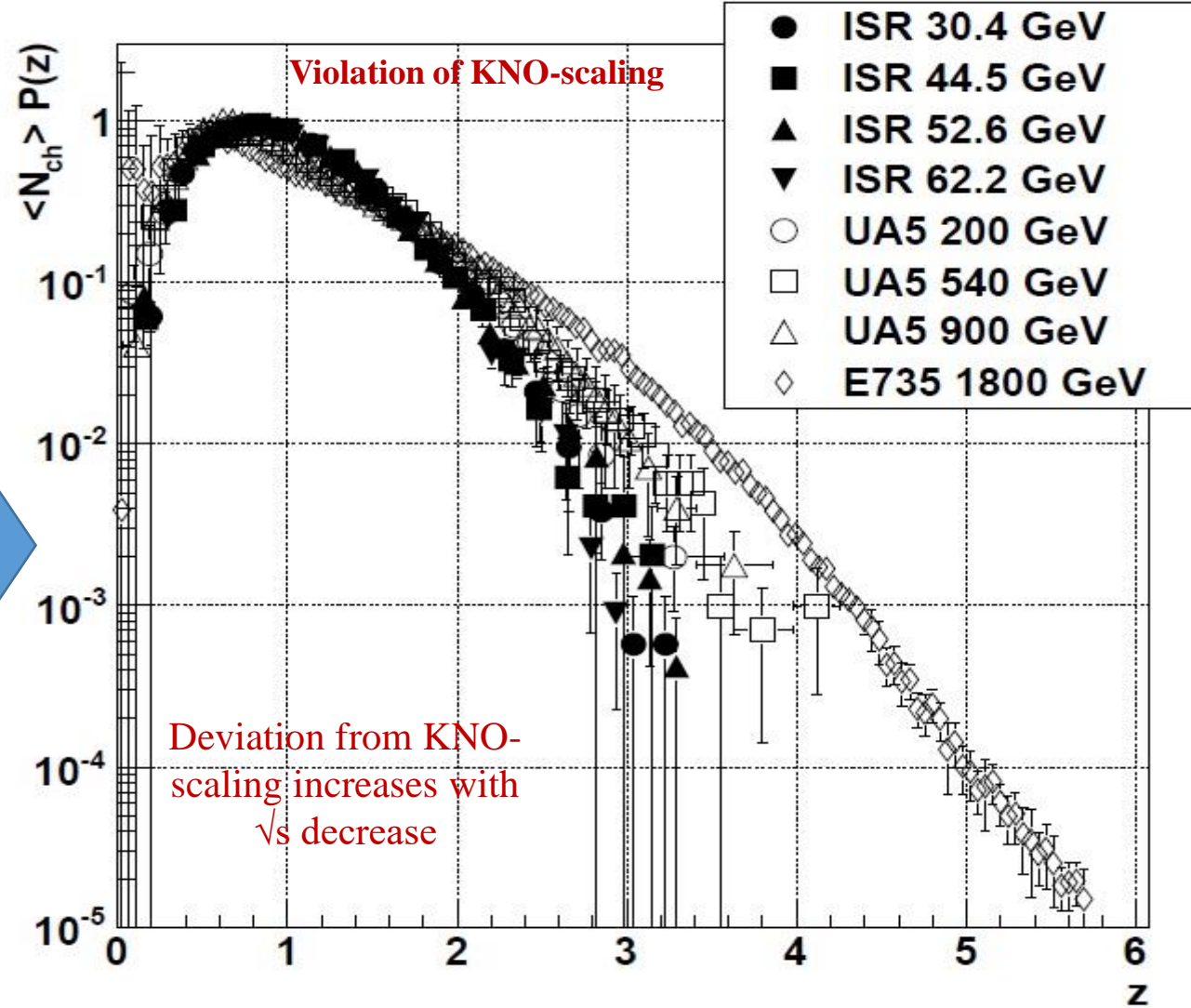
09/03/2023



KNO distributions

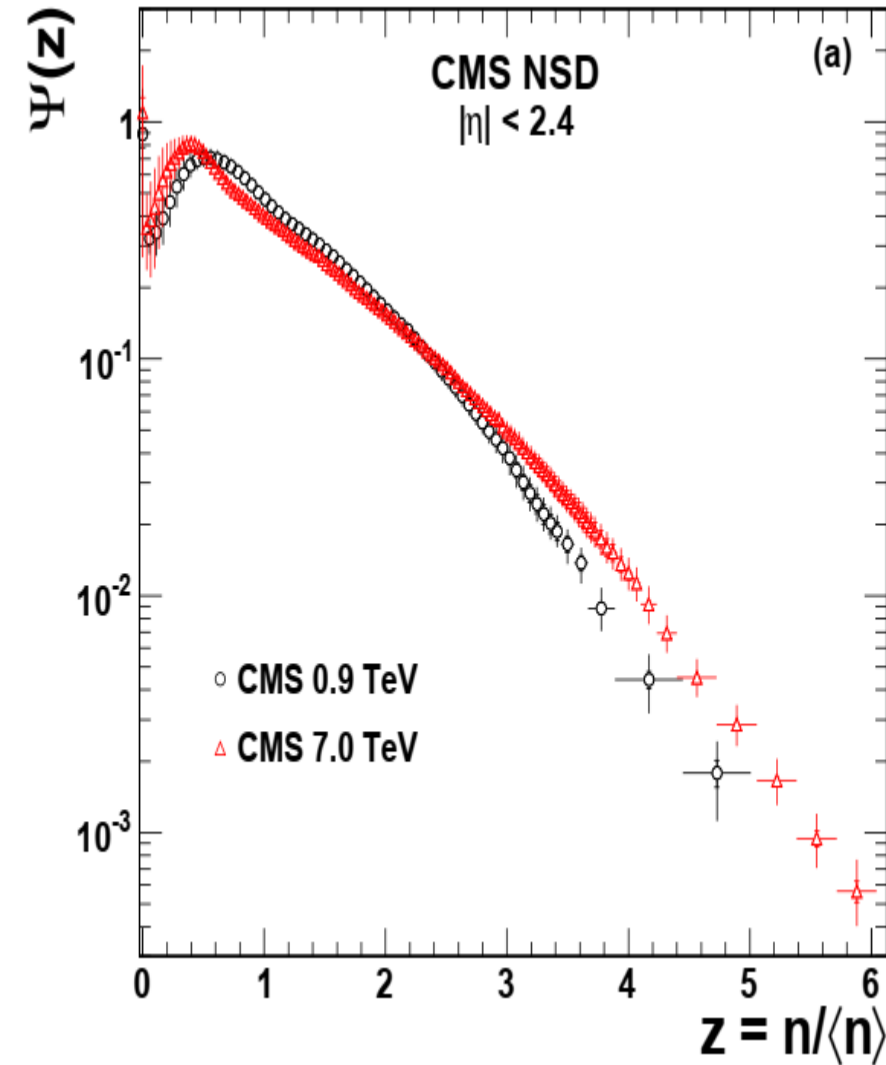


Events multiplicity distributions at energies \sqrt{s} in pp and p anti-p collisions



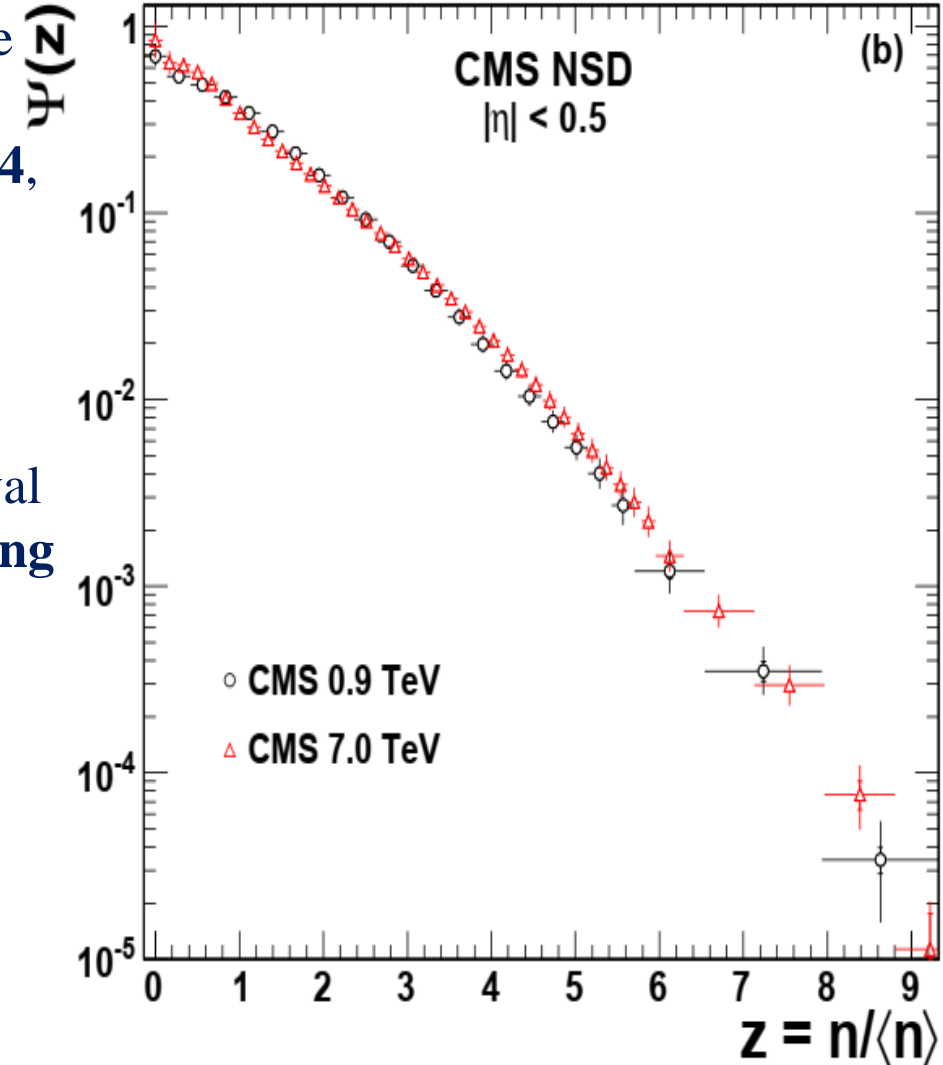
KNO function distributions at energies \sqrt{s} in pp and p anti-p collisions

Can be interpreted as a consequence of particle production through (soft) MPI

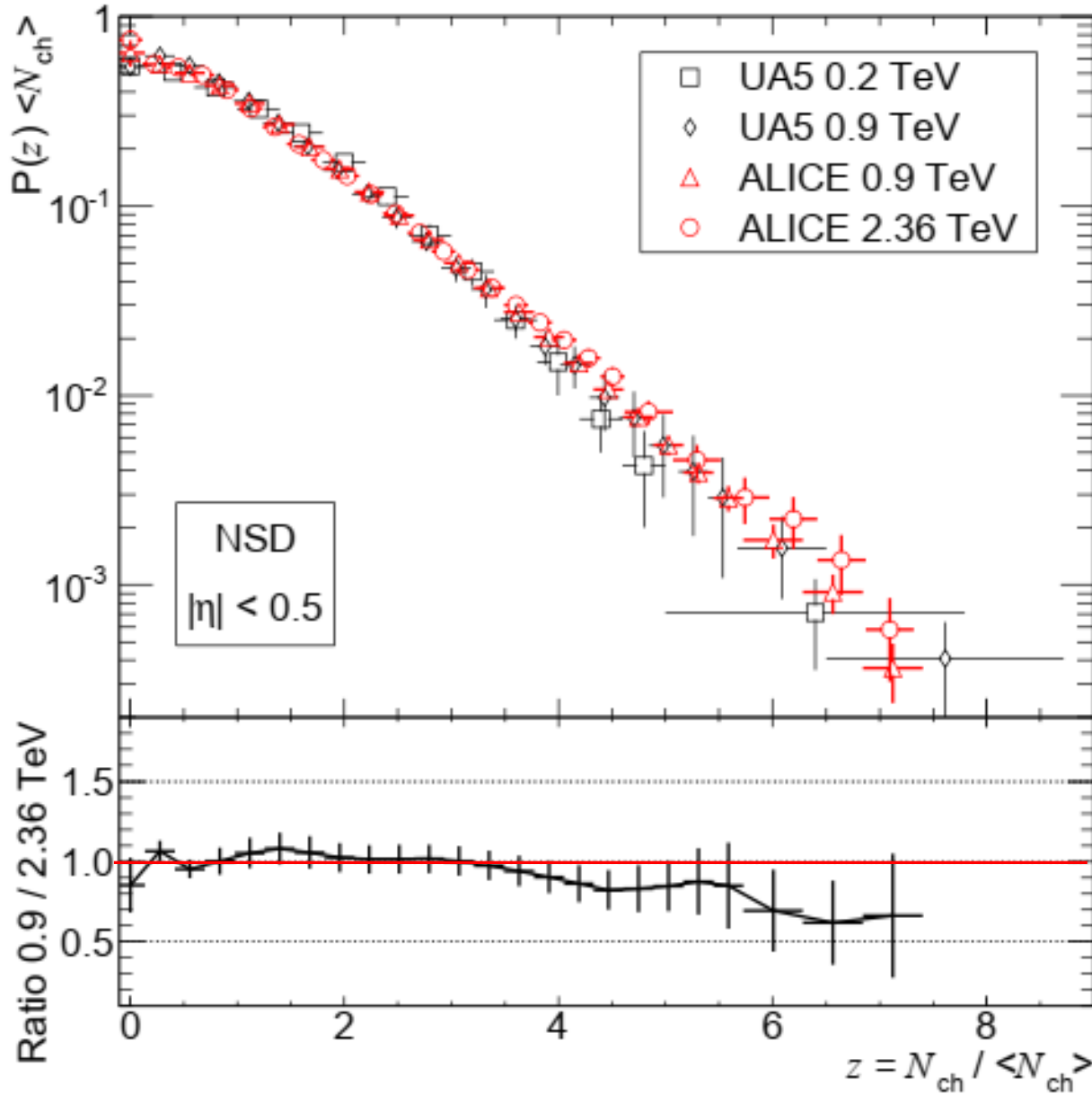


The multiplicity distributions are shown in KNO form for a large pseudorapidity interval of $|\eta| < 2.4$, where we observe

- a **strong violation of KNO scaling** between **0.9 and 7 TeV**, and for
- a small pseudorapidity interval of $|\eta| < 0.5$, where **KNO scaling holds**.
- Scaling is a characteristic property of the multiplicity distribution in cascade processes of a single jet with self-similar branchings and fixed coupling constant.



□ The charged hadron multiplicity distributions in KNO form at **0.9 & 7 TeV** in two pseudorapidity intervals: $|\eta| < 2.4$ and $|\eta| < 0.5$



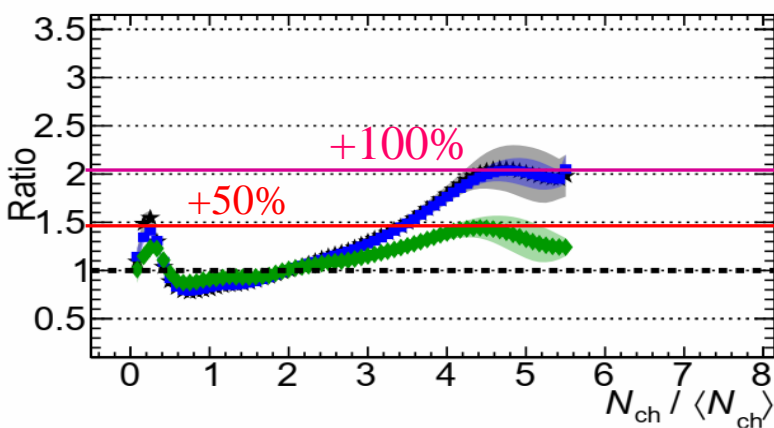
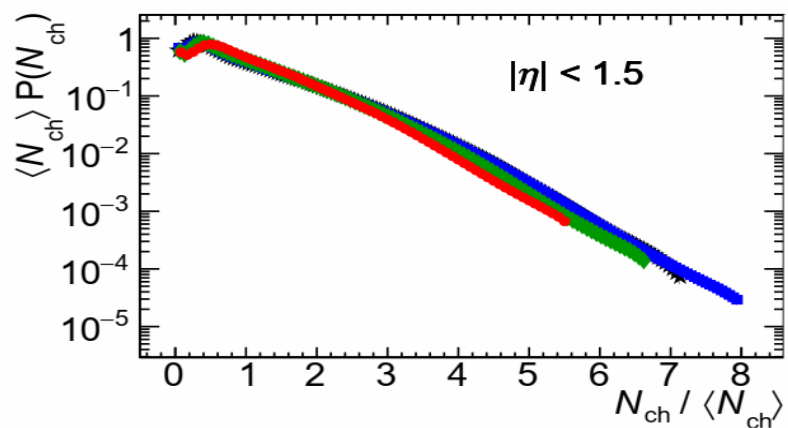
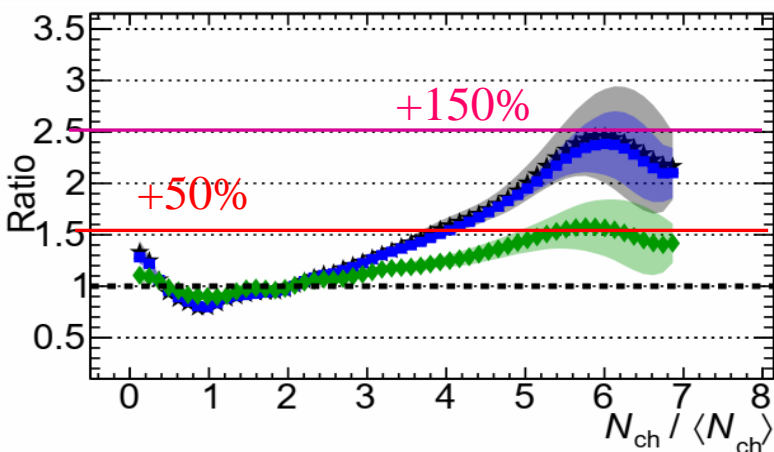
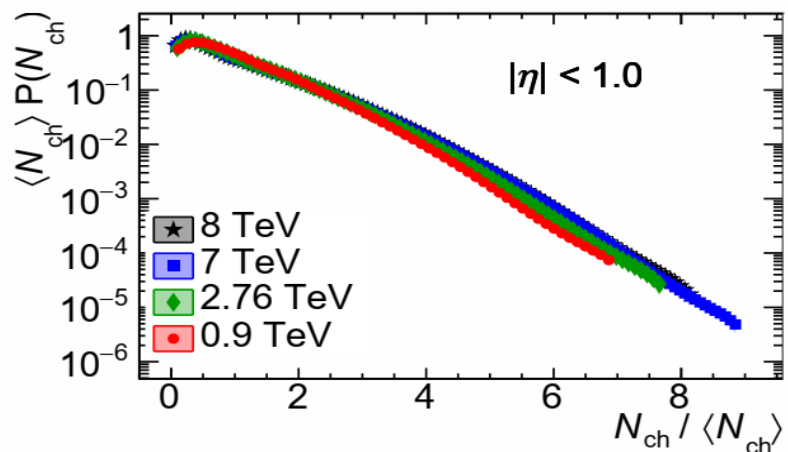
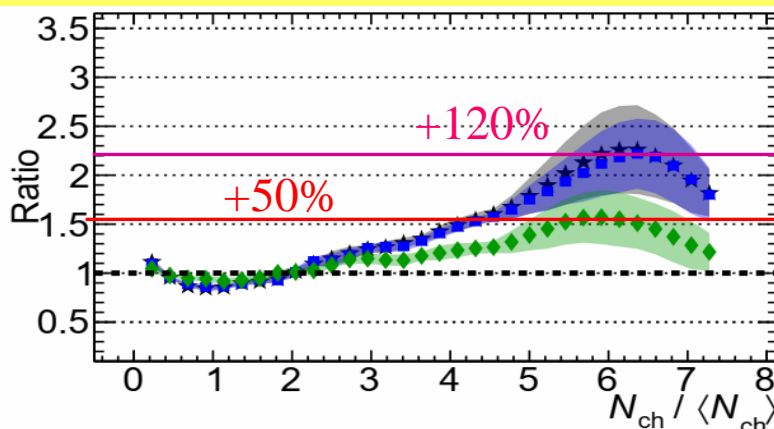
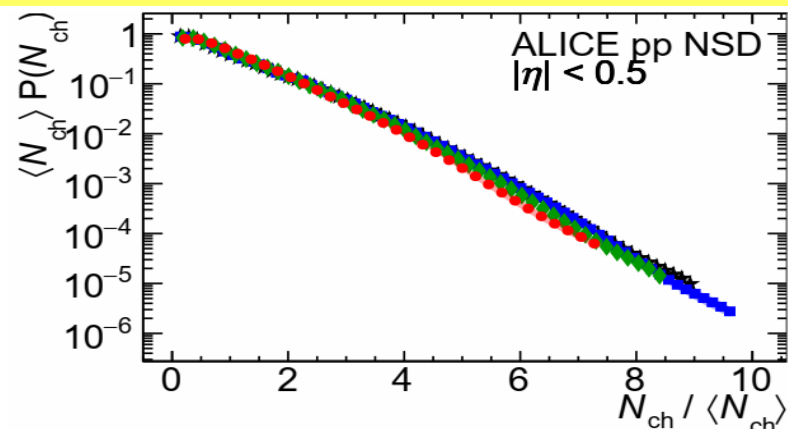
The shape evolution of the multiplicity distributions with energy was studied in terms of KNO-scaling variables

Comparison of multiplicity distributions in KNO variables measured by **UA5 Collaboration** in proton-antiproton collisions at $\sqrt{s} = 0.2$ and 0.9 TeV, and by **ALICE Collaboration** at $\sqrt{s} = 0.9$ and 2.36 TeV, for NSD events in $|\eta| < 0.5$.

In the lower part the ratio between ALICE measurements at **0.9 and 2.36 TeV** is shown. The error bars represent the combined statistical and systematic uncertainties.

- While KNO scaling gives a reasonable description of the data from **0.2 to 2.36 TeV**, the ratio between the **0.9 and 2.36 TeV** data shows a slight departure from unity above $z=4$

A slight, but only marginally significant evolution in the shape is visible in the data for $z > 4$, possibly indicating an increasing fraction of events with the highest multiplicity. This issue will be studied further using the data collected from forthcoming higher-energy runs at the LHC

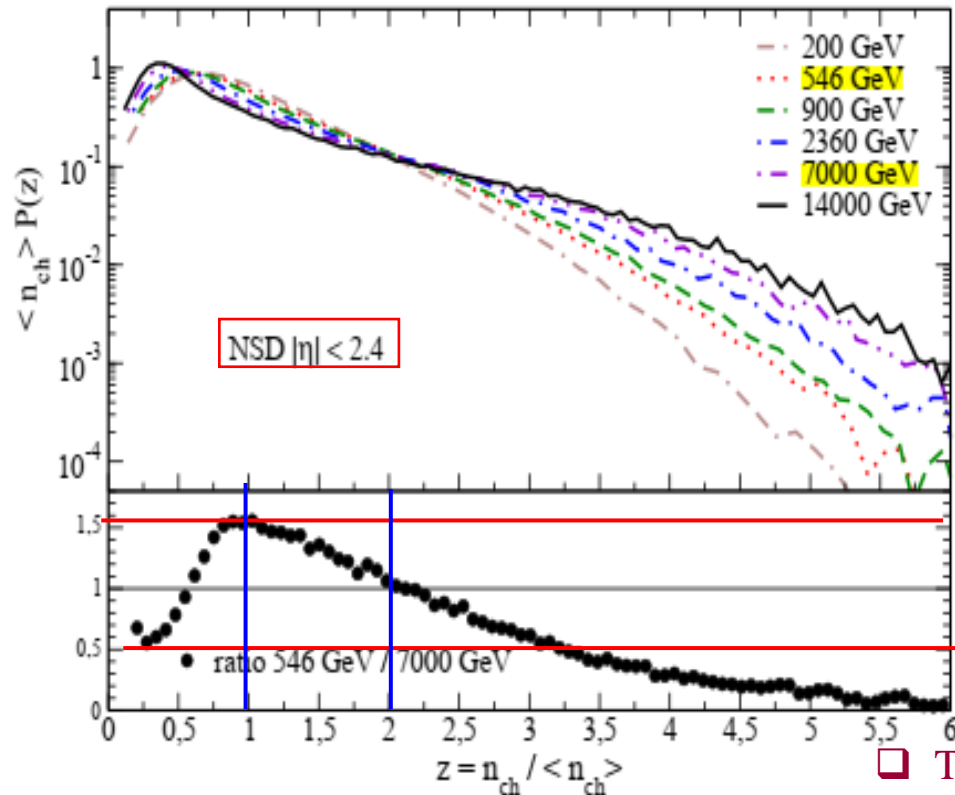


KNO-scaled distribution $\langle N_{ch} \rangle P(N_{ch})$ vs the KNO variable $N_{ch} / \langle N_{ch} \rangle$ at 0.9, 2.76, 7 and 8 TeV, for three pseudorapidity intervals: $|\eta| < 0.5$, 1.0 and 1.5. In each case, ratios to the distribution at 0.9 TeV are shown. As $N_{ch} / \langle N_{ch} \rangle$ takes different values at different energies, ratios were obtained by interpolating the KNO-scaled distributions, and uncertainties were taken from the nearest data point. Bands represent the total uncertainties

Ratios between the two highest energies and 0.9 TeV exceed the value 2 at $N_{ch} / \langle N_{ch} \rangle$ larger than 5.5, 5 and 4.5, for $|\eta| < 0.5$, for $|\eta| < 1$ and $|\eta| < 1.5$.

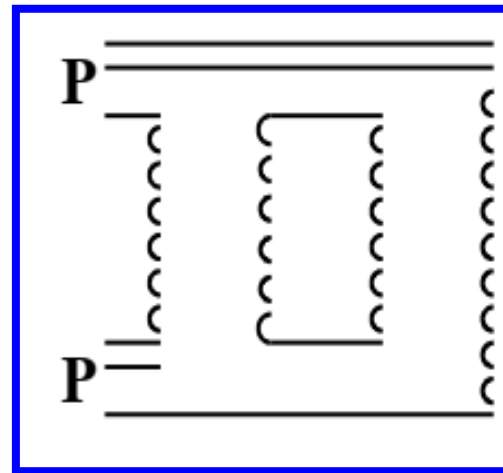
- This confirms that **KNO scaling violation increases with increasing pseudorapidity intervals.**
- The **shape of the KNO scaling violation** reflects the fact that the high-multiplicity tail of the distribution increases faster with increasing energy and with increasing pseudorapidity interval than the low ($N_{ch} \leq 20$) multiplicity.

Charged-particle multiplicity and transverse momentum distributions in pp collisions at 0.2–14 TeV within the MC QGSM based on Gribov's Reggeon field theory were studied and the special attention was given to the origin of violation of the KNO scaling

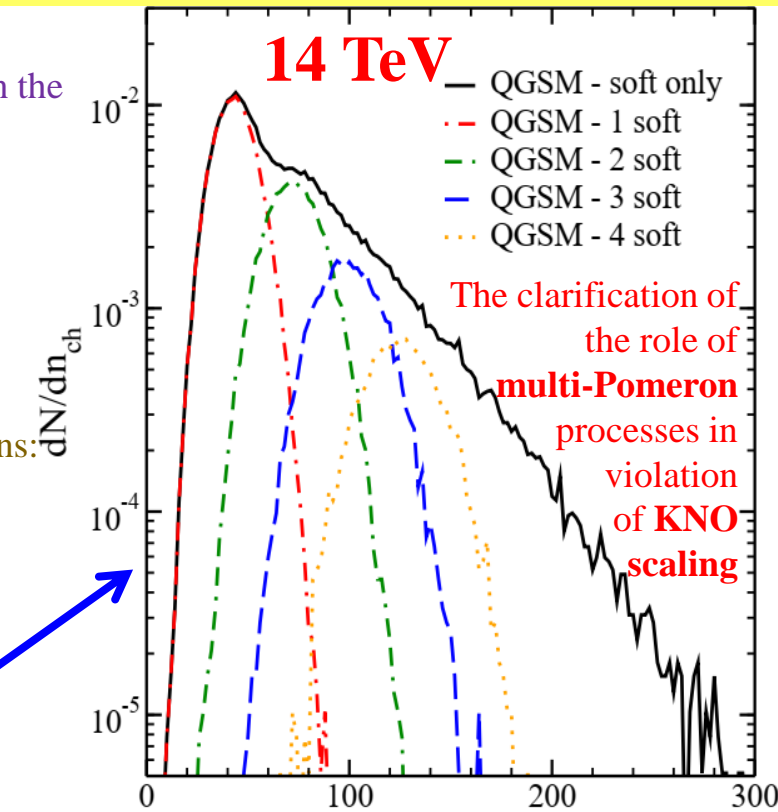


Charged particle multiplicity distributions in the KNO variables in QGSM non-diffractive pp (pp) collisions at energies 0.2, 0.564, 0.9, 2.36, 7 and 14 TeV

- The differences between the neighbor energies seem **not to be very dramatic**, the tendency in the modification of the distributions is **quite clear**.
- The **high-multiplicity tail is pushed up**
- Maximum of the distribution is shifted towards small values of $n_{ch} / \langle n_{ch} \rangle$
- The characteristic “shoulder” in the spectrum becomes quite distinct, as presented by the distribution for top energy
- The unique intersection point for all distributions: all curves cross each other at $z \approx 2.3$

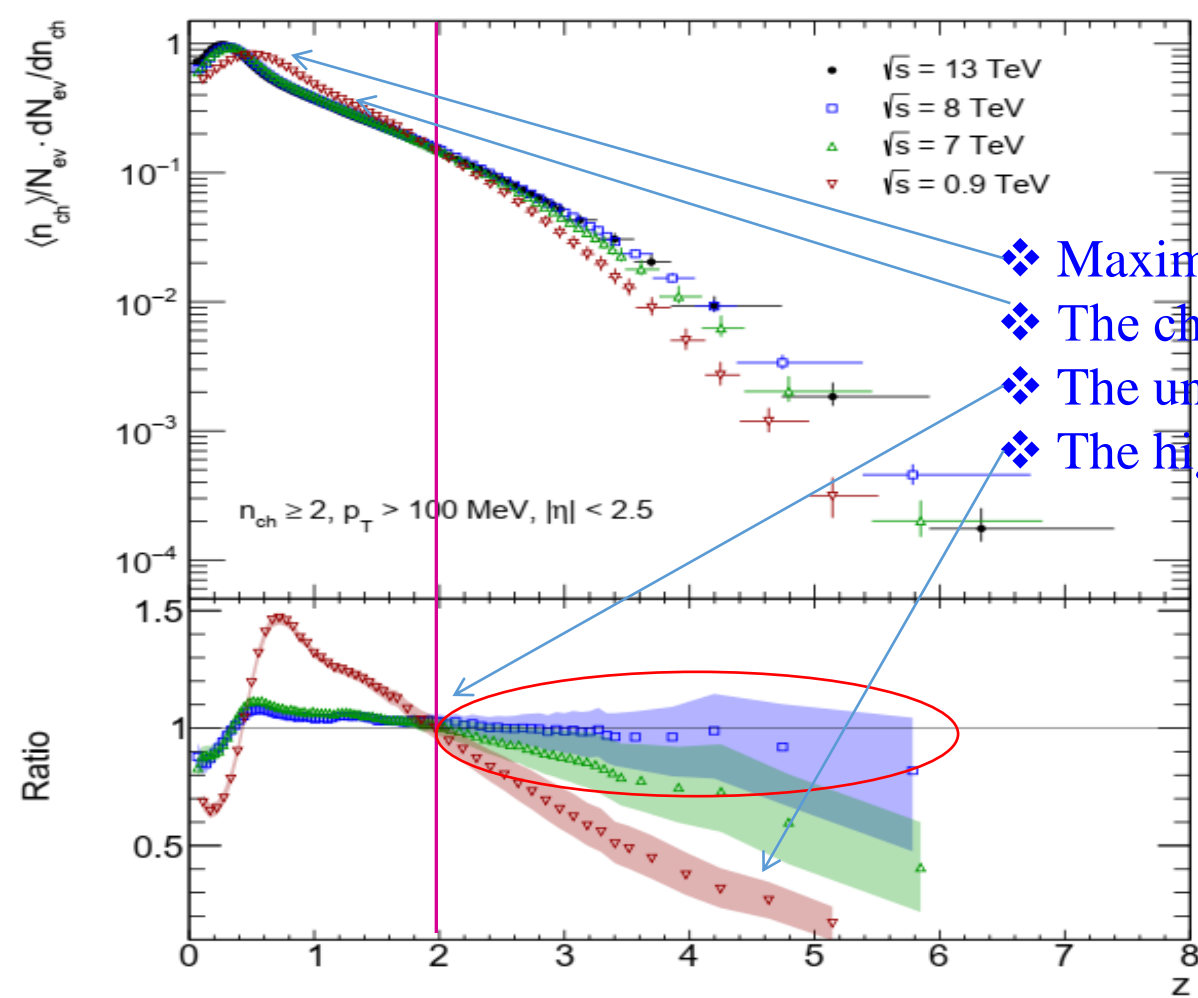


- The pronounced **peak** in the low-multiplicity interval arises solely due to single Pomeron exchange
- The maxima of distributions for **multi-Pomeron** processes are moved in the direction of high multiplicities, thus **lifting the high-multiplicity tail**.

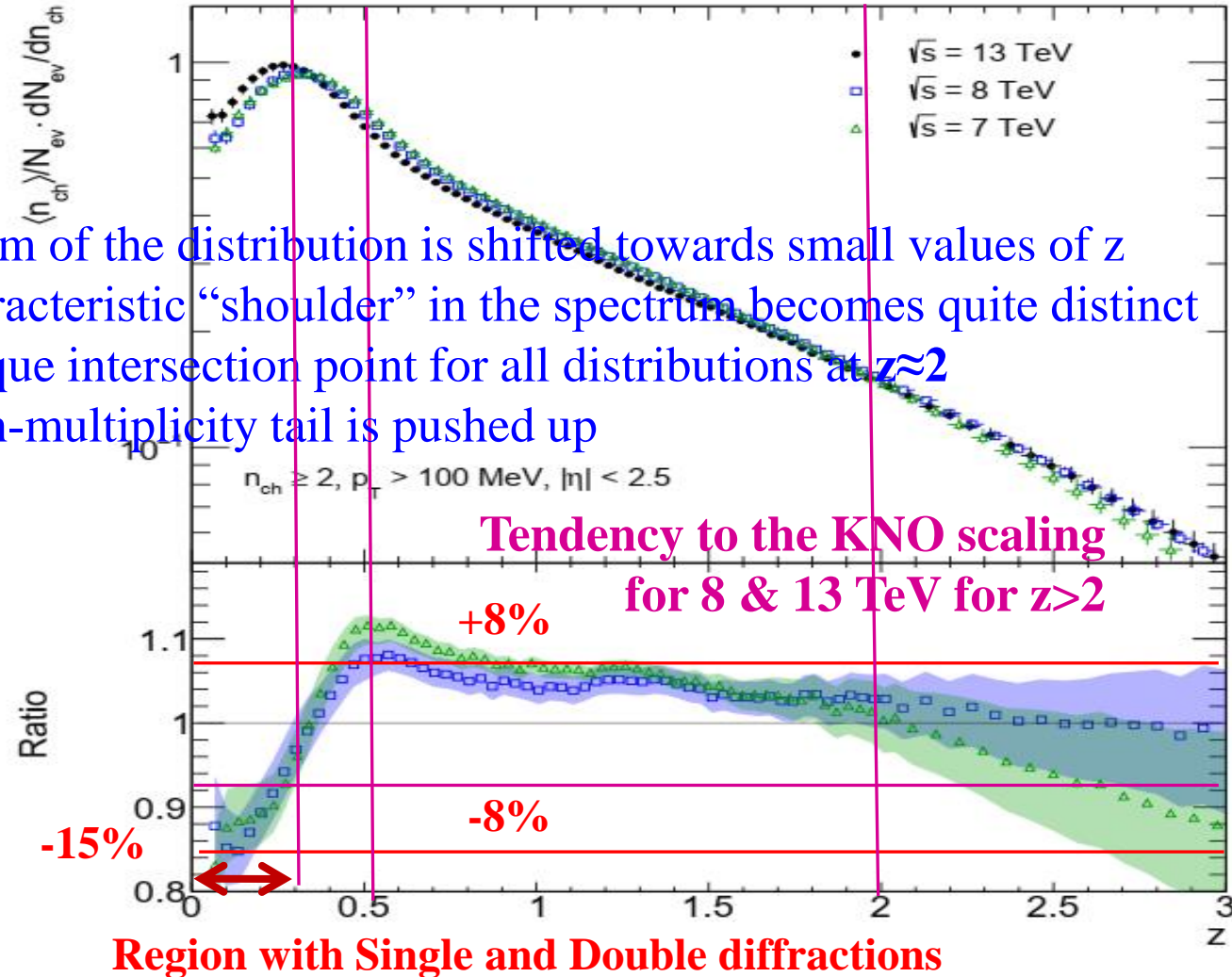


Charged particle multiplicity distribution (solid line) for processes going via the exchange of $n \geq 1$ soft **Pomerons** in pp collisions at $\sqrt{s}=14$ TeV. Contributions of the **first four terms** are shown by dash-dotted ($n=1$), double-dash-dotted ($n=2$), dashed ($n=3$) and dotted ($n=4$) lines, respectively.

KNO CHARGED-PARTICLE MULTIPLICITIES DISTRIBUTIONS: **ATLAS**, $p_T > 100$ MEV



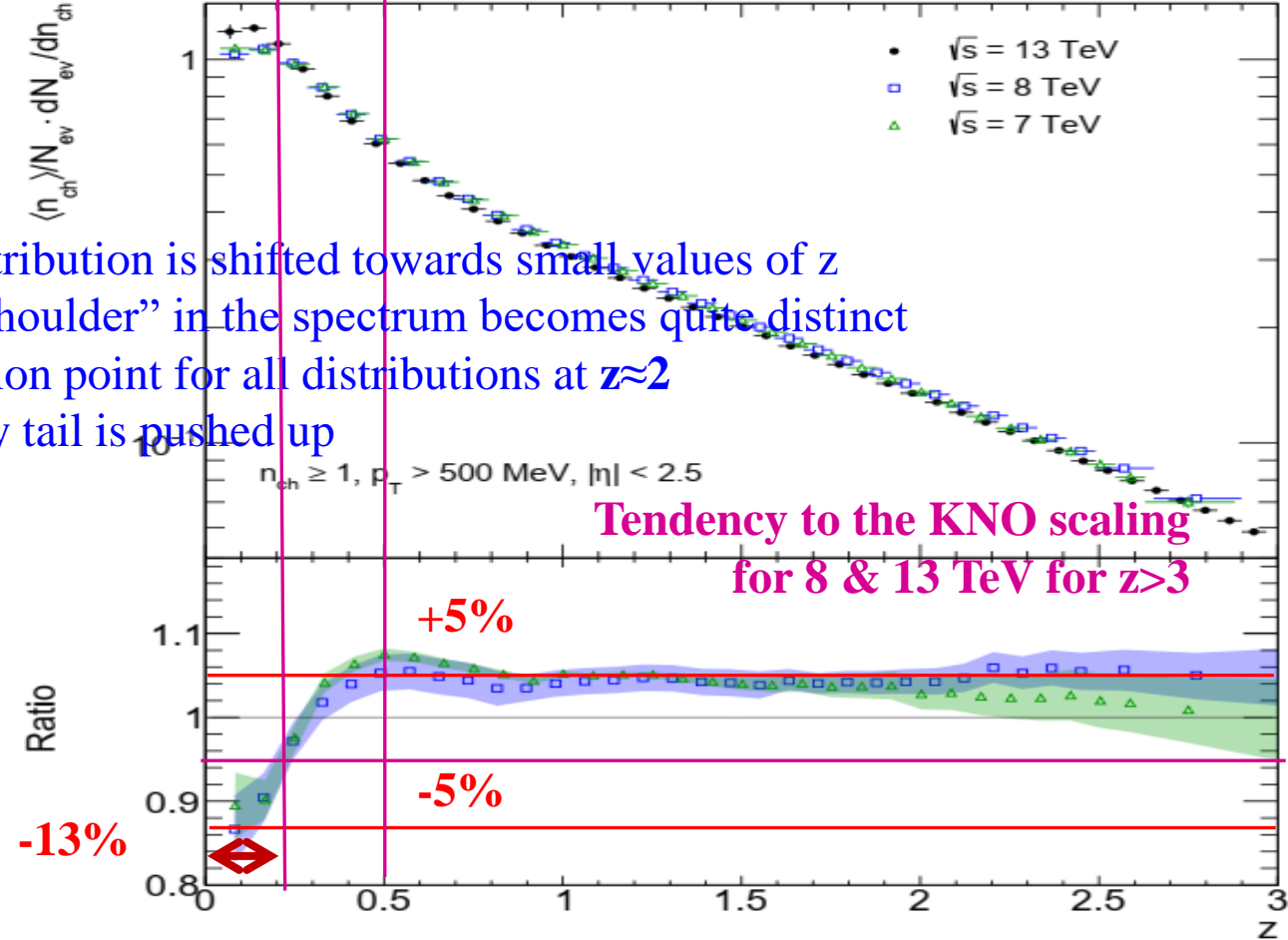
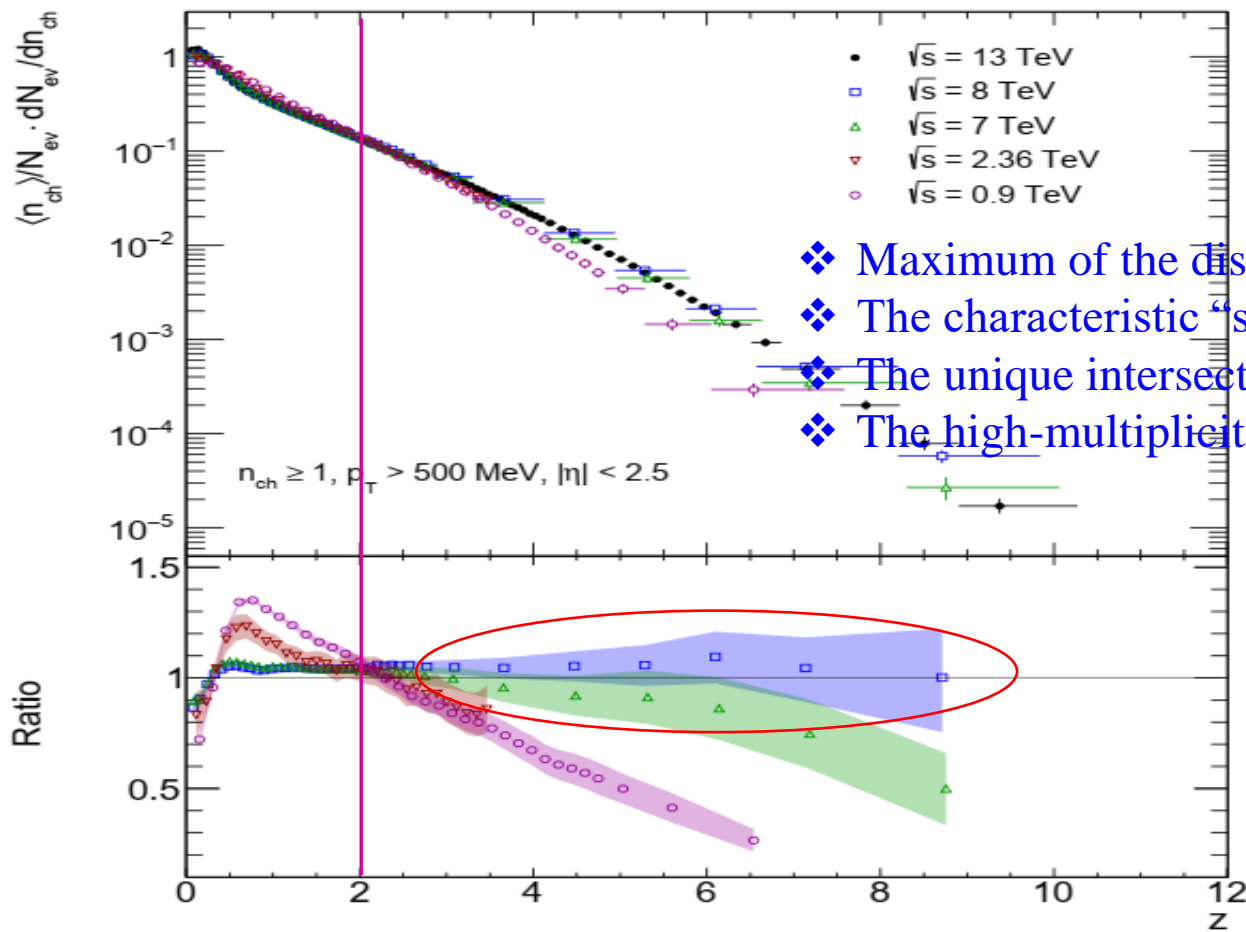
- ❖ Maximum of the distribution is shifted towards small values of z
- ❖ The characteristic “shoulder” in the spectrum becomes quite distinct
- ❖ The unique intersection point for all distributions at $z \approx 2$
- ❖ The high-multiplicity tail is pushed up



□ KNO scaled charged-particle multiplicity distributions as a function of a normalized multiplicity for events ($n_{ch} \geq 2$, $p_T > 100 \text{ MeV}$, $|\eta| < 2.5$) at the $\sqrt{s} = 0.9, 7, 8, 13 \text{ TeV}$ and for zoom multiplicity region up to 3 at $\sqrt{s} = 7, 8, 13 \text{ TeV}$.

□ The ratios to the distribution at 13 TeV are shown.

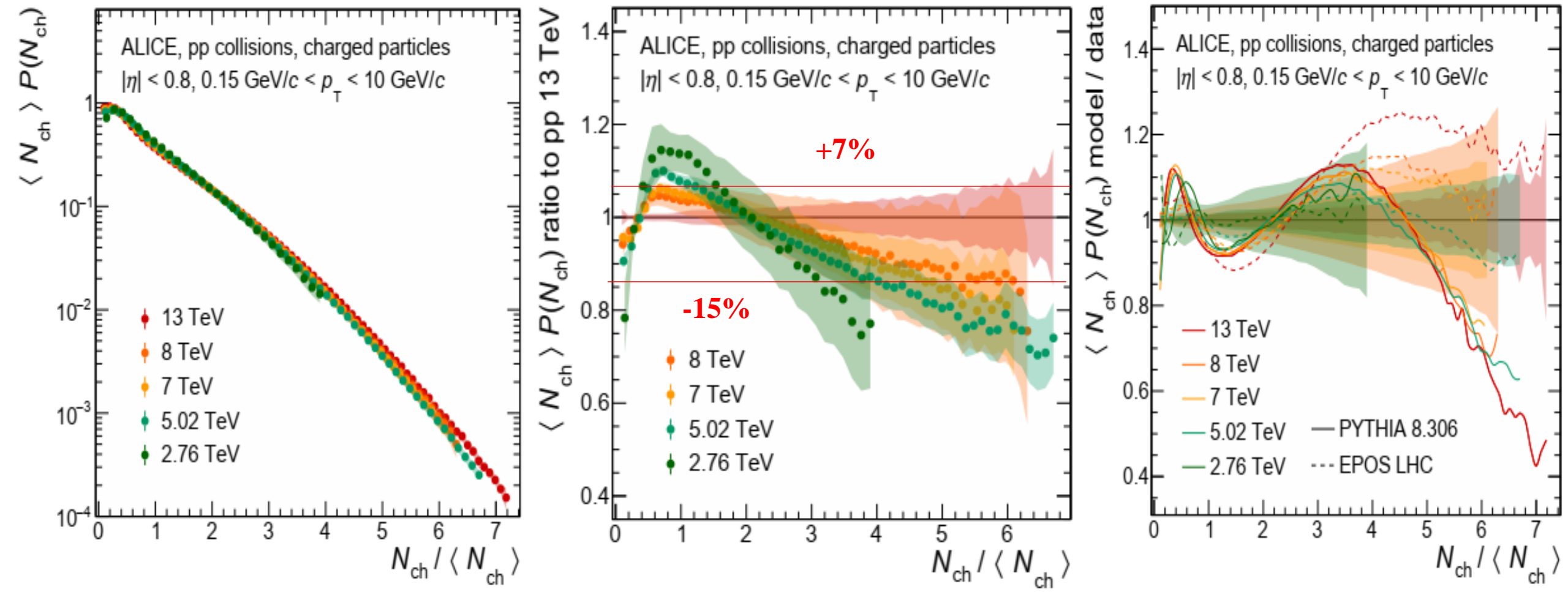
KNO CHARGED-PARTICLE MULTIPLICITIES DISTRIBUTIONS: **ATLAS**, $p_T > 500$ MEV



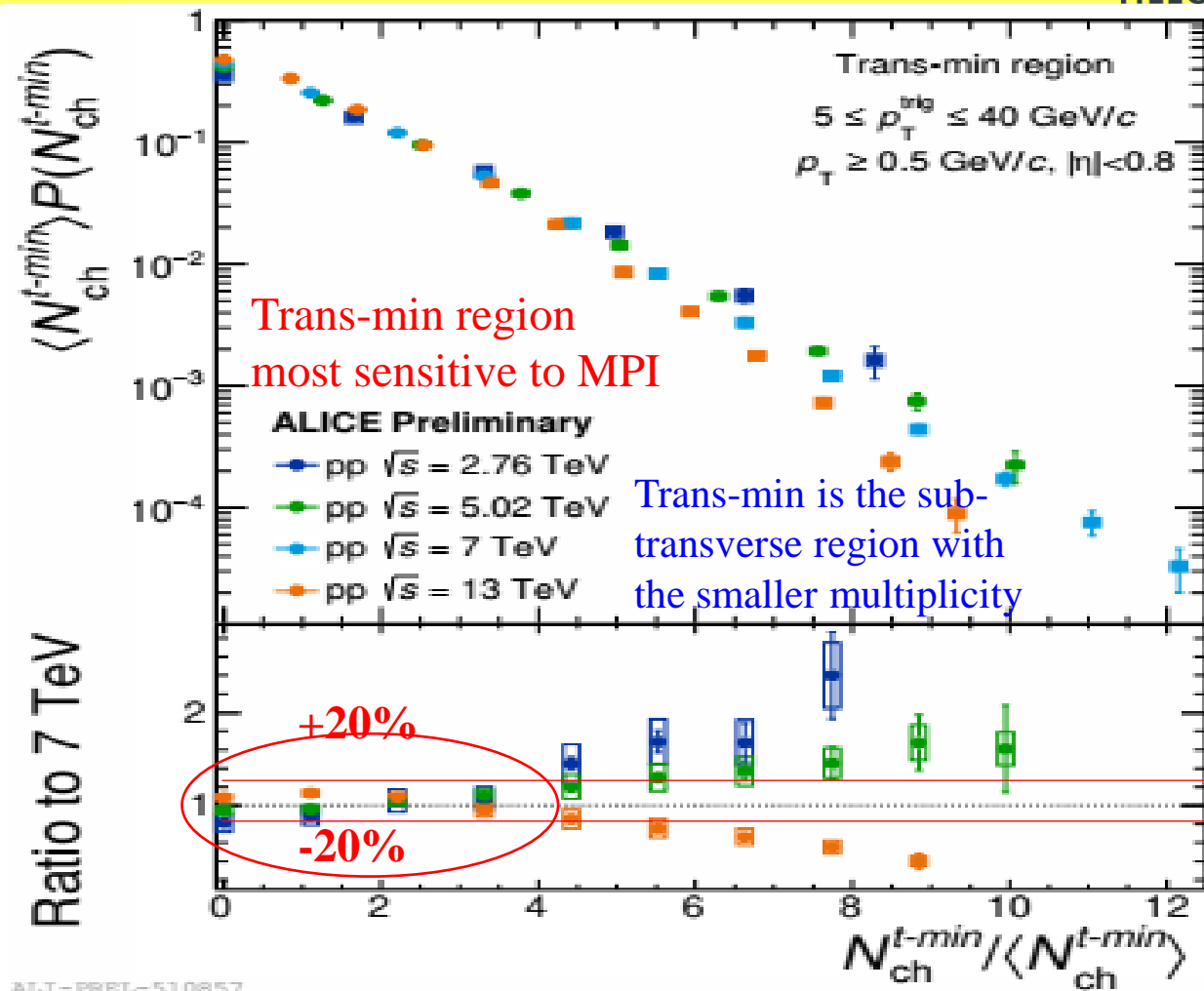
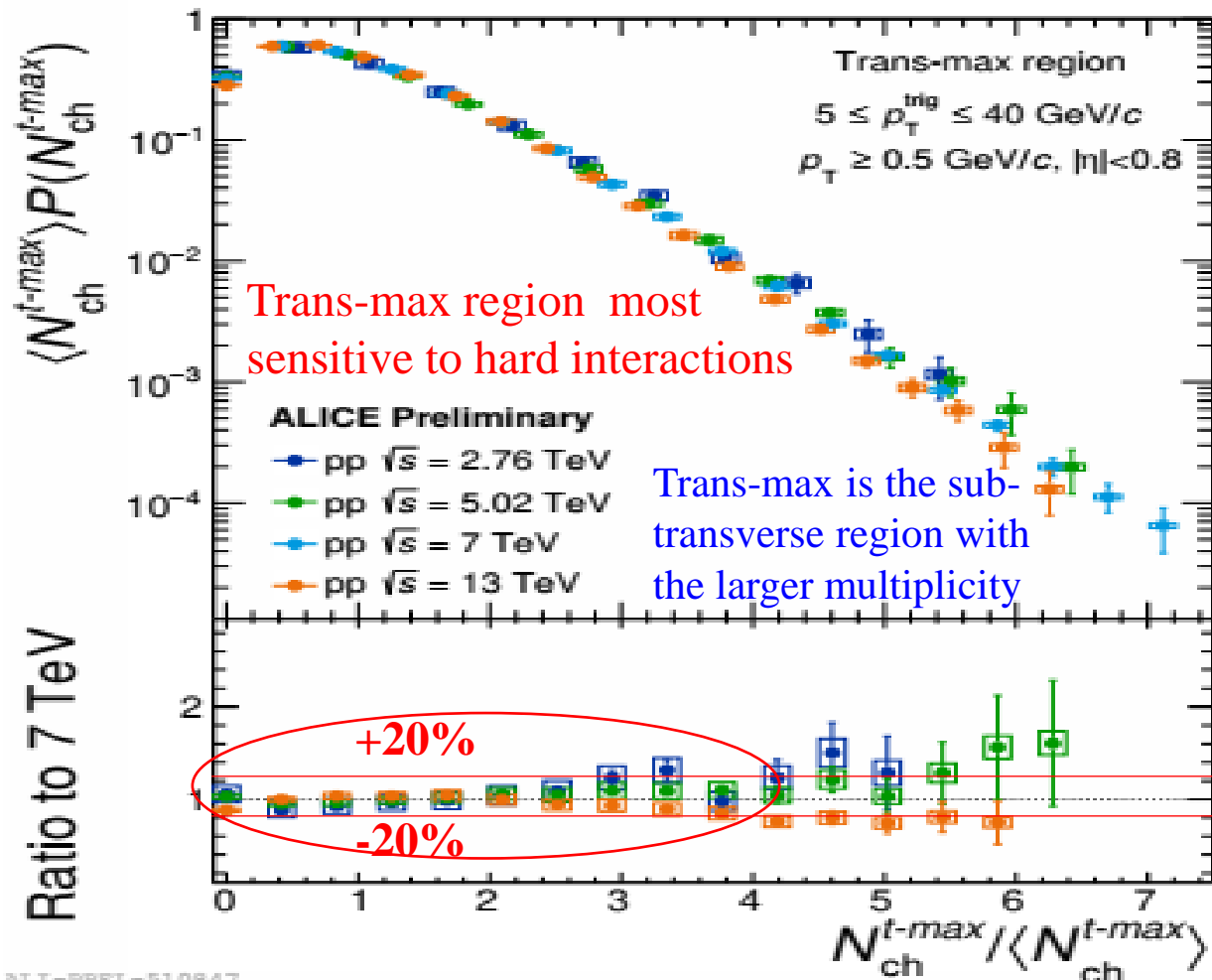
Region with Single and Double diffractions

\square KNO scaled charged-particle multiplicity distributions as a function of a normalized multiplicity for events ($n_{ch} \geq 1$, $p_T > 500$ MeV, $|\eta| < 2.5$) at the $\sqrt{s} = 0.9, 7, 8, 13$ TeV and for zoom multiplicity region up to 3 at $\sqrt{s} = 7, 8, 13$ TeV

\square The ratios to the distribution at 13 TeV are shown. Yuri Kulchitsky, JINR

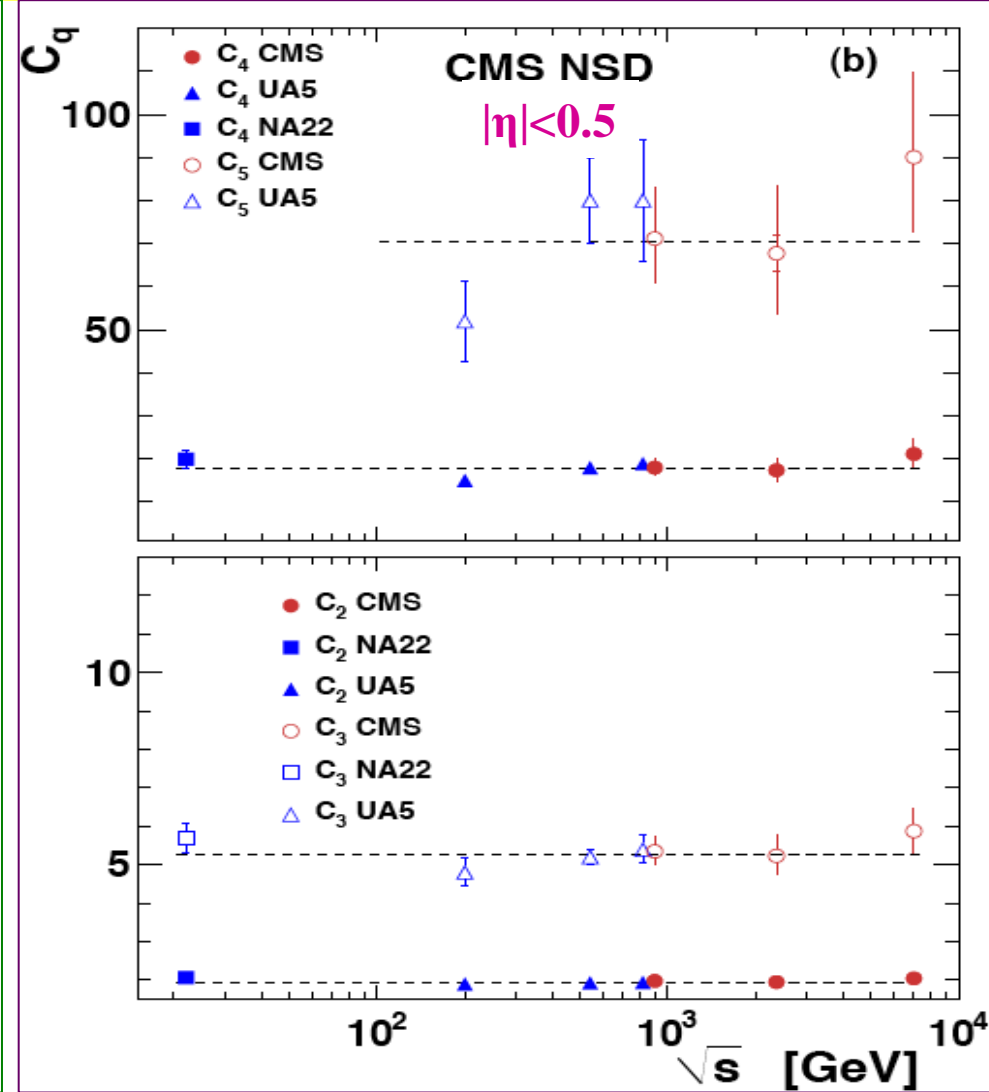
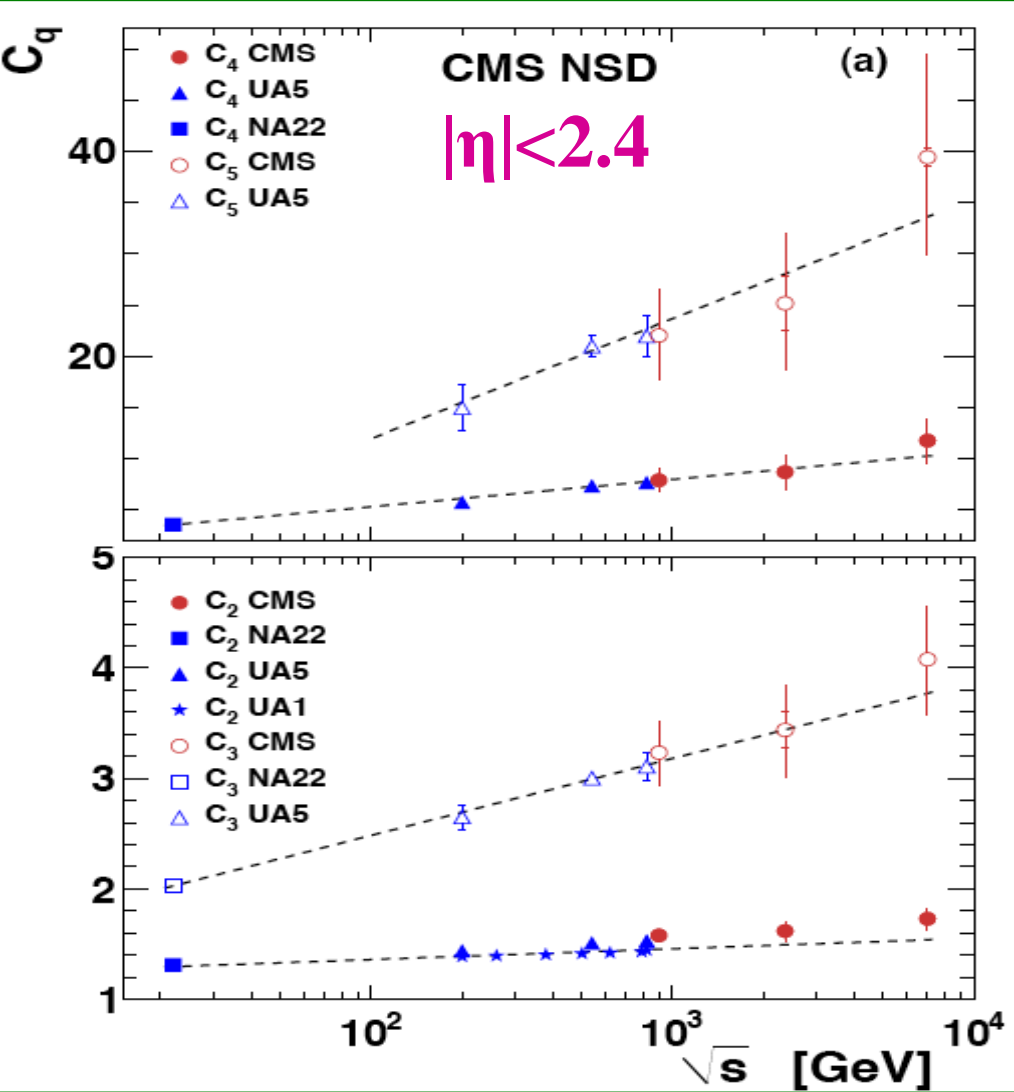


- The KNO scaled charged-particle multiplicity distributions as a function of the scaled multiplicity at the different CM energies $\sqrt{s} = 2.36, 5.02, 7, 8, 13$ TeV for events with $N_{ch} > 0$, $|\eta| < 0.8$ and $0.15 < p_T < 10$ GeV.
- The ratios of the KNO scaled primary charged-particle distributions to the interpolated distribution at $\sqrt{s} = 13$ TeV.
- The ratio of **Pythia 8** and **EPOS LHC** model predictions to data at various energies for the KNO scaling of charged-particle multiplicity distributions.



- The ALICE KNO scaled primary charged-particle multiplicity distributions as a function of the scaled multiplicity for pp collisions at the different CM energies $\sqrt{s} = 2.36, 5.02, 7$ and 13 TeV for events in $|\eta| < 0.8, p_T > 0.5 \text{ GeV}$, $5 \leq p_T^{\text{trig}} \leq 40 \text{ GeV}$ in the **UE trans-max**; and **UE trans-min** regions at $\sqrt{s} = 2.76, 5.02, 7$ and 13 TeV

- The KNO multiplicity distributions are normalized to that at $\sqrt{s} = 7 \text{ TeV}$.



If KNO scaling holds C_q are independent from \sqrt{s}

\sqrt{s} dependence of the normalized moments C_q of the multiplicity distribution for:

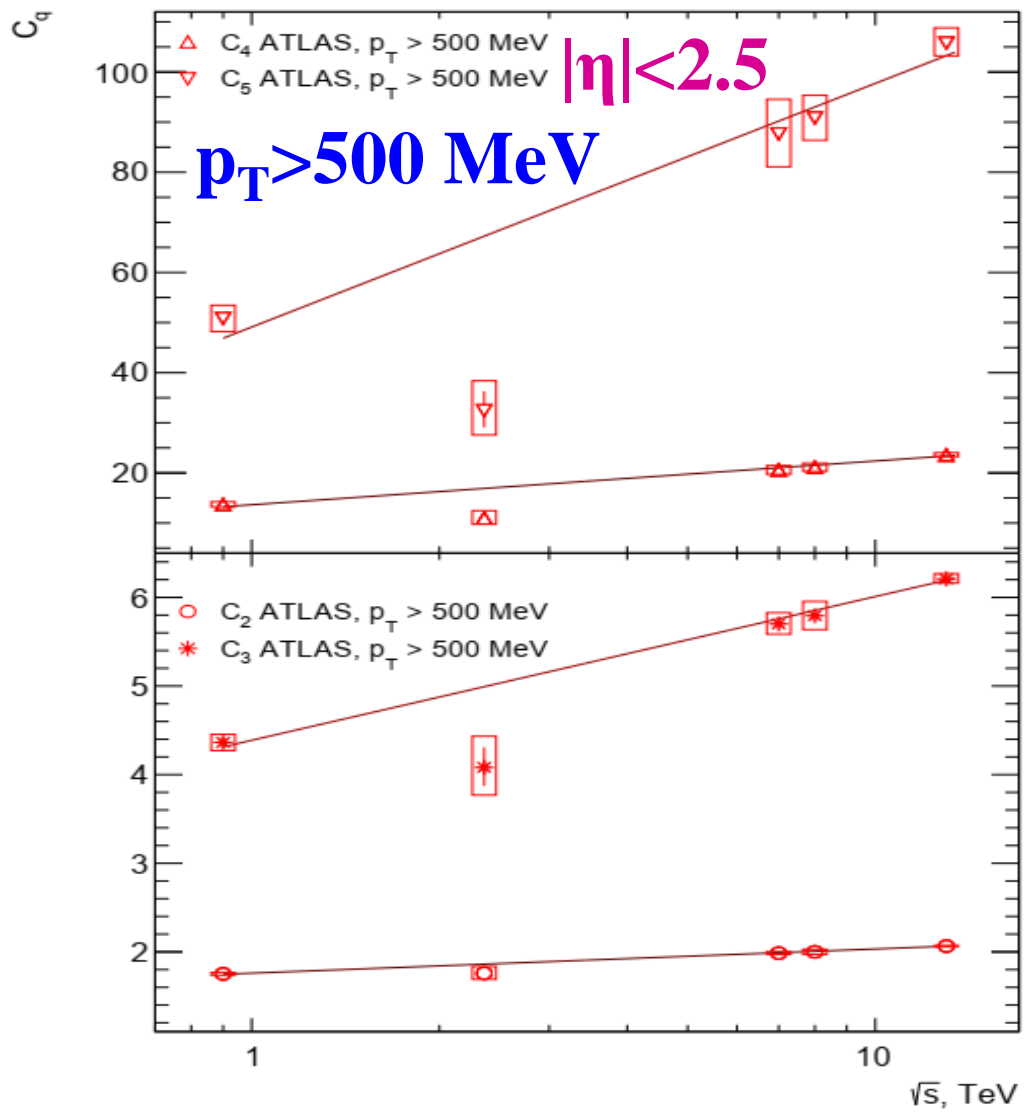
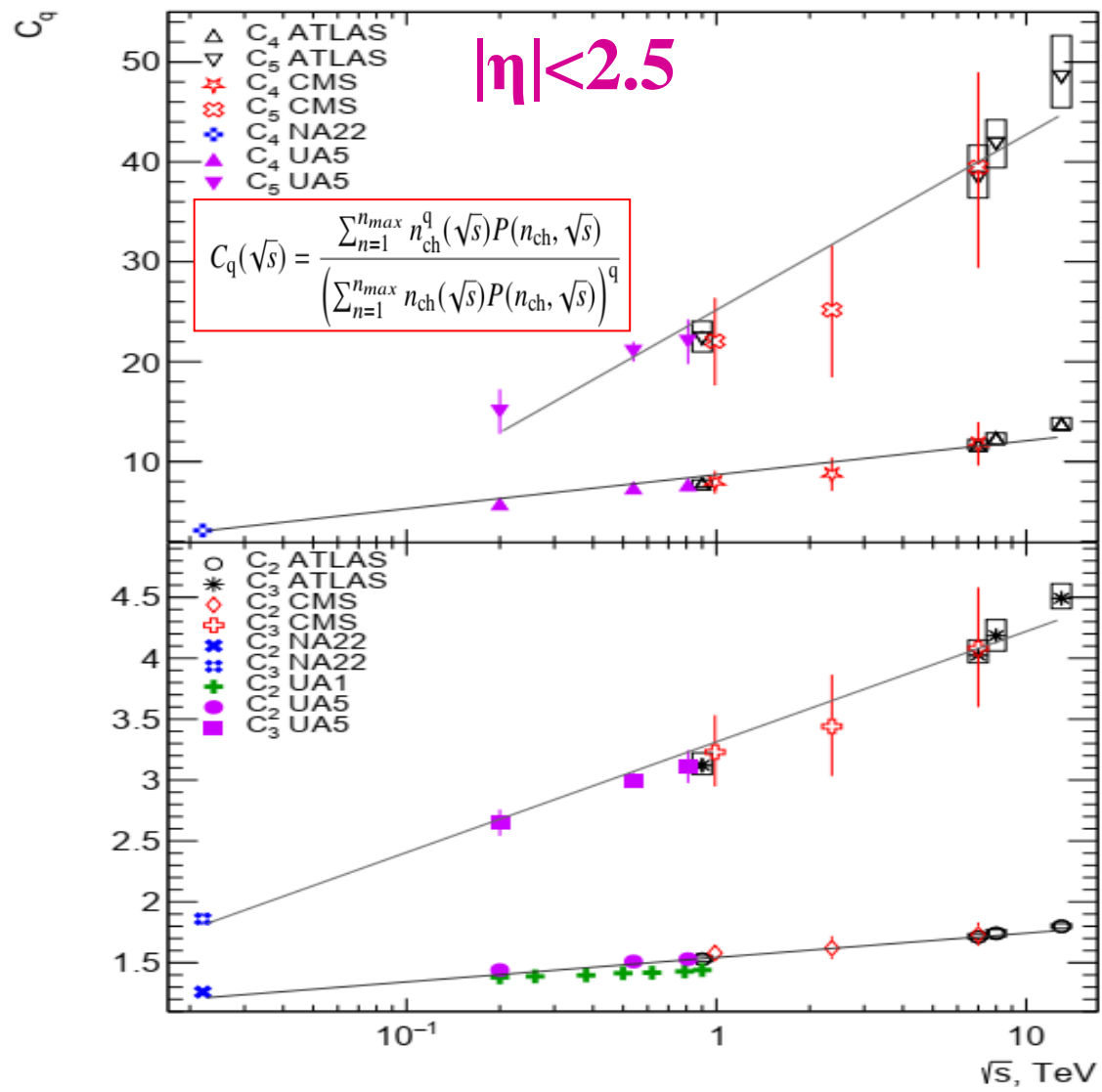
- (a) $|\eta| < 2.4$ and
- (b) $|\eta| < 0.5$

(a) $\rightarrow \ln(s)$ linear fits
 (b) \rightarrow constant fits

- Violation sensitive for $|\eta| < 2.4$
- No clear violation for $|\eta| < 0.5$ at least up to the order 4.

$$C_q(\sqrt{s}) = \frac{\sum_{n=1}^{n_{max}} n_{ch}^q(\sqrt{s}) P(n_{ch}, \sqrt{s})}{\left(\sum_{n=1}^{n_{max}} n_{ch}(\sqrt{s}) P(n_{ch}, \sqrt{s})\right)^q}$$

NORMALIZED ORDER-Q MOMENTS $C_Q = \langle N_{CH} \rangle^Q / \langle N_{CH} \rangle^Q$: ATLAS



If KNO scaling holds C_q are independent from \sqrt{s}

\sqrt{s} dependence of the normalized moments C_q of the multiplicity distribution for: $|\eta| < 2.5$

- The normalized moments C_q of the primary charged-particle multiplicity distributions measurement by the ATLAS for events with energies at $\sqrt{s} = 0.9, 2.36, 7, 8, 13 \text{ TeV}$ for $|\eta| < 2.5, n_{ch} \geq 2, p_T > 100 \text{ MeV}$ & $n_{ch} \geq 1, p_T > 500 \text{ MeV}$

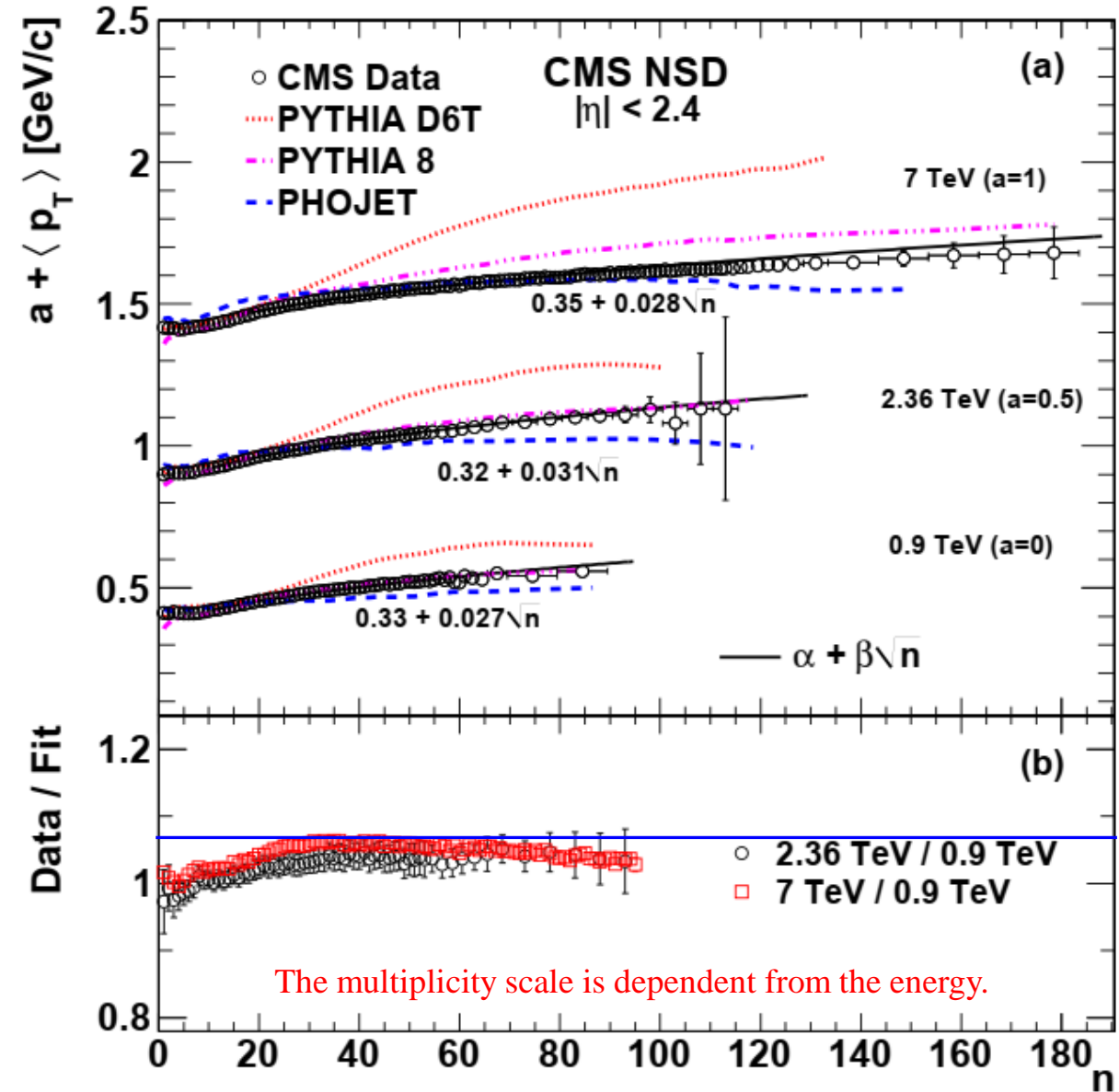
- The results of CMS and lower-energy experiments NA22, UA1, and UA5 are included.

AVERAGE TRANSVERSE MOMENTUM MULTIPLICITY DISTRIBUTIONS

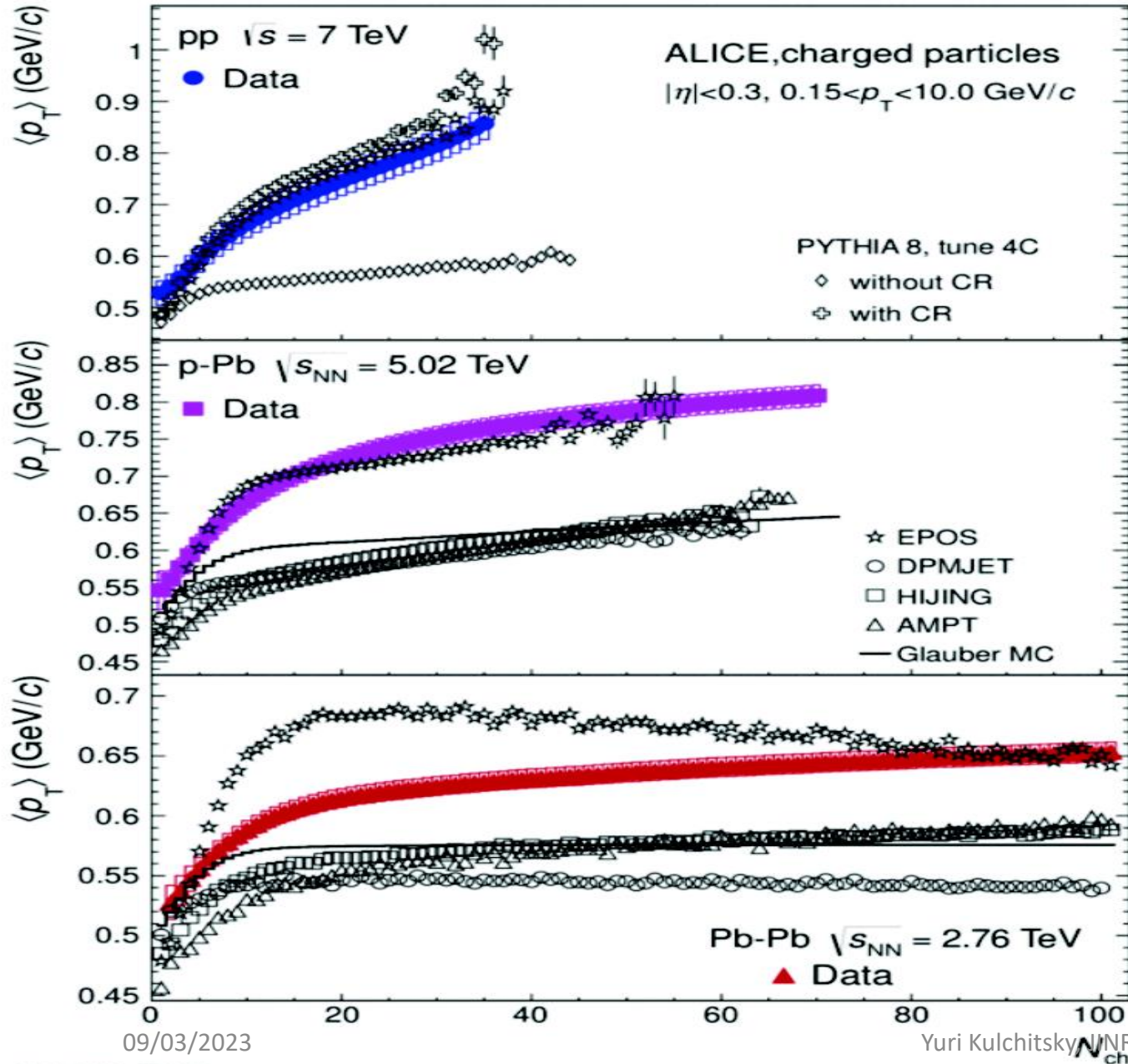


Run: 312837
Event: 135456971
2016-11-14 07:42:28 CEST

High-multiplicity event with 319 reconstructed tracks.
The shown tracks are from a single vertex and have $p_T > 0.4$ GeV



- A comparison of $\langle p_T \rangle$ versus n for $|\eta| < 2.4$ with two different PYTHIA models and the PHOJET model at 0.9, 2.36, and 7 TeV. For clarity, results for different energies are shifted by the values of a shown in the plots.
- Inspired we fit a first-degree polynomial in \sqrt{n} to the multiplicity dependence of $\langle p_T \rangle$ for $n > 15$ at each energy, yielding a good description which is valid at all three energies.
- The ratios of the data obtained at 7 and 2.36 TeV with respect to the data at 0.9 TeV show that the rise of the average transverse momentum with the multiplicity is **roughly energy-independent**.
- PHOJET produces too few charged hadrons overall but gives a good description of the average transverse momentum $\langle p_T \rangle$ at fixed multiplicity n . Among the three classes of models, PYTHIA 8 gives the best overall description of the multiplicity distribution and the dependence of the average transverse momentum on n .

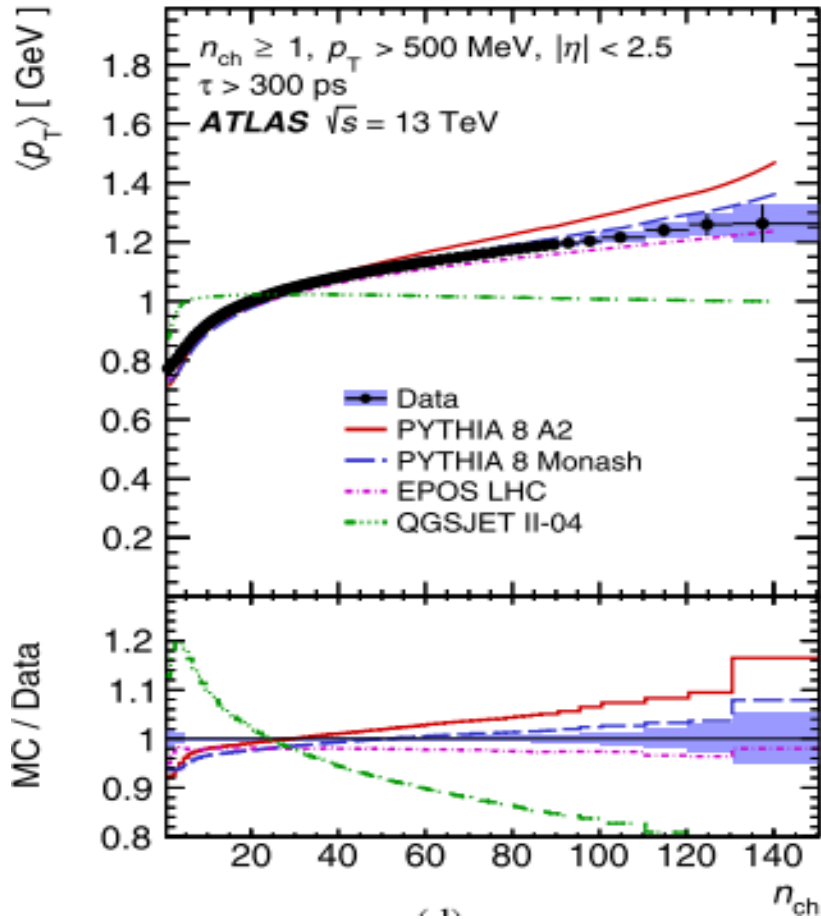


p-p: Color Reconnection in MPI unavoidable to describe $\langle p_T \rangle$ vs N_{ch} and dN_{ch}/dh . \sqrt{s} scaling \rightarrow properties driven by N_{ch}

p-Pb: EPOS OK, however shape of dN_{ch}/dh qualitatively similar to the Pythia 8 predictions for tune 4C CR (i.e. with Color Reconnections).

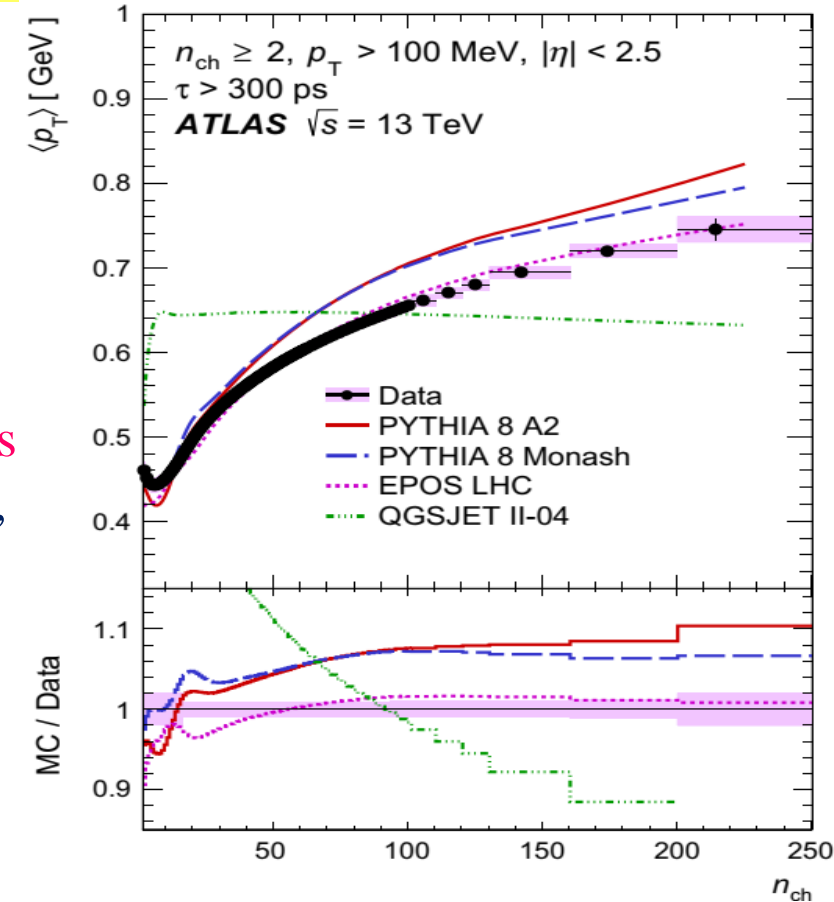
Pb-Pb: Bad description by HI MCs, shape of in agreement with Pythia 8 predictions for tune 4C NOCR (i.e. with no Color Reconnections).

MEAN TRANSVERSE MOMENTUM $\langle p_T \rangle$ VERSUS n_{ch}

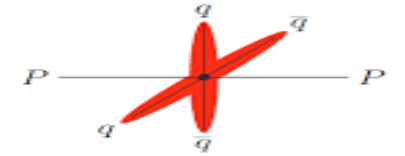


For $p_T > 500 \text{ MeV}, p_T > 100 \text{ MeV}$:

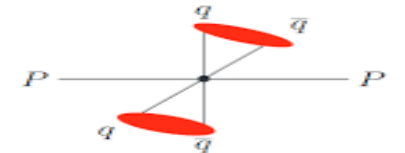
- Increases towards higher n_{ch} , as modelled by a *colour reconnection mechanism* in **PYTHIA 8** and by the *hydrodynamical evolution model* in **EPOS**
- The **QGSJET-II** generator, which has *no model for colour coherence effects*, describes the data poorly.
- For low n_{ch} , **PYTHIA 8 A2, EPOS** underestimate the data
- For **higher n_{ch}** all generators overestimate the data
- EPOS** describes the data reasonably well and to within 2%



Before colour reconnection

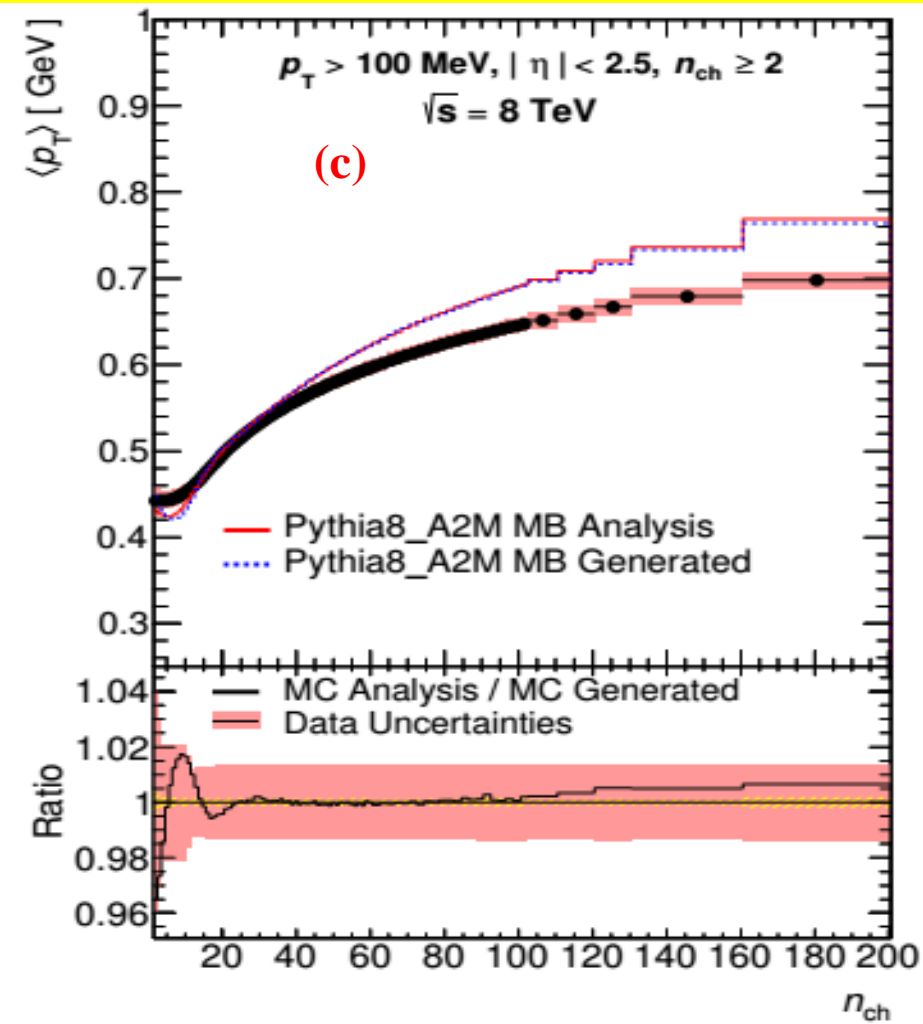
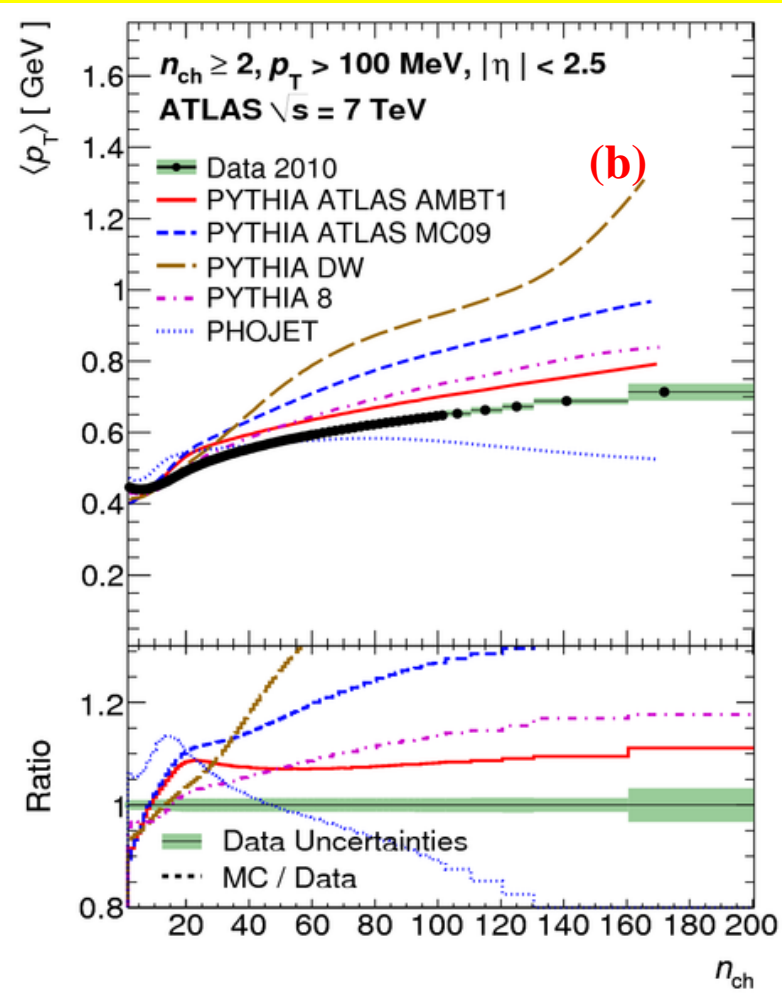
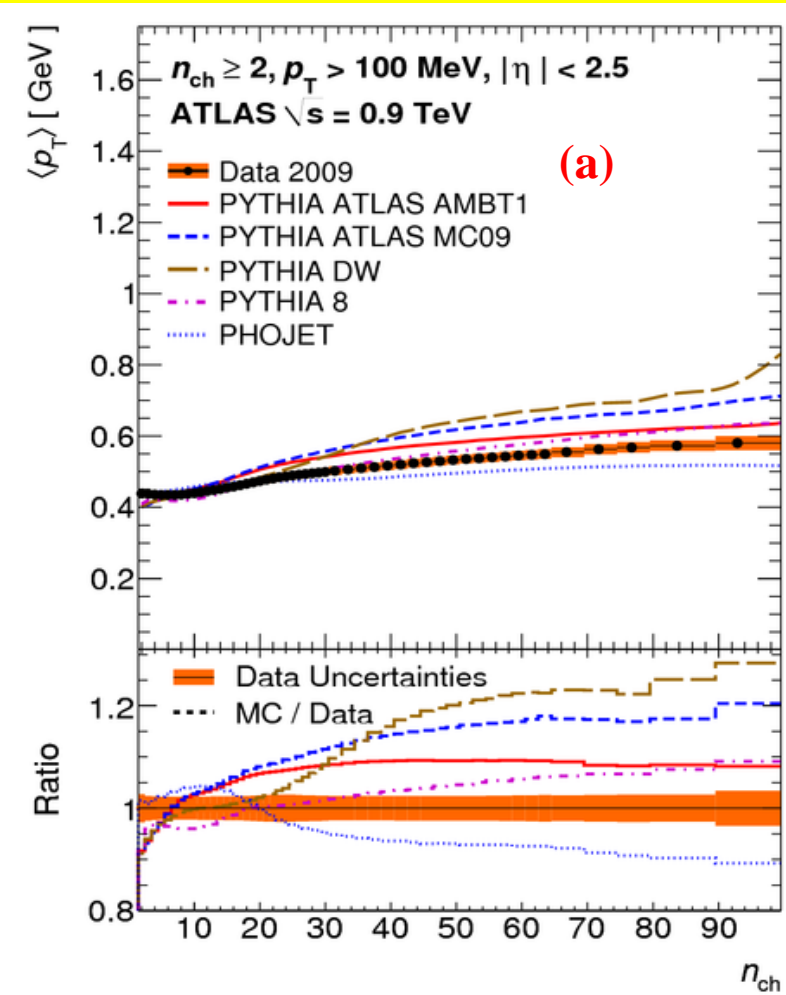


After colour reconnection?

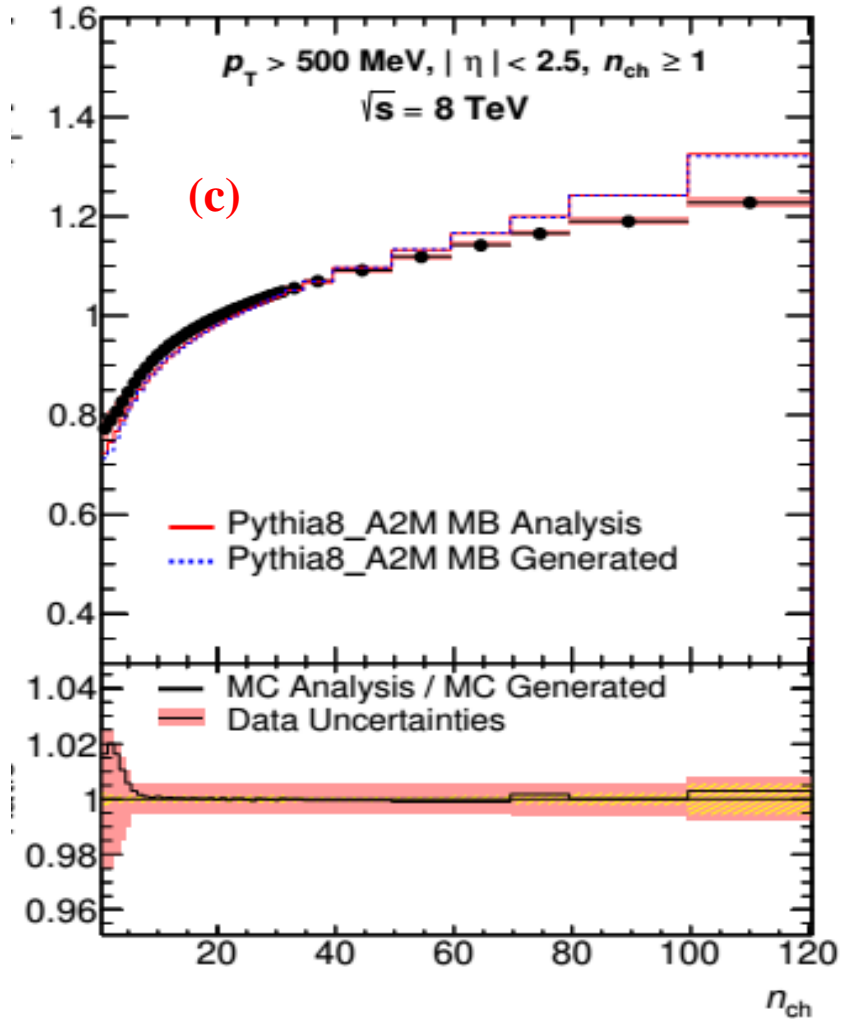
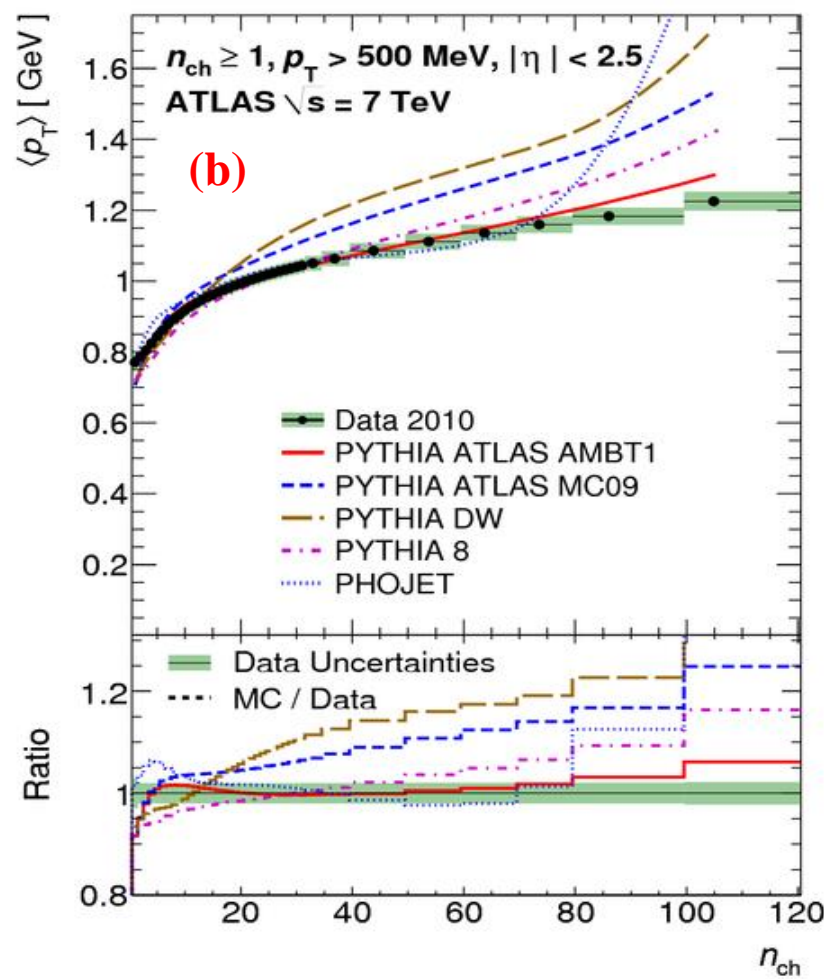
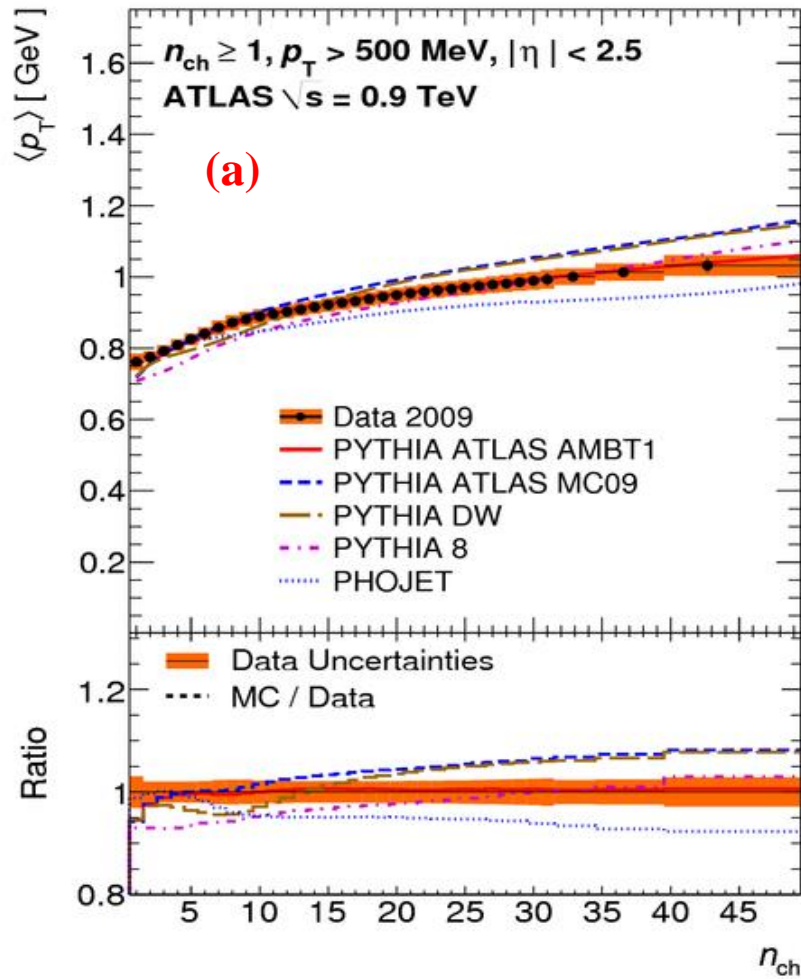


Primary charged-particle the $\langle p_T \rangle$ vs. n_{ch} for events with $n_{ch} \geq 1, p_T > 500 \text{ MeV}$ and $n_{ch} \geq 2, p_T > 100 \text{ MeV}$ in $|\eta| < 2.5$

Colour reconnection: strings from independent parton interactions do not independently produce hadrons, but fuse before hadronization

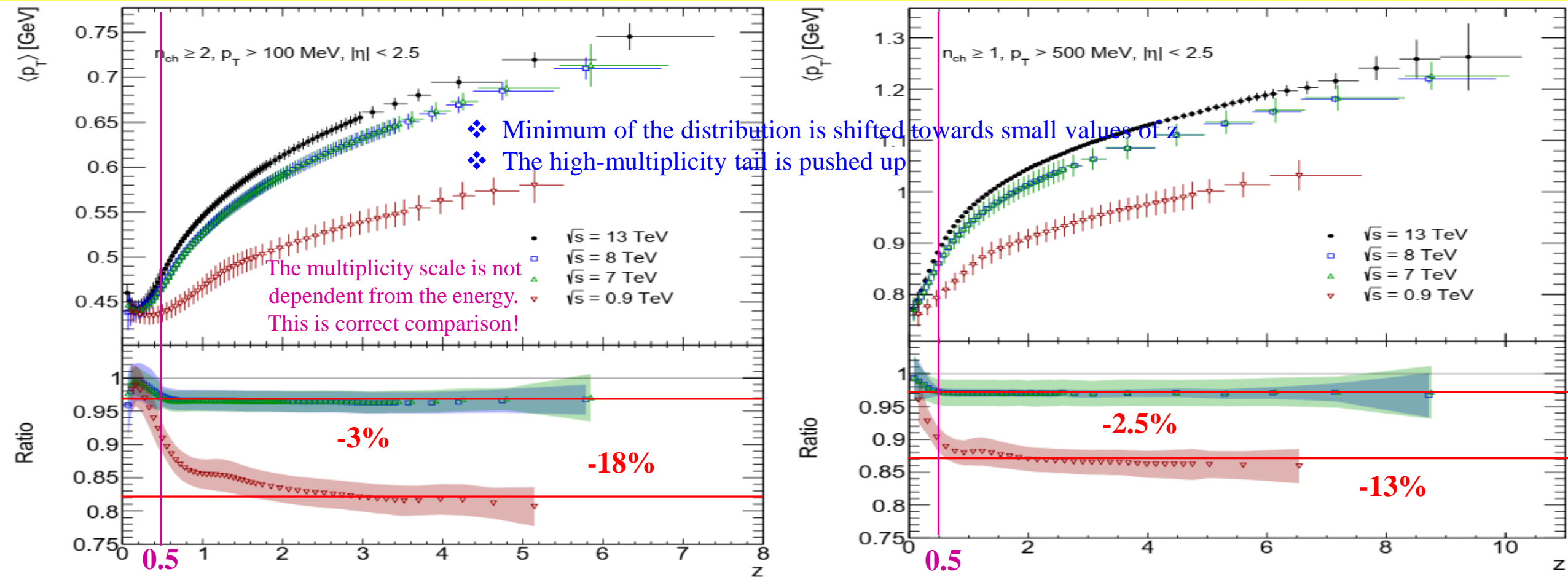


Average transverse momentum as a function of the number of charged particles for events with $n_{ch} \geq 1, p_T > 100$ MeV and $|\eta| < 2.5$ at $\sqrt{s} = 0.9$ (a), 7 (b) and 8 TeV (c)

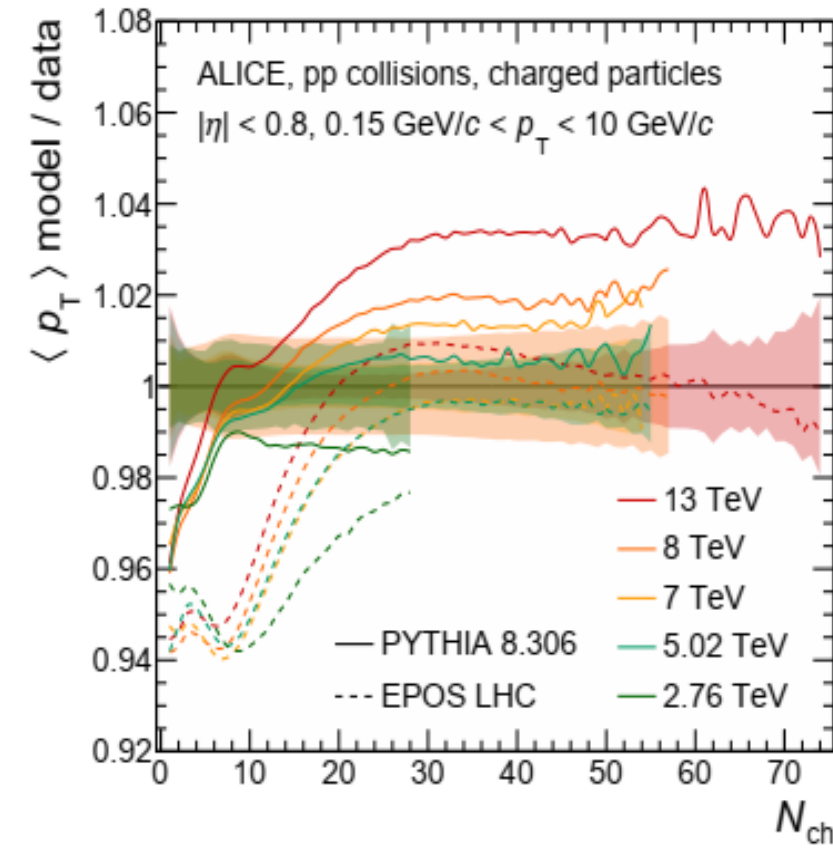
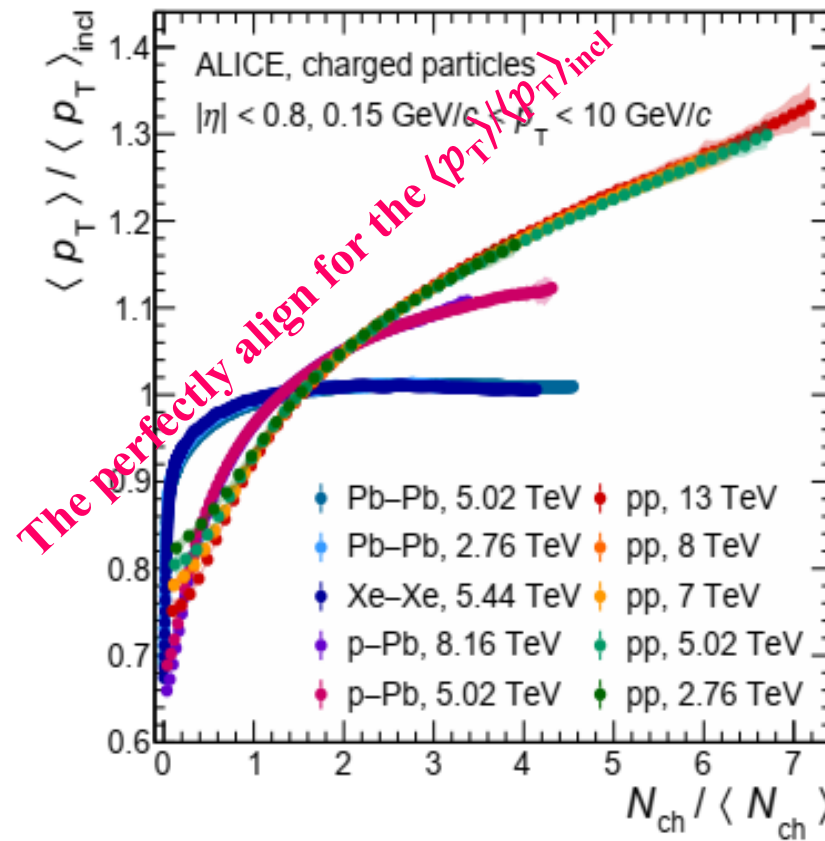
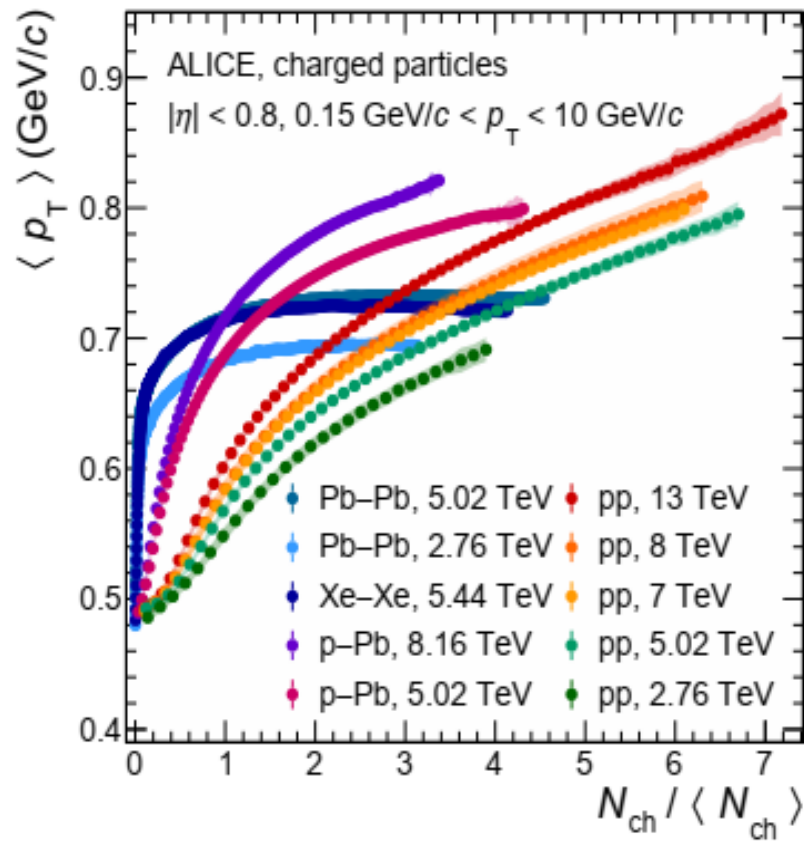


Average transverse momentum as a function of the number of charged particles for events with $n_{ch} \geq 1, p_T > 500$ MeV and $|\eta| < 2.5$ at $\sqrt{s} = 0.9$ (a), 7 (b), 8 TeV (c).

THE AVERAGE TRANSVERSE MOMENTUM DISTRIBUTIONS: ATLAS



Top panel: The average transverse momentum, $\langle p_T \rangle$, as a function of a normalized multiplicity z for events with $n_{ch} \geq 2, p_T > 100 \text{ MeV}$ and $n_{ch} \geq 1, p_T > 500 \text{ MeV}$ for $|\eta| < 2.5$ measurement by the ATLAS Collaboration at the energies 0.9 TeV, 7 TeV, 8 TeV and 13 TeV. The error bars and boxes represent the statistical and systematic contributions, respectively. **Bottom panel:** The ratios to the distribution at 13 TeV are shown. Ratios and their uncertainties were obtained by interpolating the distribution at 13 TeV. Bands represent the total uncertainties of ratios.



- The average charged-particle transverse momentum and normalized on $\langle p_T \rangle_{\text{incl}}$, $\langle p_T \rangle / \langle p_T \rangle_{\text{incl}}$ distributions as a function of the scaled multiplicity for pp , p -Pb, Xe -Xe and Pb -Pb collisions at the different CM energies $\sqrt{s} = 2.36, 5.02, 7, 8$ and 13 TeV for pp , $\sqrt{s} = 5.02$ and 8.16 TeV for p -Pb, $\sqrt{s} = 5.44 \text{ TeV}$ for Xe -Xe and $\sqrt{s} = 2.76$ and 5.02 TeV for Pp -Pb for events in the kinematic range $N_{ch} > 0, |\eta| < 0.8$ and $0.15 < p_T < 10 \text{ GeV}$.

- The ratio of Pythia 8 and EPOS LHC model predictions to data at various energies are shown for $\langle p_T \rangle$ distributions

	$\sqrt{s_{NN}}$ (TeV)	$\langle p_T \rangle_{\text{incl}}$ (MeV/c)
pp	2.76	589.7 ± 2.6
	5.02	612.2 ± 2.7
	7	627.1 ± 1.6
	8	631 ± 5
	13	654.0 ± 1.0

SUMMARY

- ❑ Comparison of the charged-particle multiplicity $P_n(z)$, the average transverse momentum $\langle p_T(z) \rangle$ distributions on KNO scale were done using the **ATLAS** results at $\sqrt{s} = 0.9, 2.36, 7, 8, 13$ TeV for $|\eta| < 2.5$ and (1) $n_{ch} \geq 2, p_T > 100$ MeV; (2) $n_{ch} \geq 1, p_T > 500$ MeV
- ❑ The $P_n(z)$ distributions on KNO scale have the **similar shape** & decrease with energy increase
- ❑ Study of the **KNO scaling** was done at **0.9–13 TeV** (in the **first time** at **13 TeV**)
- ❑ The test of $\Psi(z)$ for **0.9/13 TeV** confirms that **$\Psi(z)$ violation** increases with **decreasing energy**
- ❑ The **KNO scaling** is **hold** for highest energies within $\pm 8\%$ for $p_T > 100$ MeV; $\pm 5\%$ for $p_T > 500$ MeV: the **better KNO scaling** for **higher $p_T > 500$ MeV** is observed
- ❑ The $\langle p_T(z) \rangle$ on the KNO scale have the **same shape** & **increase** with energy increase
- ❑ The results of comparisons $P_n(z)$ & $\langle p_T(z) \rangle$ on KNO scale can be useful for MC tuning
- ❑ Discussion of the CMS & ALICE results for the **KNO scaling**, $P_n(z)$, $\langle p_T(z) \rangle$ distributions

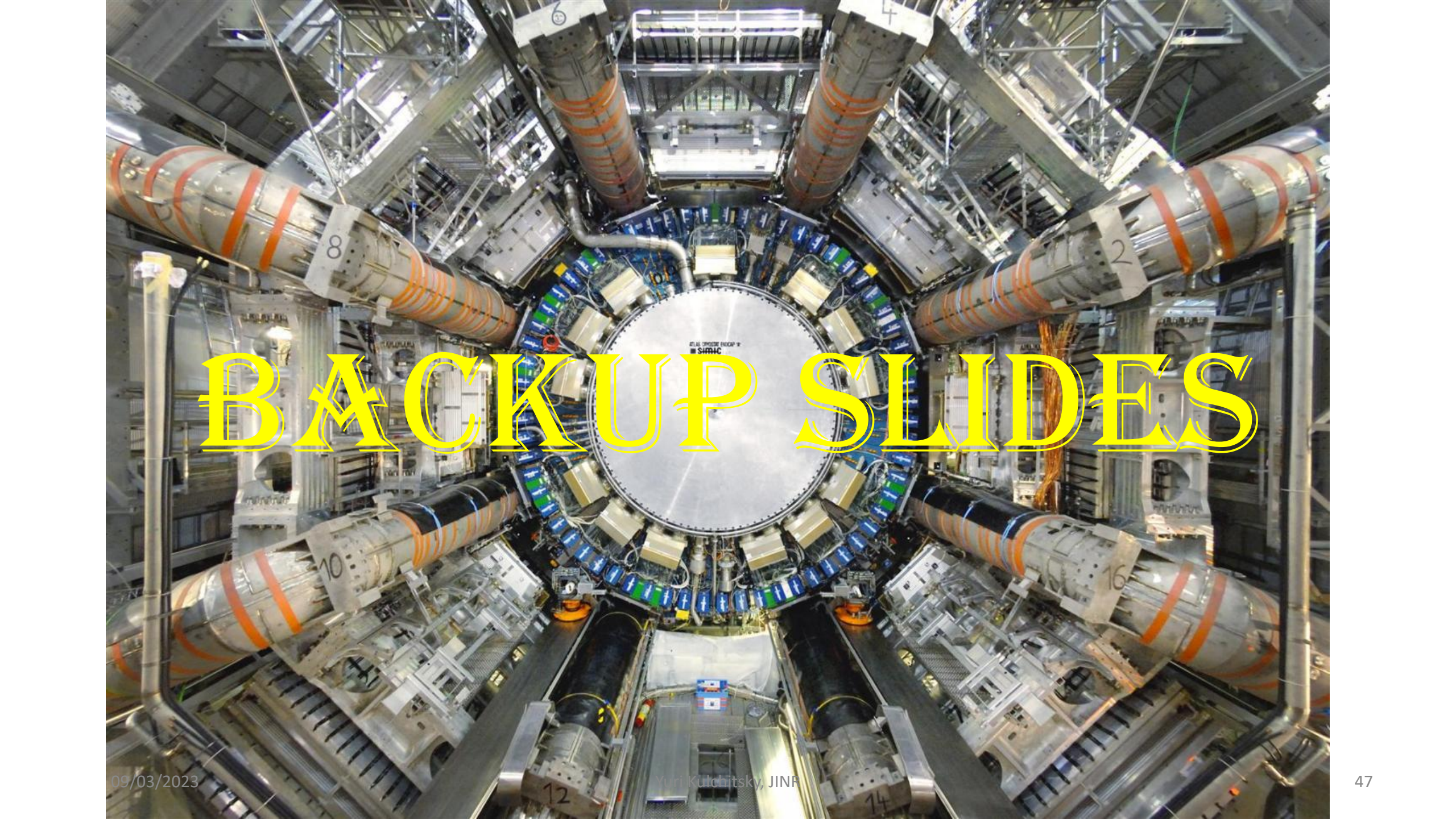
THANKS A LOT, TO ATLAS COLLEAGUES!

THANK YOU
VERY MUCH
FOR ATTENTION!



Run: 312837
Event: 135456971
2016-11-14 07:42:28 CEST

High-multiplicity event with 319 reconstructed tracks.
The shown tracks are from a single vertex and have $p_T > 0.4$ GeV



ATLAS OPERATIONAL EXPERIMENT
IN SIFRAC

BACKUP SLIDES

1. ATLAS Collaboration, *Charged-particle multiplicities in pp interactions at $\sqrt{s}=900$ GeV measured with the ATLAS detector at the LHC*; *Phys. Lett. B* 688 (2010) 21-42
2. ATLAS Collaboration, *Charged-particle multiplicities in pp interactions measured with the ATLAS detector at the LHC*; *New J. Phys.* 13 (2011) 053033
3. ATLAS Collaboration, *Charged-particle distributions in pp interactions at $\sqrt{s}=8$ TeV measured with the ATLAS detector*; *Phys. Lett. B* 758 (2016) 67-88
4. ATLAS Collaboration, *Charged-particle distributions at low transverse momentum in $\sqrt{s}=13$ TeV pp interactions measured with the ATLAS detector at the LHC*; *Eur. Phys. J. C* (2016) 76:502
5. ATLAS Collaboration, *Charged-particle distributions in $\sqrt{s}=13$ TeV pp interactions measured with the ATLAS detector at the LHC*; *Physics Letters B* 758 (2016) 67–88
6. The ATLAS collaboration, *The Pythia 8 A3 tune description of ATLAS minimum bias and inelastic measurements incorporating the Donnachie-Landshoff diffractive model*; *ATL-PHYS-PUB-2016-017*

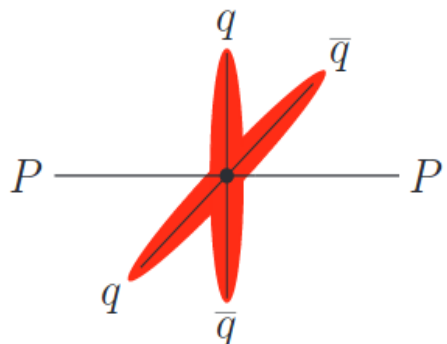
KNO SCALING STUDY AT THE LHC EXPERIMENTS

1. **CMS Collaboration**, *Charged Particle Multiplicities in pp Interactions at $\sqrt{s} = 0.9, 2.36,$ and 7 TeV*, ***JHEP 01 (2011) 079***, *arXiv:1011.5531 [hep-ex]*
2. **ALICE Collaboration**, *Charged-particle multiplicity measurement in proton-proton collisions at $\sqrt{s} = 0.9$ and 2.36 TeV with ALICE at LHC*, ***Eur. Phys. J. C 68 (2010) 89***, *arXiv:1004.3034 [hep-ex]*.
3. **ALICE Collaboration**, *Charged-particle multiplicities in proton–proton collisions at $\sqrt{s}= 0.9$ to 8 TeV*, ***Eur. Phys. J. C 77 (2017) 33***, *arXiv:1509.07541 [nucl-ex]*
4. Yuri Kulchitsky & Pavel Tsiareshka, *Study of KNO scaling in pp collisions at \sqrt{s} from 0.9 to 13 TeV using results of the ATLAS at the LHC*, ***Submitted to Eur. Phys. J. C (2022)*** , *arXiv:2202.06697 [hep-ex]*,
5. **ALICE Collaboration**, *Multiplicity dependence of charged-particle production in pp , p -Pb, Xe - Xe and Pb - Pb collisions at the LHC*, (2022), *arXiv:2211.15326 [nucl-ex]*
6. **ALICE Collaboration (F. Fan)**, *Particle production as a function of underlying-event activity and very forward energy with ALICE*, *20th International Conference on Strangeness in Quark Matter 2022*, *arXiv: 2208.11348 [nucl-ex]*

COLOUR RECONNECTION

Colour reconnection addresses the problem of how the colour fields rearrange themselves after the collision

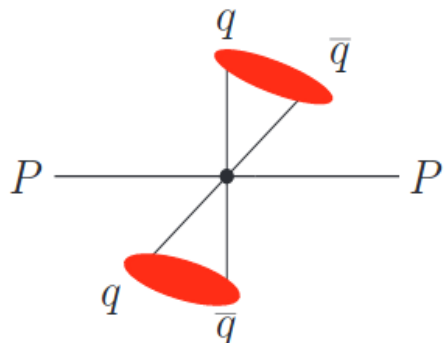
Before colour reconnection



Experimentally driven in order to describe the rise of average transverse momentum as a function of number of particles

Increases towards higher n_{ch} , as modelled by a **colour reconnection mechanism** in **PYTHIA 8**

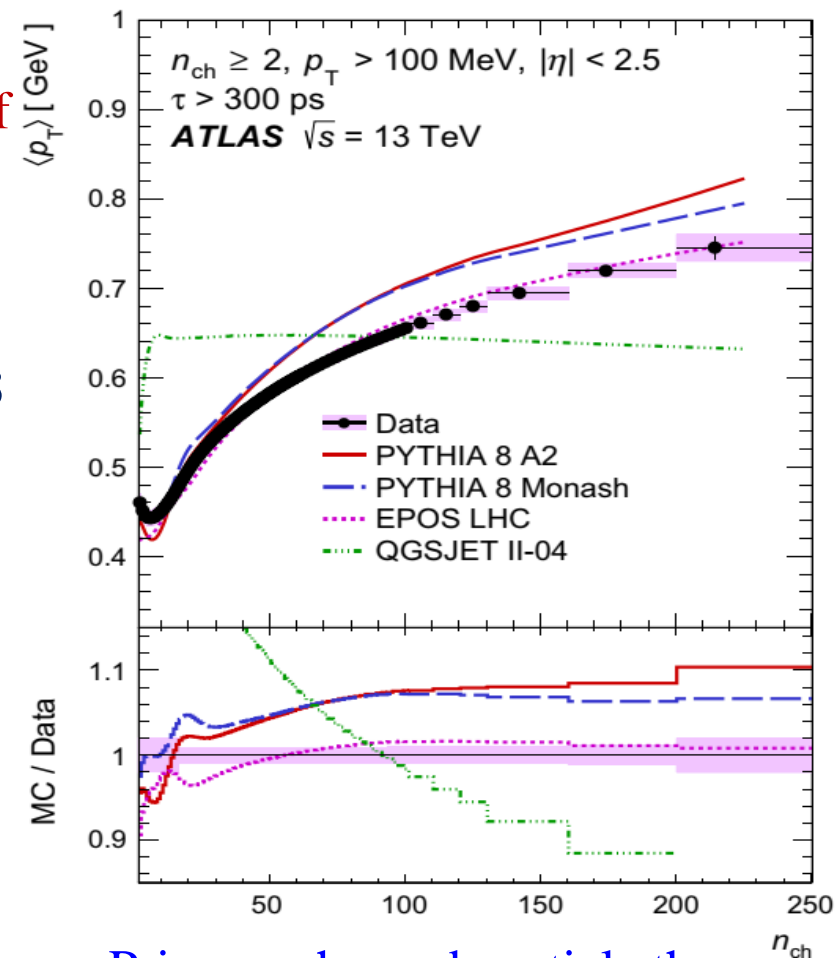
After colour reconnection?



The **QGSJET-II** generator, which has **no model for colour coherence effects**, describes the data poorly.

Monte Carlo event generators (e. g. PYTHIA 8) have various models to implement such arrangements: MPI-based, QCD-inspired, Gluon-move

- New tunes have been obtained for the two alternative colour reconnection models implemented in PYTHIA 8: QCD-inspired and gluon-move models
- They are based on 13 TeV data and describe simultaneously observables sensitive to soft and semi-hard processes



Primary charged-particle the $\langle p_T \rangle$ vs. n_{ch} for events with $n_{ch} \geq 2, p_T > 100 \text{ MeV}$ in $|\eta| < 2.5$